COMPREHENSIVE REPORT

1974 - 1977

FINAL REPORT

1974 - 1977

UNITED STATES ENERGY RESEARCH AND DEVELOPMENT ADMINISTRATION

EY-76-S-05-3018

"A PHYSICO-CHEMICAL STUDY OF SOME AREAS OF FUNDAMENTAL SIGNIFICANCE TO BIOPHYSICS"

August 18, 1977

S. P. McGlynn
Principal Investigator
Boyd Professor of Chemistry

TABLE OF CONTENTS

FOREWORD

In the last three years, we have submitted three annual reports and one proposal. In addition, we have published ~50 papers, most in journals of excellent repute. It is the sum of those entities which constitutes (or should constitute) this Comprehensive Report.

We make an attempt, in the following, to summarize all the above efforts. However, our attempt falls quite short. Hence, we have no recourse but to suggest that a proper perspective will be gained only by reading from the list of Section II.A.

I. STATEMENT OF OTHER SUPPORT

The work described in the Comprehensive Report (1974 - 1977) and in the Annual Report (1976 - 1977) was supported by no other U.S. agency (Federal, State or Private). Apart from a stipend to Dr. Klaus Wittel from The Deutsche Forschungsgemeinschaft, ~$15,000.00 for 15 months, ERDA (ERDA-Division of Biomedical Research--Physics and Technological Program) was the sole supporting agency.

II. BIBLIOGRAPHY, SYMPOSIA, LABORATORY GUESTS, IN-HOUSE SYMPOSIA, PERSONNEL DEPARTING, AND EQUIPMENT PURCHASED AND/OR FABRICATED

II. BIBLIOGRAPHY, SYMPOSIA, LABORATORY GUESTS, IN-HOUSE SYMPOSIA, PERSONNEL DEPARTING, AND EQUIPMENT PURCHASED AND/OR FABRICATED

A. Bibliography of Titles

1974 - 1977

131. Lui, Yau H., "Electronic Spectroscopy of Highly-Polar Aromatics," A Ph.D. Dissertation submitted to LSU in August, 1974 and for which a Ph.D. Degree was awarded to Mr. Lui.

132. Felps, Walter Sidney, "Molecular Rydberg States," A Ph.D. Dissertation submitted to LSU in May, 1975 and for which a Ph.D. Degree was awarded to Mr. Felps.

133. Lui, Y. H. and McGlynn, S. P., "Electronic Spectroscopy of Highly-Polar Aromatics, X. Luminescence of the Fluorobenzonitriles," J. Luminescence, 9, 449(1975).

134. McGlynn, S. P. and Meeks, J. L., "Photoelectron Spectra of Carbonyls. Acetaldehyde, Acetamide, Biacetyl, Pyruvic Acid, Methyl Pyruvate and Pyruvamide," J. Elec. Spectrosc., 6, 269(1975).

135. Lui, Y. H. and McGlynn, S. P., "Electronic Spectroscopy of Highly-Polar Aromatics. XI. Luminescence of the Cyanoanilines," J. Luminescence, 10, 113(1975).

136. Lui, Y. H. and McGlynn, S. P., "Electronic Spectroscopy of Highly-Polar Aromatics. XII. Luminescence of the Aminoacetophenones," not yet submitted for publication.

137. Meeks, J. L., Arnett, J. F., Larson, D. B. and McGlynn, S. P., "Photoelectron Spectroscopy of Carbonyls. Urea, Oxamide, Oxalic Acid and Oxamic Acid, J. Amer. Chem. Soc., 97, 3905(1975).

138. Meeks, J. L. and McGlynn, S. P., "Photoelectron Spectroscopy of Carbonyls. Oxamide, Parabanic Acid and Their N-Methyl Derivatives," J. Amer. Chem. Soc., 97, 5079(1975).

139. Meeks, J. L. and McGlynn, S. P., "Photoelectron Spectroscopy of Carbonyls. Oxalyl Chloride, Ethyl Oxalyl Chloride, Ethyl Oxamate and N,N-Dimethyl Ethyl Oxamate," Spectrosc. Letters, 8(7), 439(1975). Corrigenda, Spectrosc. Letters, 8(11), 941(1975).

140. Meeks, J. L. and McGlynn, S. P., "Photoelectron Spectroscopy of Carbonyls. Carbonates, Oxalates and Esterification Effects," J. Electron Spectrosc., 8, 85(1976).

141. Khalil, O. S. and McGlynn, S. P., "Electronic Spectroscopy of Highly-Polar Aromatics. XIII. Absorption and Luminescence of Nitroanilines," J. Luminescence, 11, 185(1976).

142. Hochmann, P. and McGlynn, S. P., "Rydberg States. II. A Correlation Algorithm," in VACUUM ULTRAVIOLET RADIATION PHYSICS, E. -E. Koch, R. Haensel and C. Kunz, Eds., Pergamon/Vieweg, Braunschweig, Germany, 1975.

143. Annual Report 1974 - 1975. A Bibliography of Titles and Reports of Research Accomplished or in Progress (Incomplete Work) for the Period 1974 - 1975 of Research Contract No. AT-(40-1)-3018.

144. Felps, S., Hochmann, P., Brint, P. and McGlynn, S. P., "Molecular Rydberg Transitions. The Lowest-Energy Rydberg Transitions of s-Type in CH_3X and CD_3X, X = Cl, Br and I," J. Mol. Spectrosc., 59, 355(1976).

145. Dougherty, D., Wittel, K., Meeks, J. L. and McGlynn, S. P., "Photoelectron Spectroscopy of Carbonyls. Ureas, Uracils and Thymine," J. Amer. Chem. Soc., 98, 3815(1976).

146. Khalil, O. S., Meeks, J. L. and McGlynn, S. P., "Electronic States and "Geometric Isomerism" of p-Disubstituted Cyanoanilines," Chem. Phys. Letters, 39, 457(1976).

147. Wittel, K., Meeks, J. L. and McGlynn, S. P., "Electronic Structure of the Cyanato and Thiocyanato Groups. Ground State and Excited States," in THE CHEMISTRY OF CYANATES AND THEIR THIO DERIVATIVES, S. Patai, Ed., in press.

148. Chattopadhyay, S., Hochmann, P. and McGlynn, S. P., "Molecular Rydberg Transitions. V. Atomic Correlation Lines," J. Chem. Phys., 65, 3341(1976).

149. Dougherty, D., Arnett, J. F., Bloomfield, J. G., Newkome, G. R. and McGlynn, S. P., "Photoelectron Spectra of Carbonyls. Propella-enes and Propella-ones," J. Phys. Chem., 80, 2212(1976).

150. Brint, P., Dougherty, D. and McGlynn, S. P., "Photoelectron Spectra of Carbonyls. The Non-bonding n-MO's of Dicarbonyl Compounds," not yet submitted for publication.

151. Brint, P. and McGlynn, S. P., "The Low-Energy $^1\Gamma_{n\pi^*}$ Excited States of Tetramethyl-1,3-cyclobutanedione," not yet submitted for publication.

152. Brint, P., Wittel, K., Felps, W. S. and McGlynn, S. P., "Molecular Rydberg Transitions. III. A Linear Combination of Rydberg Orbitals (LCRO) Model for the Two-Chromophoric System 2,2,4,4-Tetramethyl-cyclobutane-1,3-dione (TMCBD)," J. Amer. Chem. Soc., 98, 7980(1976).

153. Annual Report 1975 - 1976. A Bibliography of Titles and Reports of Research Accomplished or in Progress (Incomplete Work) for the period 1975 - 1976 of Research Contract No. AT-(40-1)-3018.

154. Wang, Hung-tai, "Atomic and Molecular Rydberg States: A Correlative Approach," A Ph.D. Dissertation submitted to LSU in August, 1976 and for which a Ph.D. Degree was awarded to Mr. Wang.
(7 copies appended to this Report)

155. Carsey, Thomas Preston, "Excited Electronic States: Polar Aromatics and Inorganic Anions," A Ph.D. Dissertation submitted to LSU in May, 1977 and for which a Ph.D. Degree was awarded to Mr. Carsey.
(7 copies appended to this Report)

156. Dougherty, David Russell, "The Photoelectron Spectroscopy of Dicarbonyls and Biological Molecules," A Ph.D. Dissertation submitted to LSU in May, 1977 and for which a Ph.D. Degree was awarded to Mr. Dougherty.
(7 copies appended to this Report)

157. Brint, P. and McGlynn, S. P., "Excited Electronic State of α-, β-, and γ-Dicarbonyls," J. of Photochemistry, 5, 153(1976).
(7 reprints appended to this Report)

158. Wittel, K., Felps, W. S., Klasinc, L. and McGlynn, S. P., "Molecular Rydberg Transitions. VI. trans-Dibromoethylene. The Relation between Vacuum Ultraviolet and Photoelectron Spectroscopy," J. Chem. Phys., 65, 3698(1976).
(7 reprints appended to this Report)

159. Dougherty, D. and McGlynn, S. P., "Photoelectron Spectroscopy of Carbonyls. 1,4-Benzoquinones," J. Amer. Chem. Soc., 99, 3234(1977).
(7 reprints appended to this Report)

160. Wittel, K. and McGlynn, S. P., "The Orbital Concept in Molecular Spectroscopy," Chem. Revs., in press.
(7 preprints appended to this Report)

161. Wang, H. -t., Felps, W. S. and McGlynn, S. P., "Molecular Rydberg States. VII. Water," accepted for publication in J. Chem. Phys.
(7 preprints appended to this Report)

162. Findley, G., Wittel, K., Felps, W. S. and McGlynn, S. P., "Molecular Rydberg Transitions. VIII. The Geometry of Ethylene in the R_{1S} State," accepted for publication in the Internat. J. Quantum Chem.
(7 preprints appended to this Report)

163. Hochmann, P. and McGlynn, S. P., "Molecular Rydberg Transitions. IX. Term Value/Ionization Energy Correlations," in preparation.
(7 preprints appended to this Report)

164. Hochmann, P. and McGlynn, S. P., "Molecular Rydberg Transitions. X. Correlation Algorithms for Rydberg Term Values," in preparation.
(7 preprints appended to this Report)

165. Dougherty, D. and McGlynn, S. P., "Photoelectron Spectroscopy of Carbonyls. Biological Molecules," accepted for publication in J. Chem. Phys.
(7 preprints appended to this Report)

166. McGlynn, S. P., Dougherty, D., Mathers, T. and Abdulner, S., "Photoelectron Spectroscopy of Carbonyls. Biological Considerations," accepted for publication in the "Proceedings of the 10th Jerusalem Conference on Excited States in Organic and Biochemistry".
(7 preprints appended to this Report)

167. Findley, G. L. and McGlynn, S. P., "A Group-Theoretic Analysis of the Genetic Code," submitted to J. Chem. Phys.
(7 preprints appended to this Report)

168. Dougherty, D., Younathan, E. S., Voll, R., Abdulner, S. and McGlynn, S. P., "Photoelectron Spectroscopy of Biological Molecules," submitted to Biochemistry.
(7 preprints appended to this Report)

169. Wang, H. -t., Felps, W. S., Findley, G. L., Rao, A. R. P. and McGlynn, S. P., "Molecular Rydberg States. XI. Quantum Defect Analogies between Molecules and Rare Gases," accepted for publication in J. Chem. Phys.
(7 preprints appended to this Report)

170. McGlynn, S. P., review of DONOR-ACCEPTOR BOND, (by E. N. Guryanova, I. P. Goldstein and I. P. Romm, Wiley: New York and Chichester, 1975), Nature, 262, 82(1976).
(7 reprints appended to this Report)

171. McGlynn, S. P., "Louisiana Higher Education System Lacks Respect," Baton Rouge State-Times, June 1, 1977.
(7 reprints appended to this Report)

172. Scott, J. D., Felps, W. S., Findley, G. L. and McGlynn, S. P., "Molecular Rydberg Transitions. XII. Magnetic Circular Dichroism of Methyl Iodide," submitted to J. Chem. Phys.
(7 preprints appended to this Report)

173. McGlynn, S. P., Wang, H. -t., Findley, G. L., Felps, W. S. and Rao, A. R. P., "Quantum Defect Analogies between Molecules and Rare Gases," submitted to "Proceedings of the Vth International Conference on Vacuum Ultraviolet Radiation Physics."
(7 preprints appended to this Report)

174. Khalil, O. S., Seliskar, C. J. and McGlynn, S. P., "CNDO/s-CI Computations on the Electronic States of Nitroanilines," submitted to J. Mol. Spectrosc.
(7 preprints appended to this Report)

175. McGlynn, S. P., "A Few Priorities," LSU/Alumni News, 53, 4(1977).
(7 reprints appended to this Report)

176. Felps, W. S., Wittel, K. and McGlynn, S. P., "Molecular Rydberg Transitions. XIII. cis-Dibromoethylene," submitted to J. Mol. Spectrosc.
(7 preprints appended to this Report)

177. Felps, W. S., Scott, J. D. and McGlynn, S. P., "The $\sigma \rightarrow \sigma^*$ Excitation in CH_3I," submitted to J. Chem. Phys.
(7 preprints appended to this Report)

178. Carsey, T. P. and McGlynn, S. P., "Spin-Orbit Coupling in Metal Anion Systems," to be submitted for publication.
(7 preprints appended to this Report)

179. Annual Report 1976 - 1977. A Bibliography of Titles and Reports of Research Accomplished or in Progress (Incomplete Work) for the period 1976 - 1977 of Research Contract No. EY-76-S-05-3018.
(7 copies submitted to the Energy Research and Development Administration--Division of Biomedical and Environmental Research--Physics and Technological Program on August 15, 1977)

180. Three Year Comprehensive Report 1974 - 1977. A Bibliography of Titles Submitted in 1974 - 1977. A Brief Resume of Principal Results Obtained during the Years 1974 - 1977, with Comments Relating to the Importance of these Results, Opinion of Principal Investigator Concerning Research Performed under Contract No. EY-76-S-05-3018, Expenditure Statement, and Report on Equipment Purchased and/or Fabricated during the Period 1974 - 1977 of the Research Contract No. EY-76-S-05-3018.
(7 copies submitted to the Energy Research and Development Administration--Division of Biomedical and Environmental Research--Physics and Technological Program on August 15, 1977)

(i) Comments

The bibliography of titles consists of fifty (50) titles. These may be divided as follows:

Articles:	Published	21
	Accepted for Publication	7
	Submitted for Publication	7
	Ready for Publication	6
	SUB-TOTAL	41
Ph.D. Dissertations		5
Reports to the Energy Research and Development Administration		4
	TOTAL	50

Two of the published articles (No's. 171 and 175) are not of a research nature. They represent my personal effort, on behalf of LSU, to increase concern for, and funding of research, pure and applied, by the State of Louisiana. However, since these articles were informed and instigated by my experiences with ERDA, and since it is my funding and publications rec :d with ERDA which led to my choice as the University spokesman, I believe these articles represent a most signif-icant ERDA impact on this State --- and it is for that reason that I include them. I might add that these articles are now instituted as Board of Supervisors' policy, and that the Legislature, via increased funding, does appear to have paid attention.

Disregarding Ph.D. Dissertations and Reports, the average cost per publication was ∿$7,000.00. This figure takes no account of the

extent to which grant expenditures contributed to the training and education of the persons employed on ERDA monies. A good appreciation of the training/educational commitment, including the present activities of the persons so employed, may be obtained by consulting the listing under Departing Personnel.

Nor do the figures take any account of the extent to which grant expenditures contributed to the caliber of the Undergraduate Programs in this Department. This contribution was so pervasive, yet so ill defined, that it cannot be categorized. However, such effects did occur and they were important.

B. SYMPOSIA ATTENDED

1974 - 1977

(i) INVITED PAPERS

1. Second Annual Symposium on Molecular Electronic Structure and Spectroscopy, Louisiana State University, Baton Rouge, Louisiana, May 21-22, 1974.

   a. S. P. McGlynn, "Electronic States of Inorganic Ions and Molecules."

   --Invited Lecture

   b. S. P. McGlynn, "Electronic Spectroscopy of α-Dicarbonyls, Carbonyls and Amides."

   --Invited Lecture

   c. S. P. McGlynn, "Electronic Spectroscopy of Polar Molecules."

   --Invited Lecture

2. S. P. McGlynn, "The Colors of Post Transition Metal Salts," Eastman Kodak Company, Rochester, New Jersey, June 24, 1974.

   --Invited Lecture

3. S. P. McGlynn, "On the Assignment of Molecular Rydberg States. Rare Gases and Halides," The University of Pittsburgh, Pittsburgh, Penn., June 25, 1974.

   --Invited Lecture

4. S. P. McGlynn, "On the Assignment of Molecular Rydberg States. Rare Gases and Halides," IVth International Conference on Vacuum Ultraviolet Radiation Physics, Hamburg, Germany, July 22-26, 1974.

   --Invited Lecture

5. S. P. McGlynn, "The Excitement of Science," The Louisiana Teachers Association, Monroe, Louisiana, November 25-27, 1974.

   --Invited Lecture

6. S. P. McGlynn, "Virtual Atomic Orbitals in Molecules," 7th Annual Mardi Gras Symposium in Theoretical Chemistry, Tulane University, New Orleans, Louisiana, February 7, 1975.

   --Invited Lecture

7. S. P. McGlynn, "Rydberg Orbitals," University of South Florida, Tampa, Florida, April 10, 1975.

--Invited Lecture

8. S. P. McGlynn, "The Colors of Post Transition Metal Salts," Baton Rouge Chapter of Sigma Xi, Baton Rouge, Louisiana, May 1, 1975.

--Invited Lecture

9. S. P. McGlynn, "Excited Electronic States of α-, β-, and γ-Dicarbonyls," VIII international Conference on Photochemistry, The University of Alberta, Alberta, Edmonton, Canada, August 7-12, 1975.

--Invited Lecture

10. S. P. McGlynn, "Analytical Applications of Fluorescence, "The Louisiana State University, Baton Rouge, Louisiana, October 1, 1975.

--Invited Lecture

11. The 27th Southeast-31st Southwest Combined Regional Meeting of The American Chemical Society, Memphis, Tennessee, October 29-31, 1975.

S. P. McGlynn, "Photoelectron Band Assignments in Monocarbonyls and α-Dicarbonyls."

--Invited Lecture

S. P. McGlynn, "Photoelectron Spectra of Urea and Uracils."

--Invited Lecture

S. P. McGlynn, "Photoelectron Spectra of Benzoic Acid and Related Molecules."

--Invited Lecture

12. S. P. McGlynn, "Molecular Rydberg States," The Florida State University, Tallahassee, Florida, November 14, 1975.

--Invited Lecture

13. S. P. McGlynn, "The Excitement of Science," Omicron Delta Kappa National Leadership Honorary, The Florida State University, Tallahassee, Florida, November 15, 1975.

--Invited Lecture

14. S. P. McGlynn, "The Color of Inorganic Ions," Michael Kasha Symposium on Energy Transfer in Organic, Inorganic, and Biological Systems, The Florida State University, Tallahassee, Florida, January 8-10, 1976.

--Invited Lecture

15. S. P. McGlynn, "Colors of Simple Polyatomic Anions," The University of Miami, Miami, Florida, January 12, 1976.

--Invited Lecture

16. S. P. McGlynn, "The Price of Precision," Planetarium Chamber, Louisiana Arts and Sciences Center, Baton Rouge, Louisiana, February 4, 1976.

--Invited Lecture

17. S. P. McGlynn, "The Need for Work," Louisiana State University Alumni Federation Scholars Program, Louisiana State University, Baton Rouge, Louisiana, February 10, 1976.

--Invited Lecture

18. S. P. McGlynn, "Molecular Rydberg Transitions," Department of Chemistry, The University of Houston, Houston, Texas, March 19, 1976.

--Invited Lecture

19. S. P. McGlynn, "A Window on the Future," O. Perry Walker Senior High School, New Orleans, Louisiana, May 20, 1976.

---Invited Lecture

20. S. P. McGlynn, "Molecular Rydberg States," Department of Chemistry, The University of Maine, Orono, Maine, August 6, 1976.

---Invited Lecture

21. S. P. McGlynn, "The Vacuum Ultraviolet Spectrum of Water," NATO Institute on "High-Energy Chemical Spectroscopy and Photochemistry," Breukelen, Holland, August 11, 1976.

---Invited Lecture

22. S. P. McGlynn, "Regularities in Rydberg Spectra," NATO Institute on "High-Energy Chemical Spectroscopy and Photochemistry," Breukelen, Holland, August 16, 1976.

---Invited Lecture

23. NATO Institute on "High-Energy Chemical Spectroscopy and Photochemistry," Breukelen, Holland, August 17, 1976.

---Session Chairman

24. S. P. McGlynn, "Report to the Board of Regents on Doctoral Program in Chemistry at Louisiana State University," Baton Rouge, Louisiana, October 19, 1976.

---Invited Lecture

25. S. P. McGlynn, "The Relevance of Science," Baton Rouge Chapter of Sigma Xi, Baton Rouge, Louisiana, March 31, 1977.

---Invited Lecture

26. S. P. McGlynn, "Electron Spectroscopy," Department of Chemistry, The University of Texas at San Antonio, San Antonio, Texas, April 1, 1977.

---Invited Lecture

27. S. P. McGlynn, "Atomic and Molecular Rydberg States," Department of Chemistry, The University of Texas at El Paso, El Paso, Texas, April 4, 1977.

---Invited Lecture

28. S. P. McGlynn, "A Little History," Coates Awards Banquet of the Baton Rouge Section of The American Chemical Society, Baton Rouge, Louisiana, April 28, 1977.

---Invited Lecture

29. S. P. McGlynn, "A Public Forum on Financing Higher Education in Louisiana," State of Louisiana Board of Regents, Baton Rouge, Louisiana, May 6, 1977.

---Invited Lecture

30. S. P. McGlynn, "Research Options in Chemical Physics and Biophysics," Department of Physics, Southern University, Baton Rouge, Louisiana, May 10, 1977.

31. S. P. McGlynn, "The UPS of Biological Materials," 1st Southwest Electron Spectroscopy Users Meeting, Texas A&M University, College Station, Texas, June 3, 1977.

---Invited Lecture

32. Special Lecturers Series, Department of Chemistry, North Texas State University, Denton, Texas, July 5-8, 1977.

S. P. McGlynn, "The Orbital Concept in Chemistry"

S. P. McGlynn, "The Colors of Post-transition Metal Salts"

S. P. McGlynn, "Codon-Amino Acid Mappings"

S. P. McGlynn, "Photoelectron Spectroscopy"

S. P. McGlynn, "Rydberg States of Atoms and Molecules"

---Invited Lectures

33. S. P. McGlynn, "The Role of Chemistry in Engineering," Department of Engineering, Louisiana State University, Baton Rouge, Louisiana, July 19, 1977.

---Invited Lecture

34. S. P. McGlynn, H. -t. Wang, G. L. Findley, W. S. Felps and A. R. P. Rau, "Quantum Defect Analogies between Molecules and Rare Gases," Vth International Conference on Vacuum Ultraviolet Radiation Physics, Montpellier, France, September 5-9, 1977.

---Invited Lecture

35. S. P. McGlynn and John D. Scott, "Field Effects in the Vacuum Ultraviolet," Synchrotron Radiation Instrumentation and Developments, Orsay, France, September 12-14, 1977.

--- Invited Lecture

36. S. P. McGlynn and D. Dougherty, "Photoelectron Spectroscopy in Biology," XIIIth European Congress on Molecular Spectroscopy, Wroclaw, Poland, September 12-16, 1977.

--- Invited Lecture

(ii) SUBMITTED PAPERS

1. The 31st Symposium on Molecular Spectroscopy, The Ohio State University, Columbus, Ohio, June 14-18, 1976.

   John D. Scott, W. S. Felps and S. P. McGlynn, "MCD Spectra of Methyl Iodide and Hydrogen Iodide in the Vacuum Ultraviolet."

   Hung-tai Wang and S. P. McGlynn, "A Correlative Study of Atomic and Molecular Rydberg States."

   Hung-tai Wang, W. S. Felps and S. P. McGlynn, "The Electronic Structure of H_2O."

2. The 32nd Annual Southwest Regional Meeting of The American Chemical Society, Ft. Worth, Texas, December, 1976.

   D. R. Dougherty and S. P. McGlynn, "The Photoelectron Spectroscopy of Carbonyls: 1,4-Benzoquinones."

   John D. Scott, W. S. Felps and S. P. McGlynn, "Vacuum Ultraviolet MCD Spectrum Associated with the First s Rydberg Transitions in Methyl Iodide."

   W. S. Felps, John D. Scott and S. P. McGlynn, "The Vacuum Ultraviolet Absorption and MCD Spectra Associated with Transitions to the Lowest-Energy p-Type Rydberg States of Methyl Iodide."

   Thomas P. Carsey. G. L. Findley and S. P. McGlynn, "The Absorption and Emission Characteristics of Highly Polar Aromatic Molecules."

   G. L. Findley, K. Wittel, W. S. Felps and S. P. McGlynn, "Intermediate-Coupling Model for Linear Molecules."

   S. Chattopadhyay, P. Hochmann and S. P. McGlynn, "Atomic Correlation Lines."

3. The 32nd Symposium on Molecular Spectroscopy, The Ohio State University, Columbus, Ohio, June 13-17, 1977.

   John D. Scott, W. S. Felps and S. P. McGlynn, "Vibronic Coupling in the First s Rydberg States of Methyl Iodide."

   Hung-tai Wang, W. S. Felps, G. L. Findley and S. P. McGlynn, "Quantum Defect Analogies between Rydberg States of Molecules and Rare Gases."

   G. L. Findley, W. S. Felps and S. P. McGlynn, "The Geometry of Ethylene in the R_{1s} State."

C. LABORATORY GUESTS

(i) 1975 - 1976

1. Professor Hans Bock
   Chemische Institute der Universität
   6 Frankfurt/Main 70
   Theodor Stern Kai 7
   West Germany
   May, 1975

2. Professor J. Wayne Rabalais
   Department of Chemistry
   University of Houston
   Houston, Texas 77004
   June, 1975

3. Dr. Haim Levanon
   Department of Physical Chemistry
   The Hebrew University of Jerusalem
   Jerusalem, Israel
   July, 1975

4. Dr. Fred Watson
   Department of Chemistry
   University of Arkansas
   Little Rock, Arkansas
   November, 1975

5. Dr. Loucas G. Christophorou
   Oak Ridge National Laboratory
   Post Office Box X
   Oak Ridge, Tennessee 37830
   February, 1976

6. Professor B. V. McKoy
   Department of Chemistry
   California Institute of Technology
   Pasadena, California
   March, 1976

7. Mr. T. Overton
   Deputy Director SCRDE
   Ministry of Defense
   Flagstaff Road
   Colchester Essex
   England
   April, 1976

8. Professor L. Vanquickenborne
Université Te Leuven
Department Scheikunde
Delestijnenlaan 200F
3030 Heverlee
Belgium
April, 1976

9. Professor L. Klasinc
Institut Ruder Boskovic
41001 Za b
Yugoslavia
Bijenecka cesta 54
Post pretinac 1016
April, 1976

(ii) 1976 - 1977

1. Professor K. Kamura
   Research Institute of Applied Electricity
   Hokkaido University
   Sapporo, Japan
   July, 1976

2. Professor O. Keller
   Royal V and M University
   Copenhagen, Denmark
   February, 1977

3. Professor D. S. McClure
   Department of Chemistry
   Princeton University
   Princeton, NJ
   February, 1977

4. Professor Michael Kasha
   Institute of Molecular Biophysics
   Florida State University
   Tallahassee, FL
   March, 1977

5. Professor Fred Watson
   Department of Chemistry
   University of Arkansas at Little Rock
   Little Rock, Arkansas
   March, 1977

6. Professor B. R. Russell
   Department of Chemistry
   North Texas State University
   Denton, Texas
   March, 1977

7. Professor Willard F. Libby
   Department of Chemistry
   University of California
   Los Angeles, California
   March, 1977

8. Professor Eugene P. Wigner
   Department of Physics
   Princeton University
   Princeton, NJ
   March, 1977

9. Professor Petr Hochmann
College of Sciences and Mathematics
The University of Texas at San Antonio
San Antonio, Texas
March, 1977

10. Professor James Meeks
Department of Chemistry
Cumberland College
Williamsberg, KY
March, 1977

11. Professor B. S. Thyagarajan
College of Sciences and Mathematics
The University of Texas at San Antonio
San Antonio, Texas
March, 1977

12. Professor Haven Aldrich
St Mary's Dominican College
New Orleans, LA
(7 days, at various times during March and April, 1977)

13. Professor Boris Dzhagarov
UNESCO Fellow
Institute of Physics
Byelorussian Academy of Sciences
Minsk, USSR
March - December, 1977

14. Professor Suheil Abdulner
Department of Chemistry
University of New Orleans
New Orleans, LA
(4 days during January - July, 1977)

15. Professor G. Guilbeau
Department of Chemistry
University of New Orleans
New Orleans, LA
(3 days during January - July, 1977)

16. Professor Kurt Schaffner
Director, Institüt für Strahlenchemie
Max-Plank Institut
Mülheim-Ruhr, Germany
April, 1977

17. Professor Rama Mohanty
New York Institute for Advanced Studies
Auburn, NY
and
Southern University
Baton Rouge, LA
(3 days during June and July, 1977)

18. Professor V. A. Kuzmin
Institute of Chemical Physics
Moscow, USSR
July 24 - 25, 1977

D. IN-HOUSE SYMPOSIA

(i) 1974 - 1975

The following four pages are the program for the 3rd Annual Symposium on Molecular Electronic Structure and Spectroscopy. This symposium is organized by members of Professor McGlynn's research group and participation is limited to members of this research group.

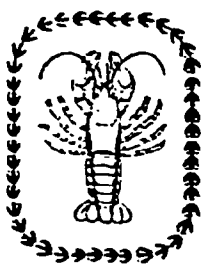

3rd ANNUAL

SYMPOSIUM ON MOLECULAR ELECTRONIC STRUCTURE & SPECTROSCOPY

UNION BUILDING
LOUISIANA STATE UNIVERSITY
BATON ROUGE, LOUISIANA

May 14 - 15, 1975

3rd ANNUAL

SYMPOSIUM ON MOLECULAR ELECTRONIC

STRUCTURE & SPECTROSCOPY

PARTICIPANTS*

Sean P. McGlynn,
Boyd Professor of Chemistry

R. Henry, Professor of Physics

P. Brint, Postdoctoral Fellow

W. S. Felps, Postdoctoral Fellow

P. Hochmann, Postdoctoral Fellow

K. Wittel, Postdoctoral Fellow

T. Carsey, Graduate Student

S. Chattopadhyay, Graduate Student

H.-t. Wang, Graduate Student

*All participants are associated with
Louisiana State University at Baton Rouge

WEDNESDAY

International A Room

Anne Wahlborg, Chairperson

9:00 - 9:05 S. P. McGlynn, OPENING REMARKS

MOLECULAR RYDBERG SPECTRA (I)

9:05 - 10:00 W. S. Felps, "Lowest Energy-Rydberg transitions of s-Type in CH_3X"

10:00 - 10:15 Break

10:15 - 11:15 H.-t. Wang, "Some Aspects of Rydberg Transitions"

11:15 - 12:15 P. Hochmann, "Model for the Interatomic and Intermolecular Correlations of Rydberg Term Values"

12:15 - 1:15 Lunch , Dining Room A

PHOTOELECTRON AND ABSORPTION SPECTRA

1:15 - 2:15 K. Wittel, "Spin-Orbit Coupling in Photoelectron Spectroscopy"

2:15 - 2:30 Break

2:30 - 3:30 P. Brint, "n-Type Molecular Orbitals of Dicarbonyl Compounds"

* * * *

THURSDAY

Red River Room

Anne Wahlborg, Chairperson

MOLECULAR RYDBERG SPECTRA (II)

9:00 -10:00 W. S. Felps, "Lowest Energy Rydberg Transitions of p-Type in CH_3X"

10:00 - 10:15 Break

10:15 - 10:45 P. Brint, "A Two-Chromophore Model for the Rydberg Spectrum of TMCBD"

10:45 - 11:15 S. Chattopadhyay, "A Correlative Approach to Rydberg Transitions in Atoms"

QUANTUM CHEMISTRY

11:15 - 12:15 R. Henry, "Use of the Variation Principle for Matrix Element of Hamiltonian"

12:15 - 1:15 Lunch, Dining Room A

HIGHLY-POLAR AROMATICS

1:15 - 2:00 T. Carsey, "Advances in the Spectroscopy of Highly Polar Aromatics"

CONCLUSION

2:00 - 2:15 General Discussion

* * * *

(ii) 1975 - 1976

The following five pages are the program for the 4th Annual Symposium on Molecular Electronic Structure and Spectroscopy. This symposium is organized by members of Professor McGlynn's research group and participation is limited to members of this research group.

4th ANNUAL

SYMPOSIUM ON MOLECULAR ELECTRONIC

STRUCTURE AND SPECTROSCOPY

VIEUX CARRÉ ROOM

UNION BUILDING

LOUISIANA STATE UNIVERSITY

BATON ROUGE, LOUISIANA

May 13 & 14, 1976

4th ANNUAL

SYMPOSIUM ON MOLECULAR ELECTRONIC

STRUCTURE AND SPECTROSCOPY

Hung -tai Wang - Director

PARTICIPANTS*

Seán P. McGlynn,
Boyd Professor of Chemistry

Thomas P. Carsey,
Graduate Student

Swapan Chattopadhyay,
Graduate Student

David Dougherty,
Graduate Student

Sid Felps,
Postdoctoral Fellow

Gary Findley,
Graduate Student

John Scott,
Postdoctoral Fellow

Hung -tai Wang,
Graduate Student

Klaus Wittel,
Postdoctoral Fellow

*All participants are associated with LSU-BR Department of Chemistry.

THURSDAY MORNING - SID FELPS, CHAIRMAN

9:00 - 9:10 S. P. McGlynn, "Opening Remarks"

MOLECULAR RYDBERG SPECTROSCOPY

9:10 - 10:10 Klaus Wittel, "Perspective in Rydberg Spectroscopy"

10:10 - 10:40 Hung -tai Wang, "Atomic and Molecular Rydberg States: A Correlation Approach"

10:40 - 11:00 Break

11:00 - 12:00 Swapan Chattopadhyay, "A Correlative Approach as Applied to Atomic Rydberg Transitions"

12:00 - 1:15 Lunch

THURSDAY AFTERNOON - SWAPAN CHATTOPADHYAY, CHAIRMAN

PHOTOELECTRON SPECTROSCOPY

1:15 - 2:15 David Dougherty, "The Photoelectron Spectroscopy of Carbonyls"

ELECTRONIC STRUCTURE AND SPECTROSCOPY

OF HIGHLY-POLAR MOLECULES

2:15 - 3:00 Gary Findley, "Luminescence Characteristics of Donor-Aromatic-Acceptor Molecules"

3:00 - 3:15 Break

SPECTROSCOPY OF INORGANIC MOLECULES

3:15 - 4:00 Thomas Carsey, "Singlet → Triplet Transitions in Metal-Anion Complexes"

FRIDAY MORNING - THOMAS CARSEY, CHAIRMAN

MOLECULAR RYDBERG SPECTROSCOPY

9:00 - 9:30 Hung -tai Wang, "The Electronic Structure of the Water Molecule"

9:30 - 10:00 Sid Felps, "Rydberg States of the Methyl Halides"

MAGNETIC CIRCULAR DICHROISM IN THE VACUUM ULTRAVIOLET

10:00 - 11:00 John Scott, "Theory of Magnetic Circular Dichroism"

11:00 - 11:15 Break

11:15 - 11:40 Sid Felps and John Scott, "MCD Spectroscopy of Methyl Iodide"

11:40 - 12:10 Klaus Wittel, "Intermediate Coupling Calculations for Linear Molecules"

12:10 - 1:30 Lunch

FRIDAY AFTERNOON

1:30 - Informal Discussion

(iii) 1976 - 1977

The following six pages are the program for the 5th Annual Symposium on Molecular Electronic Structure and Spectroscopy. This symposium is organized by members of Professor McGlynn's research group and participation is limited to members of this research group.

5th ANNUAL

SYMPOSIUM ON MOLECULAR ELECTRONIC

STRUCTURE AND SPECTROSCOPY

RED RIVER ROOM

UNION BUILDING

LOUISIANA STATE UNIVERSITY

BATON ROUGE, LOUISIANA

May 26 & 27, 1977

5th ANNUAL

SYMPOSIUM ON MOLECULAR ELECTRONIC

STRUCTURE AND SPECTROSCOPY

David Dougherty - Director

PARTICIPANTS*

Seán P. McGlynn,
Boyd Professor of Chemistry

David Bouler, Graduate Student

Thomas P. Carsey, Postdoctoral Fellow

Swapan Chattopadhyay,
Graduate Student

David Dougherty,
Postdoctoral Fellow

Sidney Felps,
Postdoctoral Fellow

Gary Findley,
Graduate Student

Terrence L. Mathers,
Graduate Student

John Scott,
Postdoctoral Fellow

*All participants are associated with LSU-BR Department of Chemistry

THURSDAY MORNING - JOHN SCOTT, CHAIRMAN

9:00 - 9:10 S. P. McGlynn, "Opening Remarks"

PHOTOELECTRON SPECTROSCOPY

9:10 - 10:10 David Dougherty, "The Photoelectron Spectroscopy of Dicarbonyls"

HYDROGEN BONDING

10:10 - 10:30 David Bouler, "Theory of Hydrogen Bonding"

10:30 - 10:50 Break

ALGEBRAIC METHODS IN MOLECULAR GENETICS

10:50 - 11:50 Gary Findley, "A Group Theoretic Analysis of the Genetic Code"

11:50 - 1:00 Lunch, Dining Room A

THURDAY AFTERNOON - SIDNEY FELPS, CHAIRMAN

ELECTRONIC STRUCTURE AND SPECTROSCOPY

1:00 - 1:20 Thomas Carsey, "Selected Highly Polar Molecules: Polarization Studies"

1:20 - 1:50 Terrence Mathers, "The Triplet State of Water"

ATOMIC RYDBERG SPECTROSCOPY

1:50 - 2:30 Swapan Chattopadhyay, "A Correlative Approach as Applied to Rydberg Transitions in Closed Shell Atoms"

2:30 - 2:50 Break

FIELD EFFECT SPECTROSCOPY

2:50 - 3:50 John Scott, "Field Effect Spectroscopy in the Vacuum Ultraviolet"

FRIDAY MORNING - THOMAS CARSEY, CHAIRMAN

MOLECULAR RYDBERG SPECTROSCOPY

9:00 - 10:00 Sidney Felps, "The Electronic Structure of cis-Dibromoethylene"

10:00 - 10:40 Swapan Chattopadhyay, "Rydberg Transitions in Open Shell Atoms and Molecules"

10:40 - 11:00 Break

11:00 - 11:30 Gary Findley, "Qualitative Analysis of Rydberg Potentials via the Phase Amplitude Method"

11:30 - 11:50 John Scott, "Vibronic Coupling in the First s-Rydberg State of Methyl Iodide"

11:50 - 1:00 Lunch, Dining Room A

FRIDAY AFTERNOON - TERRENCE MATHERS, CHAIRMAN

MOLECULAR RYDBERG SPECTROSCOPY

1:00 - 1:30 Sidney Felps, "The Lowest Energy p- and d-Rydberg States of Methyl Iodide"

1:30 - INFORMAL DISCUSSION

E. PERSONNEL DEPARTING LABORATORY

1974 - 1977

(i) Postdoctoral Fellows

Hochmann, P.	1970 - 1975	Assistant Professor College of Mathematics & Physics University of Texas at San Antonio San Antonio, Texas
Brint, P.	1973 - 1975	Research Scientist Department of Physics Schuster Laboratories The University Manchester M13 9PL England
Wittel, K.	1975 - 1976	Privat-Docent Chemische Institute der Universitat 6 Frankfurt/Main 70 Theodor Stern Kai 7 West Germany

(ii) Graduate Students

Wang, H. -t.	1970 - 1976	Post-Doctoral Fellow Department of Physics University of Chicago Chicago, Illinois
Carsey, T. P.	1972 - 1977	Instructor Department of Chemistry University of New Orleans New Orleans, Louisiana

F. EQUIPMENT PURCHASED AND/OR FABRICATED

(i) 1974 - 1975

1. Photoelastic effect light modulator with split-head option for vacuum operation . . . . . $ 2,685.85

(ii) 1975 - 1976

The equipment budget for this year was re-budgeted into supplies and salaries (see letter to A. H. Frost, Jr., April 29, 1976). This re-budgeting was requested because our replacement costs far surpassed our initial estimate and because Louisiana State University was able to purchase for us the equipment originally requested (see iii). Some of our replacement costs are itemized below:

Slave multimeter	$ 311.12
Diffusion pump heater	37.85
Thermocouple gauge	71.82
Parts for Hinteregger Lamp	718.91
Replacement Grating	3,744.05
Heated probe for PES	517.75
Dewar, graded seals	450.57
VUV windows	467.64
Optical flats	169.60
LiF windows	368.70
UV cells	666.41
Quartz discs	36.46
Total	$ 7,560.88

(iii) 1976 - 1977

Equipment Purchased by ERDA

1. EMI:

9635-QB: 2 matched photomultipliers, spectrosil, 50mm cathode.	$ 957.90
G-26E315: Solar Blind photomultiplier CsI cathode	1086.65
RFI/B-215FV: Photomultiplier housing, vacuum operation	339.90

2. A. H. Thomas Co.:

Sodium Press	257.72
Heating Mantle	36.86

3. Varian Ass.:

Ultrasonic cleaner	159.65

4. Plant Stores:

2 2-stage gas regulators	79.18

5. EMI Gencom:

0-5KV regulated power supply	396.55

Equipment Fabricated

1. Magnetic Circular Dichroism System (Sample cell; optics box for precision alignment of mirrors, prisms and photoelastic modulator; goniometer heads: all in high vacuum)	NC
2. Electric Linear Dichroism System (Sample cell; field plates, plate holders, HV feed through system: all in high vacuum)	NC
3. Electrometer: 10^{-3}-10^{-8} amps, 0 - 100KHz	NC
4. Wavelength to wavenumber converter	NC
5. Differentiator (1st) of a time-varying signal	NC
6. Differentiator (2nd) of a time-varying signal	NC
7. Integrator	NC
8. Programmer to maintain maximum retardation angle	NC
9. Logarithmic Amplifier	NC

EQUIPMENT PURCHASED BY LSU

1.	Superconducting magnet/He dewar system (Liquid level monitor & control; power supply; and flexible transfer line)	$20,000.00
2.	Datametrics Capacitance Manometer	4,200.00
3.	1m VUV monochromator (McPherson)	24,000.00
4.	Chromatix dye laser system	26,000.00
5.	I-beam, trolley plus block and tackle	500.00

III. VACUUM ULTRAVIOLET (VUV) STUDIES

III. VACUUM ULTRAVIOLET (VUV) STUDIES

The items of Section II.A which refer to VUV studies are:

132, 142, 144, 147, 148, 152, 154, 158, 160, 161, 162
163, 164, 169, 172, 173, 176, 177

The work performed is diverse. Hence, we will attempt a brief summary of all of it, but will report in slight detail on some of the more trenchant parts.

A. THE CORRELATION OF RYDBERG TERM VALUES AND IONIZATION POTENTIALS

The Rydberg equation is inadequate to the task of assigning low-energy Rydberg transitions. Furthermore, its use for high-energy Rydberg transitions is often questionable and usually in need of substantiation. The thrust of our work has been the development of different assignment criteria, ones which invoke the chemical relatedness or homology of molecular species.

The term values of Rydberg states correlate linearly with ionization potentials. The form of the correlation is

$$T(\mu,\tilde{\alpha},n) = a_{\alpha n} I_{\mu} + b_{\alpha n} \qquad \ldots 1$$

The symbol $T(\mu,\tilde{\alpha},n)$ denotes the actual term value of the nth lowest-energy Rydberg state of α type and is to be distinguished from $T(\mu,\alpha,n)$ which, with respect to a model to be specified later (vide infra), is the theoretical one-electron component of $T(\mu,\tilde{\alpha},n)$; α is a symmetry label or some other appropriate designation for the Rydberg state in question; and μ denotes the cationic core on which the states $(\mu,\tilde{\alpha},n)$, n variable, converge as $n \to \infty$. The ionization potential I_{μ} is the energy difference between the μth cationic state and the ground state of the neutral species. In line with the definition of $T(\mu,\alpha,n)$, the subscript α in the slopes $a_{\alpha n}$ and in the intercepts $b_{\alpha n}$ can be supposed to be the symmetry representation of the terminal orbital of the Rydberg absorption process.

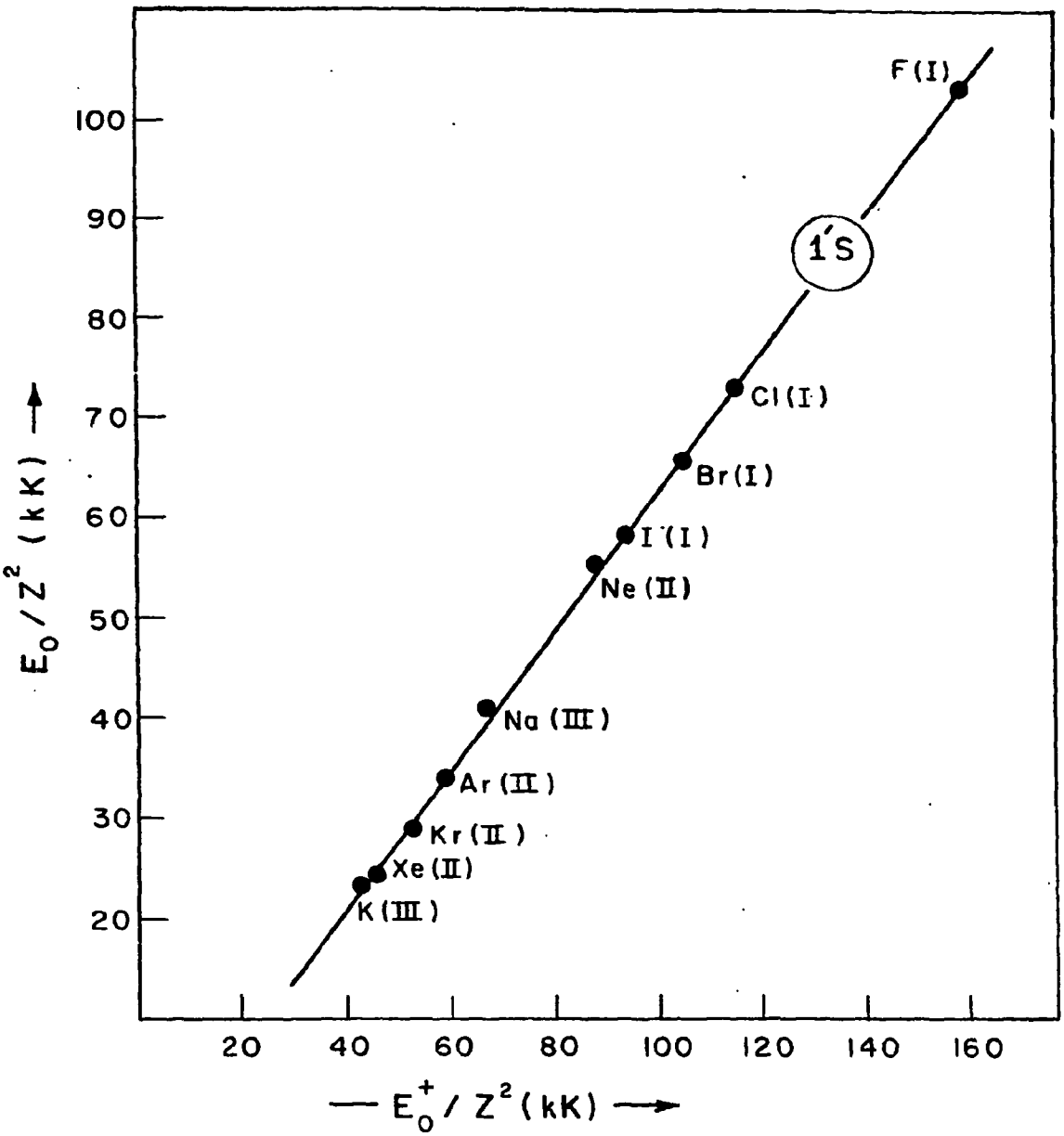

Figure 1. A plot of configuration energies E_0/Z^2 <u>versus</u> ionization energies E_0^+/Z^2 for the halogen group.

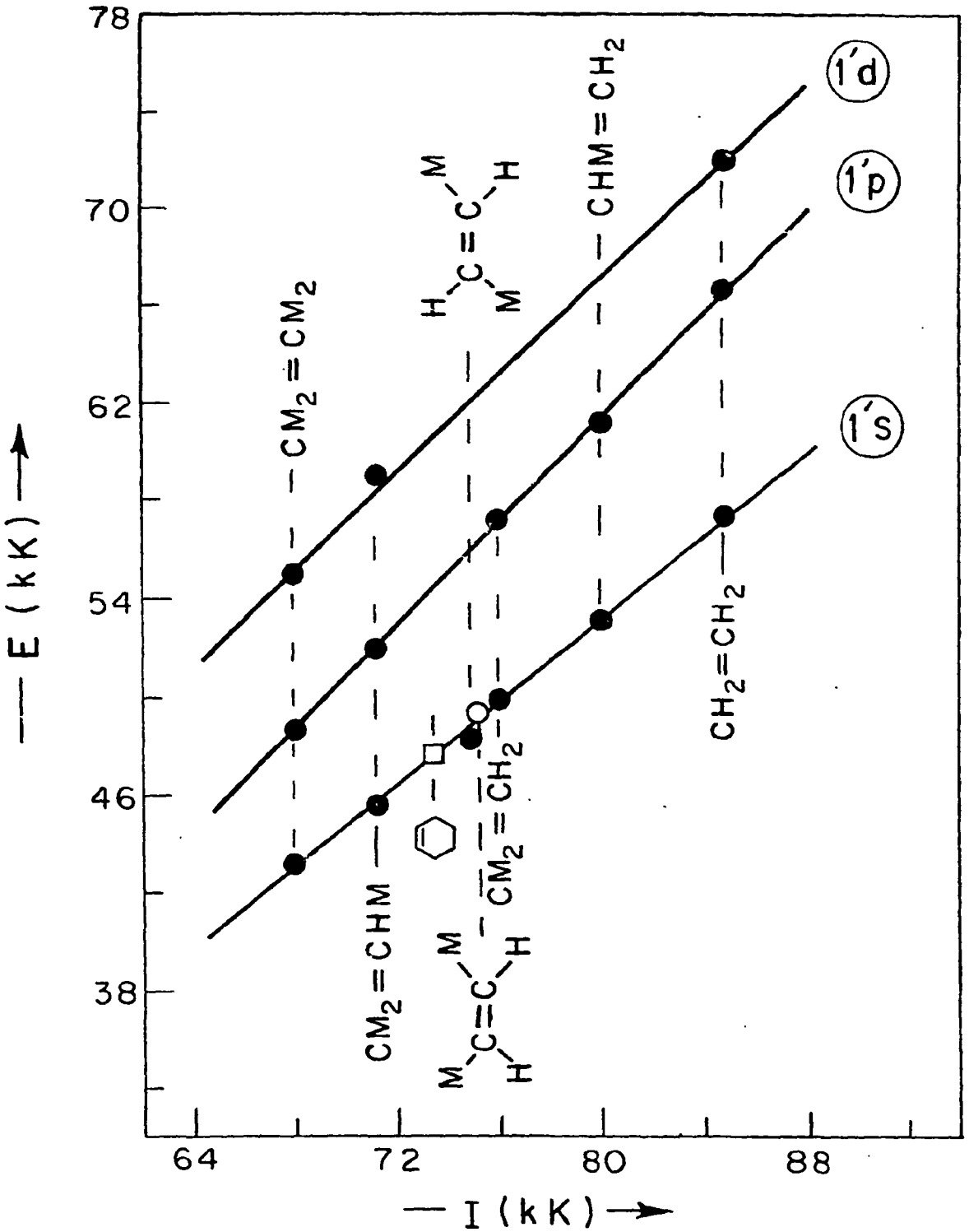

Figure 2. Correlation lines for the methylated ethylenes. M denotes the methyl group, $-CH_3$.

The correlations of Eq. 1 are purely empirical. (See items 142, 148, 163 and 164). Furthermore, these correlations are valid only within certain groups of atoms (and molecules). These groups, if atomic, lie within columns of the periodic table and, if molecular, contain fixed substituents and chromophores which lie within columns of the periodic table. Examples are given in Figures 1 and 2.

The least-squares values of the parameters $a_{\alpha n}$ and $b_{\alpha n}$ display regular intra-group behavior, and exhibit regular variations from one group to another. They contain information about the interactions of the excited optical electron with the atomic and/or molecular cores.

The major assumptions of the model which leads to the correlative algorithm are:

---The gross interatomic and intermolecular variations of Rydberg term values are reflected in a one-electron model. The appropriate one-electron Hamiltonian need only account for the Coulomb interactions of the optical electron with a rigid atomic or molecular core. The core charge density can be identified as that of the μth parental cationic state.

---A molecule XS is partitioned into two parts: A substituent part S and a Rydberg chromophoric part X. In methyl iodide, CH_3I, for example, we have S = CH_3 and X = I. The term values are assumed to be dominated by the interactions of the optical electron with the chromophoric segment X. The substituent segment S is assumed to produce effects of secondary importance. Consequently, the core charge distribution, and the core potential to which it gives rise, can be divided into a chromophoric part and a substituent part. This set of assumptions is required only for molecules.

---The charge distributions, whether associated with the chromophoric or substituent parts of the core, can be expanded in ways which reflect the major variations of the core potential caused by changes in the structure

of the chromophore and/or the substituent. The possibility of such an expansion is confined, at least initially, to atomic (or molecular) species which belong to the same group.

As is shown in items 163 and 164, the first- and second-order solutions of the Hamiltonian eigen equation which are constructed within this set of assumptions yield a variety of correlative algorithms for Rydberg term values, and among them is Eq. 1.

We denote by $T(XS,\mu,\alpha,n)$ the one-electron component of the term value $T(XS,\mu,\tilde{\alpha},n)$ of a Rydberg excited state of the species XS. We assume that $-T(XS,\mu,\alpha,n)$ is a discrete eigenvalue of the one-electron, spin-less Hamiltonian $\hat{H}(r;XS,\mu)$

$$\{\hat{H}(r;XS,\mu) + T(XS,\mu,\alpha,n)\}\varphi(r;XS,\mu,\alpha,n) = 0 \qquad ...2$$

where φ represents the orbital which is terminal to the Rydberg excitation in question. The Hamiltonian $\hat{H}$ takes account only of the coulombic interactions between the rigid core XS^+ and the optical electron. Consequently, the potential energy part of $\hat{H}$, $V(r;XS,\mu)$, is represented by

$$V(r;XS,\mu) = e^2\int dr'\rho(r';XS,\mu)|r'-r|^{-1} \qquad ...3$$

where $\rho(r;XS,\mu)$ is the charge density of the XS^+ core. It is also assumed that the density ρ is identical to that of the μth state of the cation XS^+.

It is convenient to take explicit account of the electronic and nuclear contributions to the density ρ, namely

$$\rho(r;XS,\mu) = N\Gamma(r;XS,\mu) - \sum_{\omega=1}^{K} Z_\omega \delta(r-R_\omega) \qquad ...4$$

In this expression, $\Gamma(r;XS,\mu)$ is the electron density; N is the number of electrons in the XS^+ core; Z_ω and R_ω, $\omega=1,...,K$, denote the atomic number

and position vector of the ωth nucleus; and $\delta(r-R_\omega)$ is the Dirac delta function. From the normalization of $\Gamma(r;XS,\mu)$ to unity, it follows that

$$\int dr\ \rho(r;XS,\mu) = N - \sum_{\omega=1}^{K} Z_\omega \equiv -Z \qquad \ldots 4$$

where $Z = 1,2,3,\ldots$ is the total charge of the XS^+ core.

Much of the theoretical development rests on the partitioning of the core densities Γ and ρ into chromophoric and substituent parts, and the use of this partitioning to separate the core Hamiltonian $\hat{H}(r;X/S,\mu)$ into X and S components. This effort has been successful.

(i) SIGNIFICANCE

The Rydberg equation is valid near the ionization limit and it is in this region (i.e., high n) that it is of greatest use as an assignment device. The correlative algorithm developed empirically and deduced theoretically in this work is of greatest value at low n, where the Rydberg equation is unsatisfactory. Consequently, it is not only a new assignment device -- it is an assignment device for a region in which no satisfactory criteria previously existed.

The development of a model which rationalizes the observed correlative dependencies implies a considerable understanding of core/Rydberg and chromophore/substituent separability criteria. These, in turn, lead to a knowledge of Rydberg potentials, and ways to represent them in model potential form. Thus, this work has immense importance and represents, in our opinion, the initial probings which will surely lead to other assignment tactics; ways to extract information on chromophore-substituent interactions and Rydberg-core interpretation; and the development of new, improved models.

B. QUANTUM DEFECT ANALOGIES (See items 169 and 173)

The s and d Rydberg series of Xe, HI and CH_3I have been measured in the autoionization region. The spectra are so similar that direct comparison of

the molecular spectra with the rare gas spectrum leads to the assignment of the former. The spectra of Figures 3, 4 and 5 point up this conclusion in a most dramatic way.

A phase amplitude analysis yields information on the residual atomic and molecular potentials, provides a rationale for the number of observed Feshbach resonances, and generates a facile categorization of the residual potentials as attractive/repulsive, long range/short range. It has been shown, for example, that the centrifugal barrier for $\ell \geq 2$ is as effective in molecules as in atoms, and that it inhibits ingress of the Rydberg electron into the core. As a result, the molecule in these instances becomes effectively centrosymmetric.

(i) SIGNIFICANCE

A new and very simple way of assigning Rydberg spectra has been discovered. The first attempt at the application of phase amplitude methods to molecular Rydberg spectra has been essayed and found to be successful: It leads to hitherto unavailable information on residual potentials.

C. TORSION IN THE 1s-R STATE OF ETHYLENE (See item 162)

The vacuum ultraviolet spectrum of the first s-Rydberg region of 1,1-$C_2H_2D_2$ has been measured and analyzed. The results are shown in Figure 6 and Table 1.

Using the symmetric top approximation and the Merer-Schoonveld (A. J. Merer and L. Schoonveld, Can. J. Phys., 47, 1731(1969)) potential for the lowest-energy s Rydberg (R_{1s}) state of ethylene, the energies and relative intensities of the first few torsional vibrations (ν_4') in the R_{1s} state of 1,1-$C_2H_2D_2$ have been computed. The agreement with experiment is excellent. This result negates the recent proposal (F. H. Watson, Jr. and M. N. Nycum,

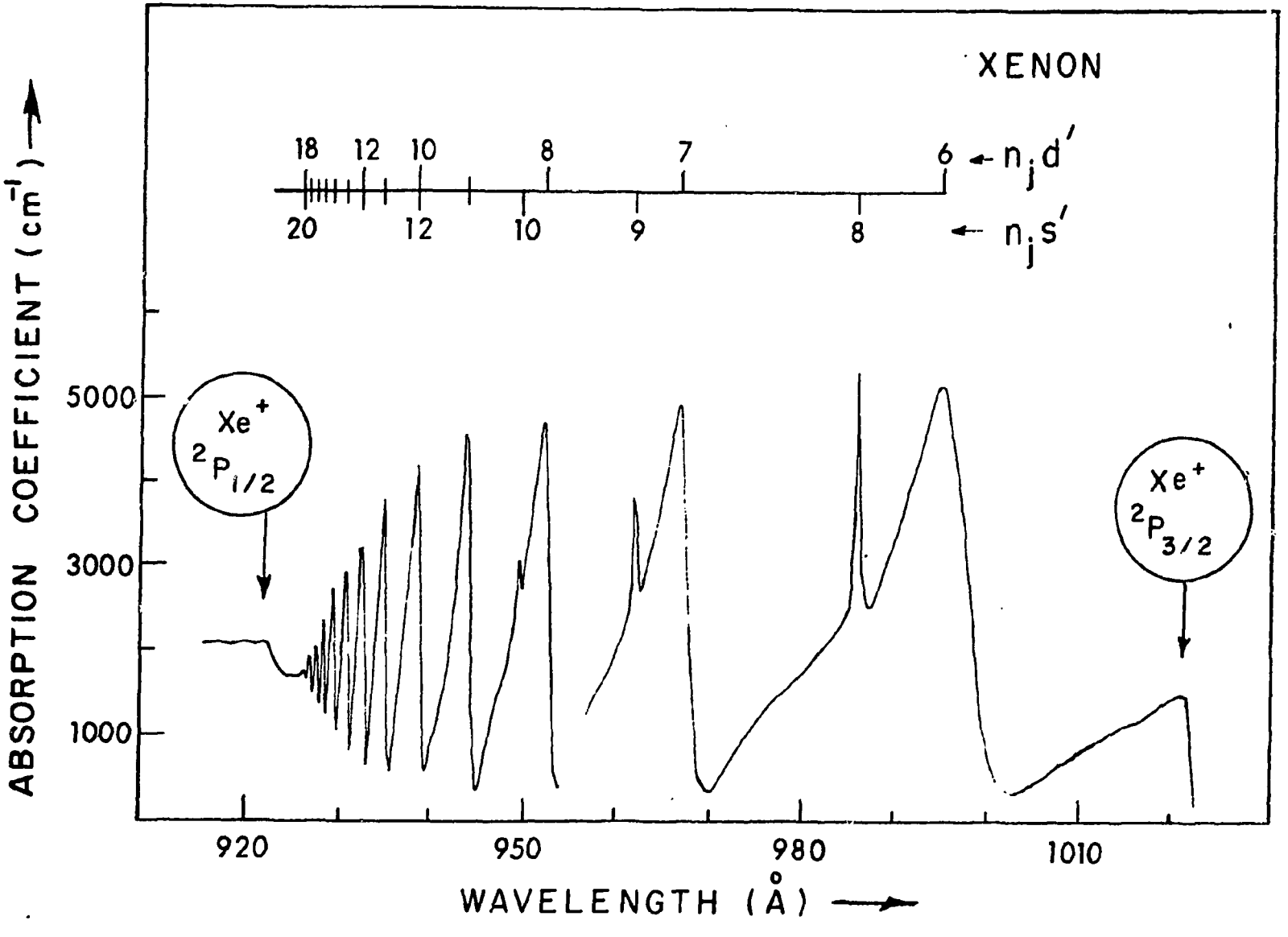

Figure 3. The autoionization spectrum of Xenon between the $^2P_{3/2}$ and $^2P_{1/2}$ ionization limits. The primed symbol $n_j\ell'$ distinguishes series converging on $^2P_{1/2}$ from those converging on $^2P_{3/2}$.

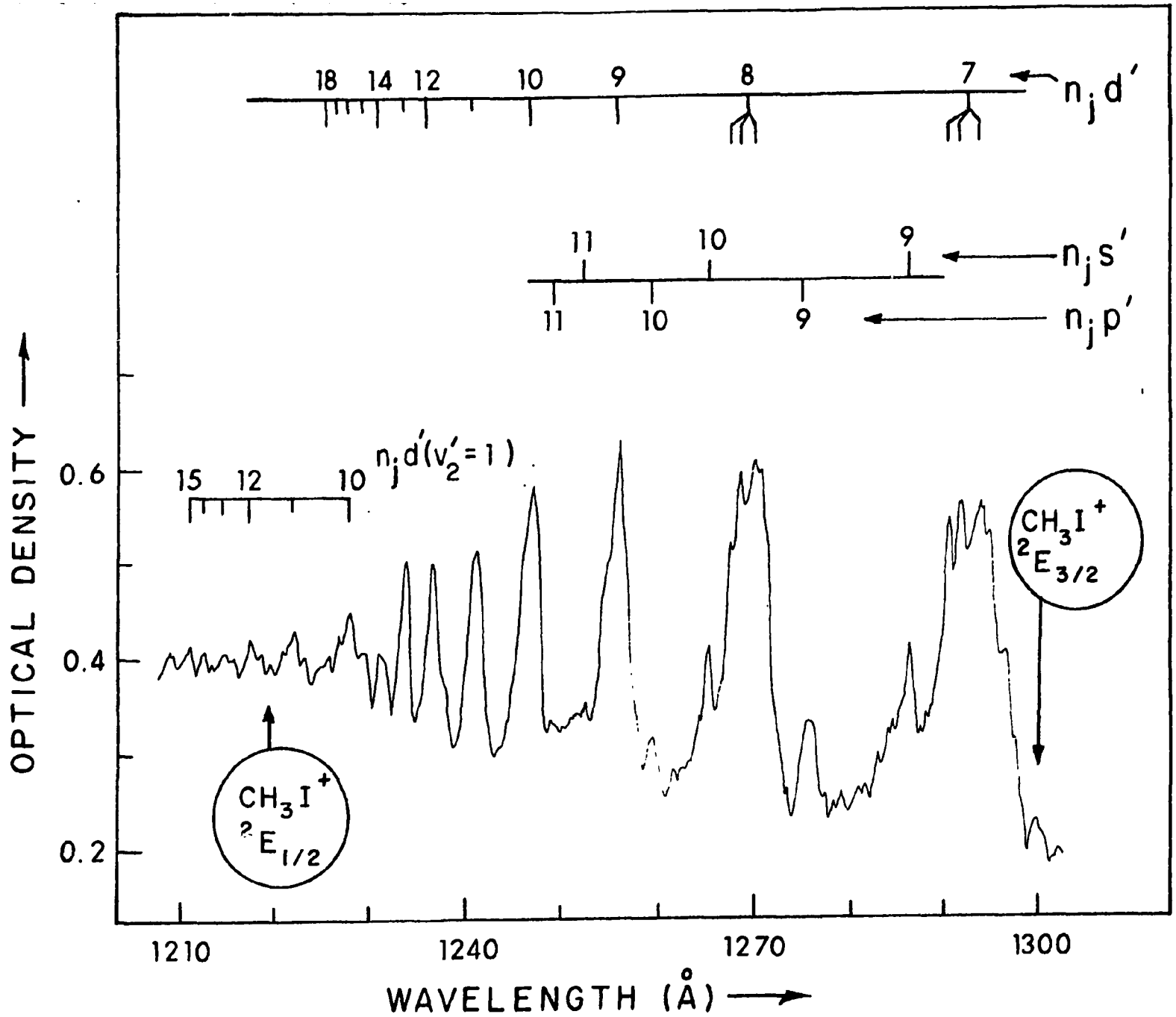

Figure 4. Absorption spectrum of CH_3I between the $^2E_{3/2}$ and $^2E_{1/2}$ ionization limits. The primed symbol $n_j\ell'$ distinguishes series converging on $^2E_{1/2}$ from those converging on $^2E_{3/2}$.

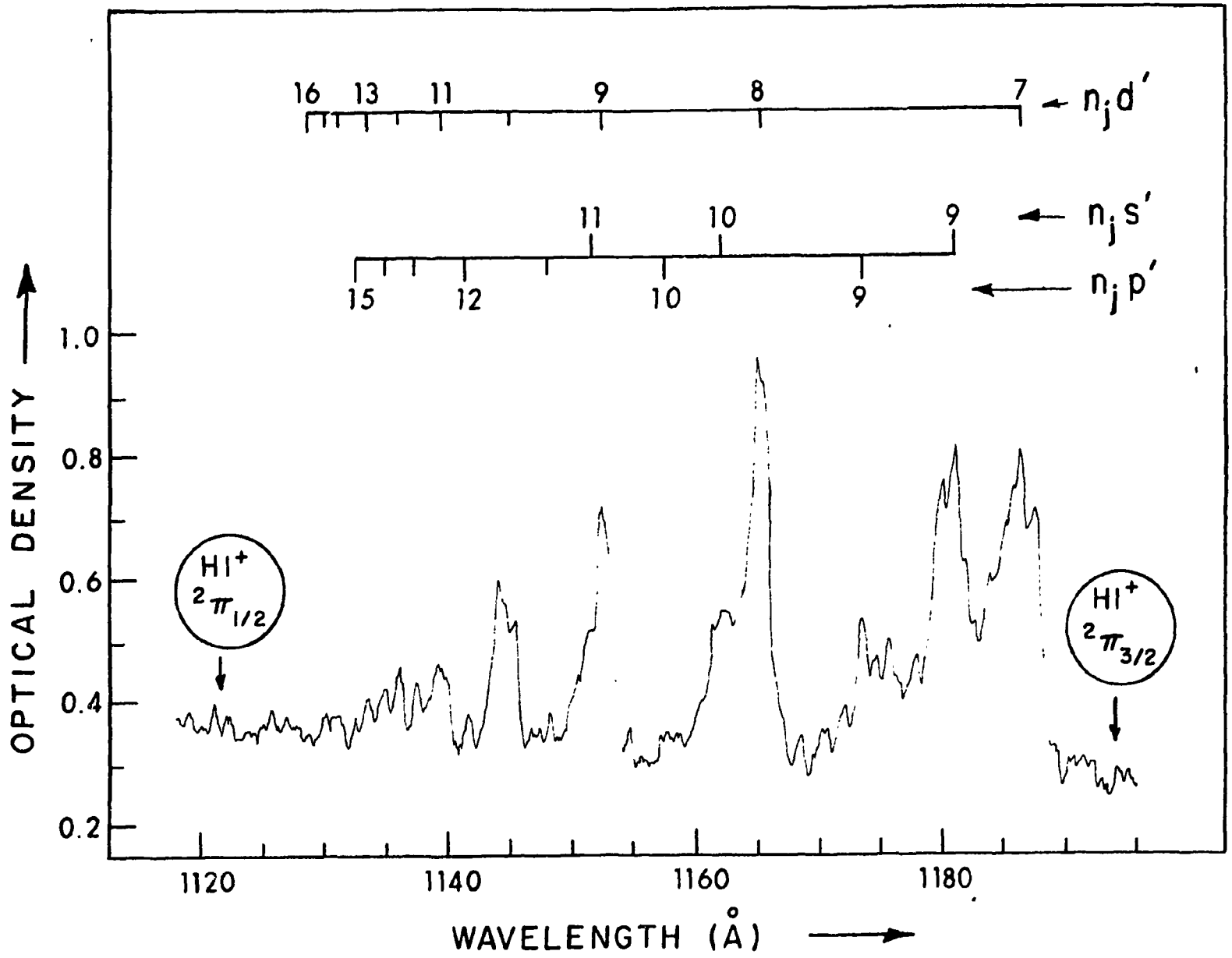

Figure 5. Absorption spectrum of HI in the region between the $^2\Pi_{3/2}$ and $^2\Pi_{1/2}$ ionization limits. The primed symbol $n_j\ell'$ distinguishes series converging on $^2\Pi_{1/2}$ from those converging on $^2\Pi_{3/2}$.

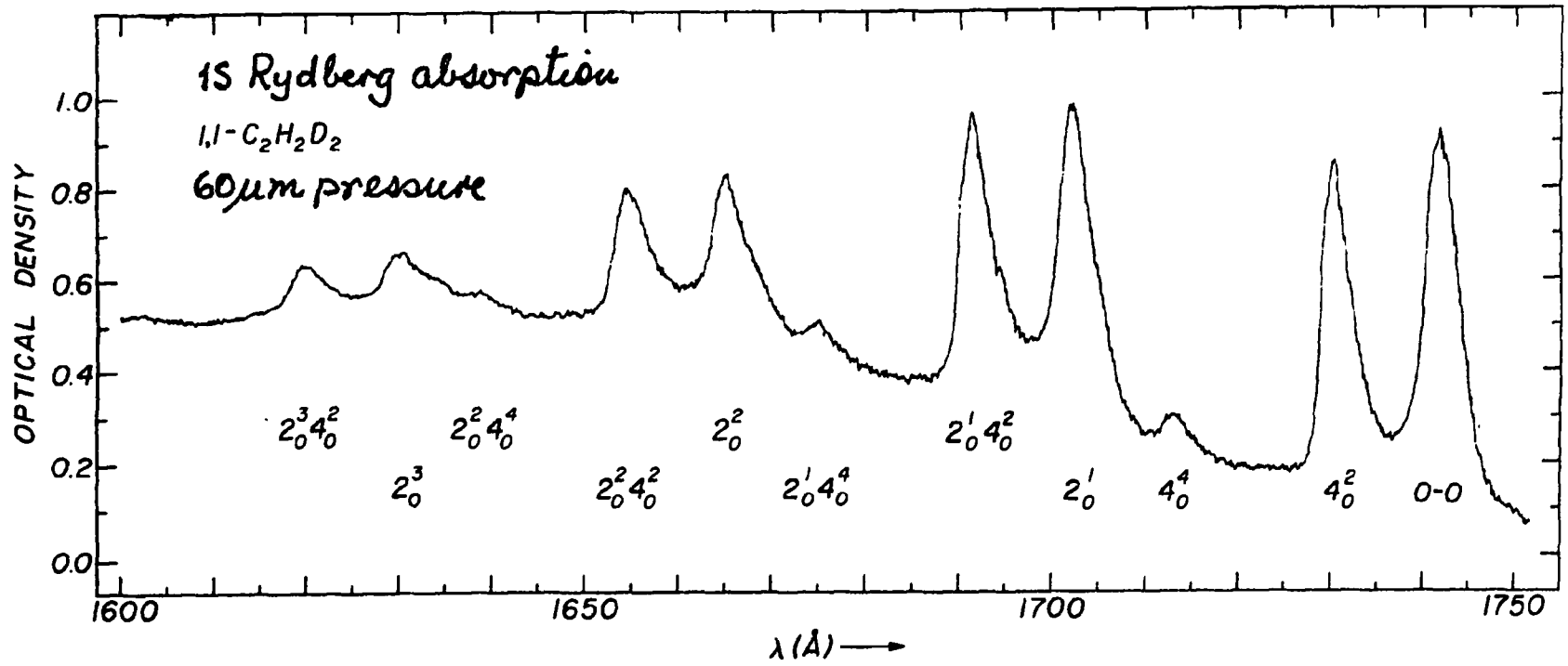
1S Rydberg absorption
1,1-$C_2H_2D_2$
60μm pressure
OPTICAL DENSITY
1.0
0.8
0.6
0.4
0.2
0.0
$2_0^3 4_0^2$
2_0^3
$2_0^2 4_0^4$
$2_0^2 4_0^2$
2_0^2
$2_0' 4_0^4$
$2_0' 4_0^2$
$2_0'$
4_0^4
4_0^2
0-0
1600
1650
1700
1750
λ (Å) ⟶

FIGURE 6

TABLE 1

CALCULATED AND EXPERIMENTAL VIBRATIONAL SPACINGS (cm^{-1}) AND RELATIVE TRANSITION INTENSITIES

		C_2H_4[a]	C_2H_3D[b]	1,1-$C_2H_2D_2$[c]	1,2-$C_2H_2D_2$[b] trans	1,2-$C_2H_2D_2$[b] cis	C_2HD_3[b]	C_2D_4[a]
ν_4''[d]	calc.	1023	936	886	837	837	784	727
	exp.	1027	1000	889	988	982	765	726
$0-\nu_4'$	calc.	-94.89	-104.59	-109.90	-115.66	-115.66	-122.01	-129.17
$1\nu_4'-0\nu_4'$	calc.	114	91	79	67	67	55	44
	exp.	96	--	--	--	--	--	--
$2\nu_4'-0\nu_4'$	calc.	464	407	378	348	348	318	288
	exp.	468	411	384	355	355	320	286
$3\nu_4'-0\nu_4'$	calc.	783	689	640	588	588	534	478
$4\nu_4'-0\nu_4'$	calc.	1139	1011	943	872	872	796	717
	exp.	1082	1035	965	901	901	819	715
$I_{2,0}/I_{0,0}$	calc.	0.68	0.80	0.89	1.00	1.00	1.15	1.37
	exp.	0.73	--	0.75	--	--	--	1.25
$I_{4,0}/I_{0,0}$	calc.	0.12	0.15	0.17	0.20	0.20	0.24	0.31
	exp.	0.09	--	0.07	--	--	--	0.23
$I_{3,1}/I_{1,1}$	calc.	0.81	0.91	0.98	1.06	1.06	1.16	1.29
	exp.	--	--	--	--	--	--	1.5

Spectrosc. Letters, 8, 223(1975)) that the $N \rightarrow R_{1s}$ transition obtains allowedness only through vibronic coupling.

The energies and relative intensities of ν_4' have also been computed for CH_3D, 1,2-$C_2H_2D_2$ (cis and trans) and C_2HD_3. The Merer-Schoonveld potential is in excellent agreement with experiment in all instances.

(i) SIGNIFICANCE

The Merer-Schoonveld/Watson-Nycum controversy has been resolved. It is shown beyond doubt that the torsional potential in the 1s-Rydberg state is that proposed by Merer and Schoonveld.

D. MOLECULAR RYDBERG STATES OF WATER (See item 161)

The optical absorption spectra of H_2O and D_2O have been investigated in the region $2000 \geq \lambda \geq 850$ Å. The 1670 Å band ($^1A_1 \rightarrow {}^1B_1$) exhibits vibrational structure in the ν_2 bending mode and the $^1B_1$ state possesses a large intravalence $4a_1$ component.

The 1280 Å absorption band has been assigned as $3a_1$; $\tilde{X}\ ^1A_1 \rightarrow 3sa_1$; $^1A_1$. The molecule is linear in the Rydberg $3sa_1$; $^1A_1$ excited state. A Renner-Teller analysis of this state (as a component of a linear $^1\Pi_u$ state) suggests the existence of a perturbing state at 1365 Å.

This perturbing state has been assigned as a bent, dominantly-Rydberg $3sa_1$; $^1B_1$ state. Arguments, based on a re-analysis of the K-shell excitation spectra, have been used to bolster this $3sa_1$; $^1B_1$ assignment.

Isotope shift studies in the 1060 - 1130 Å and 980 - 1060 Å regions lead to vibronic identifications and certain electronic origin reassignments.

The terminal electronic state of the 968 Å absorption band is linear and of species $5sa_1$; $^1A_1$.

In sum, a total of 21 electronic states comprising fragments of 6 Rydberg

series have been assigned; and one, largely-intravalence state ($4a_1$; $^1B_1$) has been identified. These assignments are summarized in Table 2.

(i) LOWER-ENERGY STATES

The singlet states below 11 eV are summarized in the potential energy diagram of Figure 7. The potential energy curves are schematic, particularly with respect to curvatures. However, the energy levels and the equilibrium values of $\measuredangle$ HOH, bent or linear, are experimental. The degenerate states of the linear molecule are split by Renner-Teller effects. According to our assignments, the bent state at 1670 Å (7.42eV) is largely intravalence [$4a_1$; $^1B_1$], and is convergent onto its partner [the $3sa_1$; $^1A_1$ state at 1432 Å (8.66eV)], as $\measuredangle$HOH approaches 180°. This convergence implies a change of orbital character as a function of $\measuredangle$HOH: The lowest-energy excited state at 180°, the $^1\Pi_u$ state, is predominantly 3s in nature. However, as $\measuredangle$HOH deviates from 180°, two states results, the lower of which minimizes at $\sim$ 105° and alters character from predominantly 3s to predominantly $4a_1$, whereas the upper remains predominantly 3s throughout its total angular extent.

The 1365 Å (9.08eV) state has a bent equilibrium conformation and it is assigned as the predominantly $3sa_1$; $^1B_1$ Rydberg state. In this energy region, all states contain considerable 3s character, regardless of the magnitude of the equilibrium value of $\measuredangle$HOH -- hence, the two largely 3s Rydberg states of equilibrium geometries 105° and 180° which we suppose to coexist in this energy region.

The $3sa_1$; $^1B_1$ potential energy curve is shown to be convergent on a $^1\Pi_u$ state at 11eV. This doubly-degenerate state must possess considerable 3p character since the 3p energy region of the linear molecule should initiate at $\sim$ 11eV.

In sum, the four states which result from Renner-Teller splitting of the

TABLE 2A

RYDBERG SERIES FOR H_2O

	$1b_1 \rightarrow nsa_1; {}^1B_1$		$1b_1 \rightarrow npa_1; {}^1B_1$		$1b_1 \rightarrow npb_1; {}^1A_1$		$1b_1 \rightarrow nda_1; {}^1B_1$		$1b_1 \rightarrow ndb_1; {}^1A_1$		$3a_1 \rightarrow nsa_1; {}^1A_1$	
n	$\nu(cm^{-1})$	n*	$\nu(cm^{-1})$	n*	$\nu(cm^{-1})$	n*	$\nu(cm^{-1})$	n*	$\nu(cm^{-1})$	n*	$\nu(cm^{-1})$	n*
3	73271	1.963	80604	2.278	82038	2.360	88629	2.892	89726	3.021	69832	1.621
4	89095	2.945			91676	3.301	94610	3.921	94970	4.024	--	--
5	94750	3.960			95910	4.336			97324	4.982	103260	3.624
6					--	--			98697	5.999		
7					99110	6.452			99512	7.008		
8									100060	8.068		
9									100410	9.063		
10									100660	10.052		
11									100850	11.067		
∞[b]	101746±8		101746±8		101746±8		101746±8		101746±8		111620±60	

TABLE 2B

RYDBERG SERIES FOR D_2O

	E $1b_1 \rightarrow nsa_1; {}^1B_1$		A $1b_1 \rightarrow npa_1; {}^1B_1$		B $1b_1 \rightarrow npb_1; {}^1A_1$		C $1b_1 \rightarrow nda_1; {}^1B_1$		D $1b_1 \rightarrow ndb_1; {}^1A_1$		E $3a_1 \rightarrow nsa_1; {}^1A_1$	
n	$\nu(cm^{-1})$	n*	$\nu(cm^{-1})$	n*	$\nu(cm^{-1})$	n*	$\nu(cm^{-1})$	n*	$\nu(cm^{-1})$	n*	$\nu(cm^{-1})$	n*
3	73260	1.958	80738	2.278	82061	2.352	88668	2.881	89847	3.018	69930	1.621
4	89142	2.934			91878	3.311	94697	3.906	95003	3.992	--	--
5	94850	3.948			95978	4.308			97437	4.964	103600	3.685
6					98116	5.392			98834	5.992		
7					99246	6.442			99641	6.985		
8									100180	8.011		
9									100550	9.049		
10									100780	9.943		
∞^b	101890±8		101890±8		101890±8		101890±8		101890±8		111680±60	

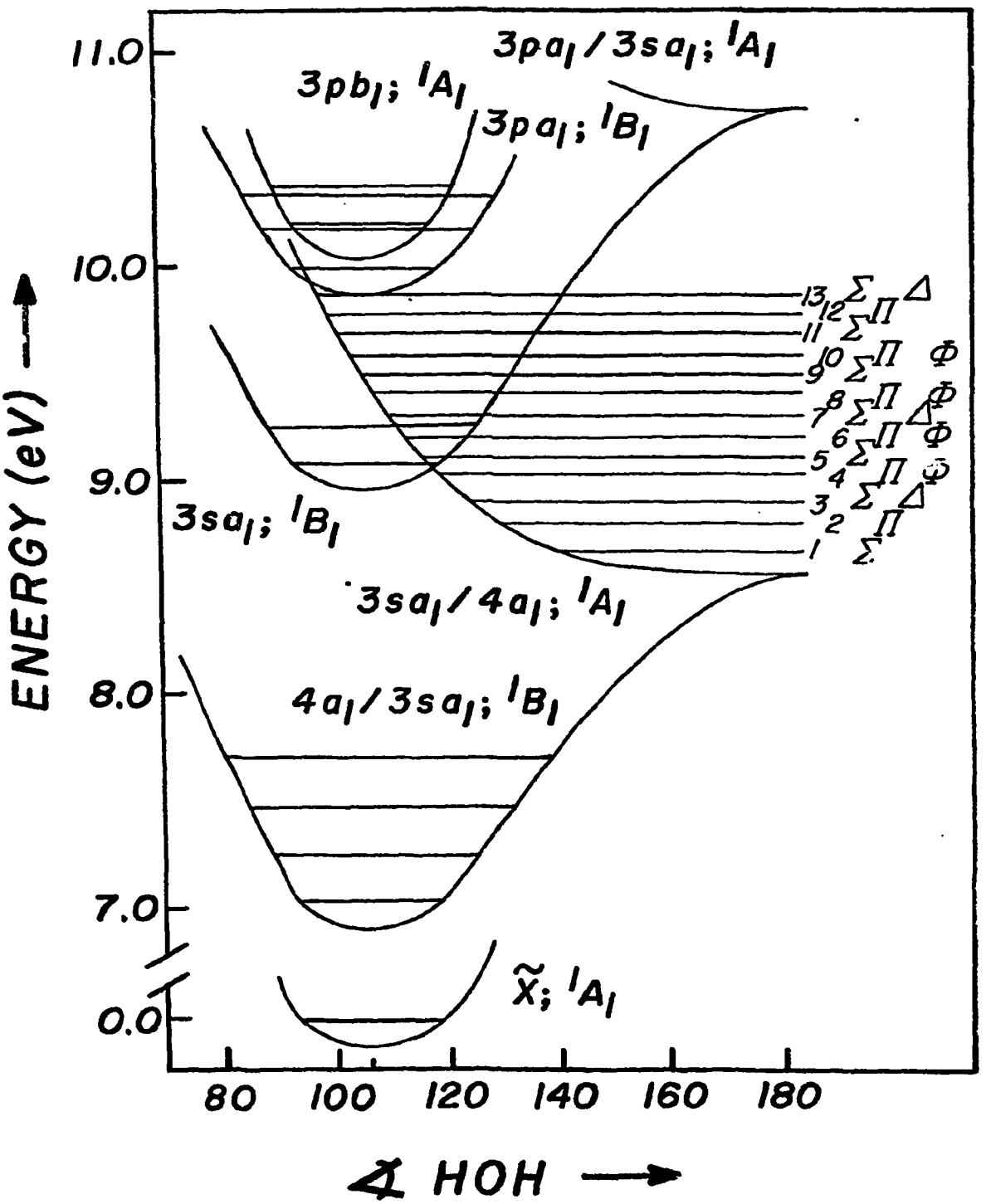
11.0
10.0
9.0
8.0
7.0
0.0
ENERGY (eV)
80
100
120
140
160
180
∠ HOH
3pa1 / 3sa1; 1A1
3pb1; 1A1
3pa1; 1B1
3sa1; 1B1
3sa1 / 4a1; 1A1
4a1 / 3sa1; 1B1
X̃; 1A1
13 12 11 10 9 8 7 6 5 4 3 2 1
Σ Π Δ Φ

FIGURE 7

two $^1\Pi_u$ states of the linear conformation can be viewed as constituted of $4a_1$, $3sa_1$, and 3p terminal MO's. The orbital constitution of these Renner-Teller components is a function of $\measuredangle$HOH and is, in our opinion, largely determined by energy. At lower energy, the intravalence $4a_1$ MO predominates; as energy increases, the $3sa_1$ Rydberg orbital begins to play a role; and, above ~ 11eV, the 3p Rydberg orbitals may well be dominant.

The $3sa_1$; $^1A_1$ state at 1432 Å probably contains $4a_1$ intravalence character also. In specific, the underlying "continuum" in the 1432 Å region may well refer to the same $3a_1$; $\tilde{X}^1A_1 \rightarrow 3sa_1$; $^1A_1$ transition, the broadness being caused by the mixing of $3sa_1$ and $4a_1$ orbitals in the upper state.

A singlet → triplet band has been observed at ~ 9.0eV and has been assigned as the $\tilde{X}^1A_1 \rightarrow 3p\ b_2$, $^3A_2$ transition. We believe that this band corresponds to the excitation of a $3a_1$ electron: The highly non-vertical appearance of this band implies that either the upper state is dissociative (and, thus, intravalence) or Rydberg with almost linear geometry. The most reasonable assignment is the $3a_1$; $\tilde{X}^1A_1 \rightarrow 3sa_1$; $^3A_1$ transition.

(ii) HIGHER-ENERGY STATES

In the region 980 Å - 1060 Å, vibrational analysis reveals not only the origins of the higher-energy npb_1; $^1A_1$ states but also the interference between vibrational levels of lower-energy Rydberg states with the electronic origins of higher-energy Rydberg states. For H_2O, the (1,0,0) band of the $5db_1$; $^1A_1$ state at 994.7 Å obscures the $10db_1$; $^1A_1$ band. As a result, Katayama et al. cite 993.6 Å as the origin of the $10db_1$; $^1A_1$ state whereas we conclude that 993.4 Å is the more likely. For D_2O, the (1,0,0) bands of the $4db_1$; $^1A_1$, $5sa_1$; $^1B_1$ and $4da_1$; $^1B_1$ states all overlap with the origin of the $5db_1$; $^1A_1$ state. Thus, we revise the true origin of the $5db_1$; $^1A_1$ state from 1026.5 Å to 1026.3 Å. The split bands at 1003.6 and 1002.4 Å are separately assigned

as the origin of the $7db_1$; $^1A_1$ state and the (1,0,0) band of the $5db_1$; $^1A_1$ state (whose origin lies at 1026.3 Å), respectively.

(iii) INTERACTIONS BETWEEN BENT AND LINEAR STATES

The two Renner-Teller component states of Π parentage in $D_{\infty h}$, one bent and the other linear, exhibit considerable interactions of the vibrational levels of these two split components. These interactions account for the alternating band shapes of the vibrational levels of the linear state. It is suspected that similar interactions exist between bent states and linear states with different values of n but similar energies (i.e., dynamic Renner-Teller effects). An example is provided by the very low intensity of the $1b_1$; $\tilde{X}^1A_1 \rightarrow 3sa_1$; $^1B_1$ transition which happens to sit astride the $3a_1$; $\tilde{X}^1A_1 \rightarrow 3sa_1$; $^1A_1$ transition of the linear molecule. Similar situations exist also for the $1b_1$; $\tilde{X}^1A_1 \rightarrow 4pa_1$; $^1B_1$, $\rightarrow 5pa_1$; $^1B_1$ and $\rightarrow npa_1$; $^1B_1$ ($n > 5$) transitions of the same series. Furthermore, the transitions $1b_1$; $\tilde{X}^1A_1 \rightarrow nda_1$; $^1B_1$ ($n = 5,6,7,...$) and $1b_1$; $\tilde{X}^1A_1 \rightarrow nsa_1$; $^1B_1$ ($n = 6,7,8,...$) all exhibit the same "disappearance" of intensity.

(iv) SIGNIFICANCE

This comprehensive study of H_2O and D_2O has produced a great deal of information about the water system. These are:

---The 1670 Å band is dominantly intravalence and not, as previously thought, Rydberg.

---Two s-Rydberg states occurs in the region 1432 - 1250 Å.
This finding leads to a more rational interpretation of K-shell spectra.

---The 1432 Å band exhibits Renner-Teller splitting up to $v' = 5$ and, thereafter, other effects due to configuration mixing with the s-Rydberg state at $\sim$ 1365 Å.

---The terminal state of the 1432 Å excitation is linear.

---New states have been discovered and assigned and some old assignments have been revised in the higher-energy region (See Table 2.

---The question of triplet assignments has been discussed and the possible alternatives have been detailed.

E. THE LINEAR COMBINATION OF RYDBERG ORBITALS (LCRO) MODEL

(See items 152 and 158)

The purpose of this work was to determine whether one R orbital situated on a center of symmetry or two R orbitals, one on each chromophore, provided the best description of the low-energy VUV spectrum of a two-chromophoric molecule with a center of symmetry. The molecule chosen was 1,1,2,2-tetramethylcyclobutanedione (TMCBD), and this molecule was treated as a combination of two acetone "bits". The results were unambiguous: An LCRO model was essential to a logical interpretation of the spectrum of TMCBD.

(i) THE ONE-CHROMOPHORE MODEL

The basis orbital set consists of a single ($\underline{n}$, ℓ, m)-set of atomic orbitals, where $\underline{n}$ = 3, 4, 5,... and ℓ = 0, 1, 2,... and one molecular orbital, n_o (i.e., the b_{2u} non-bonding MO). Symmetry adaptation of such a single ($\underline{n}$, ℓ, m)-set requires, as a minimum, that the atomic orbitals be located on the center of symmetry of the D_{2h} molecule.

The Rydberg transitions of interest, in a one-electron format, are $n_o \rightarrow$ ($\underline{n}$, ℓ, m). Of these, the ones, which are electric-dipole allowed in D_{2h} consist of one excitation of s-type and four of d-type. In particular, all excitations of p-type are forbidden.

The striking feature of the TMCBD Rydberg spectrum is the dominance of p-type excitations. One might argue that the observed excitations of "p-type" are actually "d-type". In this instance, one must then infer that core interactions have produced a change of $\delta_{1d} = 0.15$ units. If this be the case, one

might further expect that the quantum defect for the strong TMCBD Rydberg series should approach typical values of δ_d as $\underline{n}$ gets larger. This, however, does not occur. Indeed the quantum defect for the intense series is characteristic of p-type excitations and remains so for all six observed series members. Consequently, the lack of dependence of the quantum defect on transition energy establishes this series as "non-d-type"; and the magnitudes of the observed quantum defects establishes it as "p-type". Hence, comparison with acetone and with atomic systems leads to the conclusion that the one-chromophore model does not provide a reasonable description of the Rydberg spectrum of TMCBD.

(ii) THE TWO-CHROMOPHORE MODEL

The basis set consists of two ($\underline{n}$, ℓ, m)-sets of atomic orbitals, one set on each carbonyl group, and the n_o MO. Symmetry adaptation of the two sets of atomic orbitals requires, as a minimum, the use of linear combinations $(\underline{n}, \ell, m)_1 \pm (\underline{n}, \ell, m)_2$ which possess appropriate g/u transformation properties, and where the subscripts 1 and 2 denote the individual carbonyl centers. The use of such a primitive symmetry-adapted basis set leads to the molecular orbital energy diagram of Figure 8.

Only those Rydberg group orbitals which possess g transformation properties are shown in Figure 8. The g-group orbitals are those to which electric-dipole allowed excitations from n_o may occur; hence, they are the only ones pertinent to a discussion of the observed spectrum.

In summary, the two-chromophore model predicts 1 s-type, 2 p-type, and 4 d-type Rydberg transitions. All of these, with the exception of one of the d-type Rydbergs have been observed. In contrast, the one-chromophore model predicts 1 s-type and 4 d-type Rydberg transitions whereas two p-type Rydbergs have been detected.

Figure 8. An orbital energy level diagram for a set of Rydberg orbitals of tetramethylcyclobutanedione for arbitrary n. Only gerade group orbitals are shown. Observed transitions are denoted by solid vertical arrows. Electric dipole-allowed transitions which are either not observed or which are of very low intensity are denoted by dashed vertical arrows.

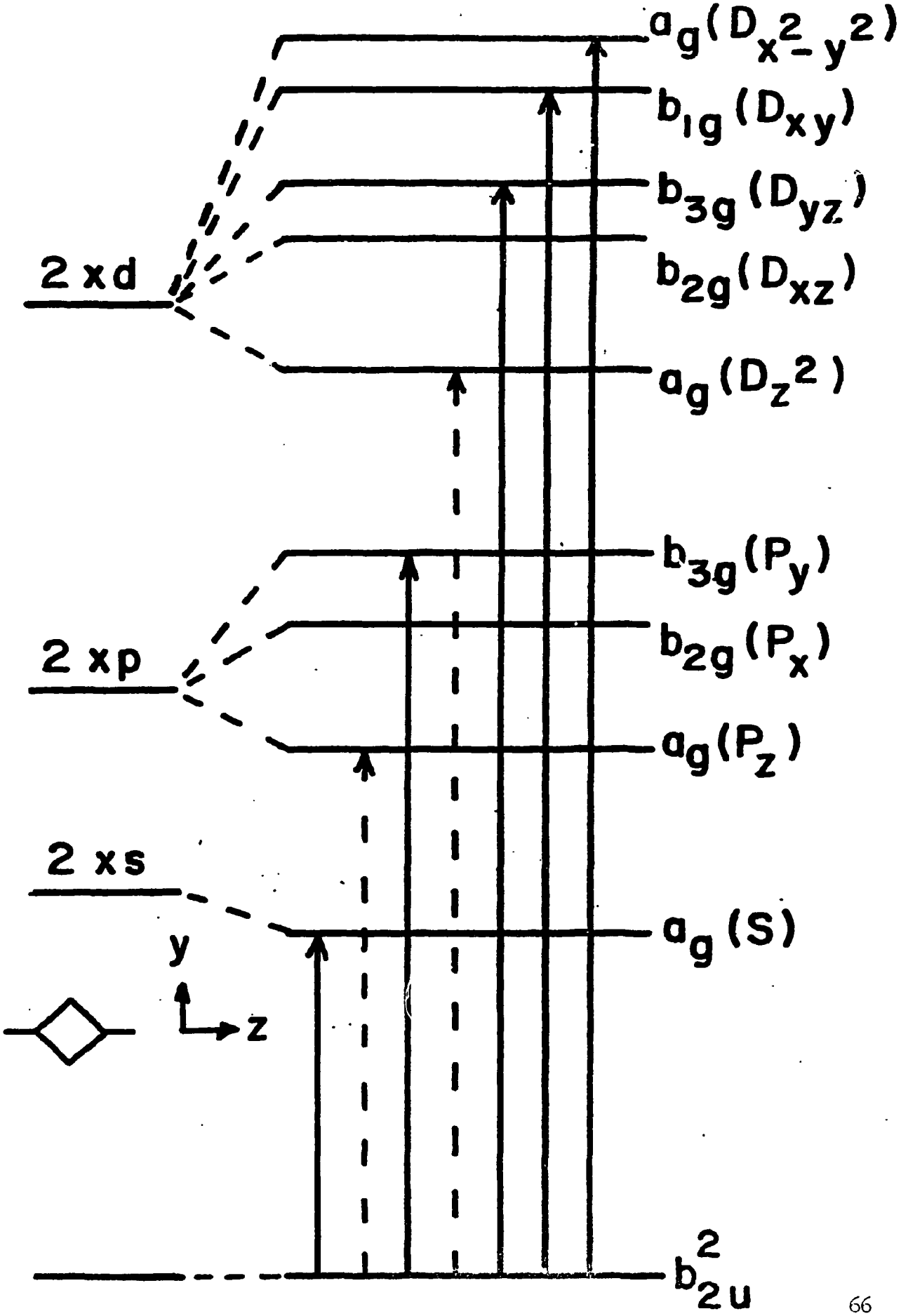
$a_g(D_{x^2-y^2})$
$b_{1g}(D_{xy})$
$b_{3g}(D_{yz})$
$b_{2g}(D_{xz})$
2 x d
$a_g(D_{z^2})$
$b_{3g}(P_y)$
$b_{2g}(P_x)$
2 x p
$a_g(P_z)$
2 x s
$a_g(S)$
y
z
b_{2u}^2

(iii) CONCLUSIONS

A two-chromophore model provides a simple description of the Rydberg spectrum of TMCBD whereas a one-chromophore model does not. One might argue that either model, processed to an appropriate degree of quantum chemical ultimacy, would fit the observed facts. While not unwilling to concede such, we emphasize that the preference for a given model may also be decided in terms of the efficiency with which the various models interpret the data at hand. On this basis, the two chromophore model is certainly the more efficient. Indeed, while the possibility exists that the one-chromophore model may be made to conform to the data, the degree of computational effort which will be required and the concomitant loss of physical insight which will result, will yield neither an efficient nor useful scheme.

The two-chromophore model, therefore, is preferred for low n. The differences between the two models should decrease rapidly with increasing n. For large n and, hence, large overlap of set $(n, \ell, m)_1$ with set $(n, \ell, m)_2$, one half of the resulting group orbitals will suffer a renormalization catastrophe and get pushed into the ionization continuum. When and if such occurs, any effort to discriminate between a one- and two-chromophore model will be largely ridiculous.

F. THE RELATIONSHIP BETWEEN VUV AND PHOTOELECTRON SPECTROSCOPY (See items 158 and 176)

The symmetry assignments of Rydberg and PES transitions are related, as is obvious on the orbital level. If one knows the symmetry of the starting orbital from the PES assignment, the symmetry of the Rydberg orbital should be more easily identified; and, if one knows the starting and final orbitals of a Rydberg transition, the corresponding PES band is identified simultaneously.

The only selection rule governing PES band intensities is Koopmans'

theorem: The only ionization processes which possess reasonable intensity are those which remove an electron from an orbital. As a consequence, the assignment of PES spectra (i.e., the symmetry labelling of cationic states) is based on computation, on experience, and on intuition -- and it may well be hazardous. On the other hand, the intensities of optical transitions, as observed in VUV spectroscopy, are governed by dipole selection rules.

It is standard practice to label Rydberg orbitals as s, p, or d. In fact, this labelling induces a considerable amount of unity into molecular Rydberg spectra. The general run of experience connects quantum defect values δ to ℓ-values as follows: $\delta_s \simeq 0.0$; $\delta_p \simeq 0.4$; and $\delta_d \simeq 0.9$. Since angular momentum quantum numbers are "good" only in the spherical group, they carry only an approximate meaning in molecules. Thus in a C_{2h} molecule, Rydberg s-orbitals must transform as a_g, p-orbitals as a_u or b_u, and d-orbitals as a_g or b_g. Consequently, the application of the dipole selection rules lead us to conclude that the observation of a Rydberg series of s-type must indicate excitation from an initial MO of a_u or b_u symmetry.

Attitudes such as the above would appear to be of help in making Rydberg and/or cationic state assignments. We will now apply them to the ionization limits IE_1, ..., IE_4 of <u>trans</u>-dibromoethylene (a C_{2h} molecule).

<u>(i) FIRST IONIZATION ENERGY</u>

The ^2A_u symmetry of the cationic ground state is well established for <u>trans</u>-dibromoethylene. Only one s-series is found to converge on the first ionization energy. The region in which the first Rydberg transitions of p-type are expected does not contain any absorption bands. These observations agree with the dipole selection rules

$a_u \rightarrow s$; $a_u \rightarrow a_g$ . . . allowed

$a_u \rightarrow p$; $a_u \rightarrow a_u$ . . . forbidden

$a_u \rightarrow b_u$ . . . forbidden

(ii) SECOND IONIZATION ENERGY

The symmetry of the second highest-energy occupied molecular orbital is not known. It may be either $4b_u$ or $5a_g$. The Rydberg series which converge on this ionization limit are: s(or p), d, and possibly p. If we disregard the "tentative" series, one must conclude that the initial MO in the absorption events must be ungerade (i.e., $4b_u$).

In support of this assignment, we note that a $5a_g$ designation for the 2nd PES band would suggest that this band be vibronically structured -- which it is not. Contra the assignment, we note our convictions that the "tentative" series are real and properly labelled -- and hence, that they should not be disregarded -- and the fact that since only s or d series terminate on IE_3 a $4b_u$ assignment for IE_3 is equally valid. In sum, while we can provide no decisive contradictory evidence against the $4b_u$ assignment of IE_2 we do not feel totally comfortable with it.

(iii) FOURTH IONIZATION ENERGY

The observed Rydberg series is labelled "d". This VUV assignment implies an ungerade cationic state. Since the assignment of this 4th PES band is $1b_g$, the obvious contradiction requires an explanation. Several possibilities are: The PES assignment is incorrect; the Rydberg transitions gain intensity through vibronic coupling or by distortion of the upper state; or the $\delta \leftrightarrow \ell$ correspondence is invalid. We will discuss each of these possibilities in turn:

---Bromine has an atomic spin-orbit coupling constant $\zeta \simeq 0.3$eV.

Consideration of the spin-orbit interaction shows that the orbitals $5a_g$ and $1b_g$ are coupled in such a way that an energy separation of at least $\sim$ 0.3eV must exist between the two corresponding cationic states. Thus, since the second and third ionization potentials differ by no more than 0.08eV, we are forced to conclude that the PES assignment is correct.

---We cannot, with certainty, establish the point group of this particular cationic state. However, the vibrational activity of the PES band can be completely interpreted in terms of a totally symmetrical mode (ν_3:a_g). Thus, no distortion appears to have occurred relative to the ground state. The same evidence, weak though it be, can be used to rule out coupling with other electronic states.

---Using the "aufbau" quantum number n, δ is found to increase roughly by $\Delta\delta = 1$ as one proceeds from member to member down a group of the Periodic Table. This increase is in accord with the increase in the number of "real precursors" (i.e., occupied orbitals to which the Rydberg orbitals must maintain orthogonality). It may well be that deviations from this $\Delta\delta = 1$ rule become large by the time one reaches the fourth row of the Periodic Table and that these deviations inhibit any ℓ identifications on the basis of quantum defect ranges. However, this supposition is not borne out by rare gas data and is not in accord with general experience.

In sum, we feel that the argument in favor of the $1b_g$ assignment is quite secure. Therefore, we tend to disregard the $\delta \leftrightarrow \ell$ correspondence, at least when used in a group-theoretical sense.

(iv) CONCLUSIONS

Further experimental work is needed to test these ideas. However, a number of points are already obvious. They are:

---We have observed identical vibrational fine structure for PES bands

and Rydberg transitions. This suggests that the higher resolution available in VUV absorption spectroscopy could be used to obtain the geometries of cationic states.

---We have thrown some doubt on the significance of quantum defect values for making assignments. The acceptance of the $\delta \leftrightarrow \ell$ correspondence leads to some contradictions with respect to the g ↔ u selection rules. The resolution of the resulting dilemma requires an LCRO description of Rydberg orbitals.

---A means of identifying cationic states has been elaborated.

G. MAGNETIC CIRCULAR DICHROISM (MCD) IN THE VUV REGION

(See items 172, 177)

We have constructed an apparatus which is capable of measuring MCD in the VUV region. A schematic of the apparatus is shown in Figure 9. This apparatus can measure absolute and relative magnetic moments (μ_e) of excited states. (As far as we know, no other apparatus with these capabilities exists).

This topic (i.e., MCD) is so relevant to the problems that beset Rydberg identifications, so powerful in its abilities to penetrate the complexities of spin-orbit and vibronic coupling, and its basis is so readily transferable to other types of field-effect measurement that we devote a lengthy discussion to it.

This discussion is preliminary. Consequently, it may contain inaccuracies and poor organization. Nonetheless, the power of the MCD method should be evident.

(i) AN EXAMPLE WORK: THE MCD OF THE 5p → 6s RYDBERG TRANSITION OF CH_3I

The 5p → 6s configuration of methyl iodide, CH_3I, consists of five electronic states. These are shown in Figure 10, which should be consulted for notation.

Figure 9. A schematic of the optical and the electronic circuitry. The components, starting topmost left, are:

S: radiation source (Hinteregger lamp)

s: entrance and exit slits to monochromator

M: monochromator (McPherson 225 1m)

m: Al mirror, spherical, MgF_2 coated (Action Research Corp.)

P: polarizer, Wollaston, MgF_2 (Karl Lambrech Corp.)

PEM: Photoelastic modulator, CaF_2 optical element, 50kHz (with associated electronics: Morvue)

w: window, either LiF or CaF_2

H: superconducting solenoid magnet (Westinghouse Corp.) contained in a liquid helium dewar (Janis Research Corp.)

C: sample cell

MOD: Power supply and oscillator for PEM

PMT: photomultiplier tube

PS: High voltage power supply for PMT, programmable (Kepco, Model 750)

L: Logarithmic amplifier

E: Electrometer

F: Filter

R: x-y Plotter

D: Differentiator

LI: lock-in amplifier (Princeton Applied Research, Model 124)

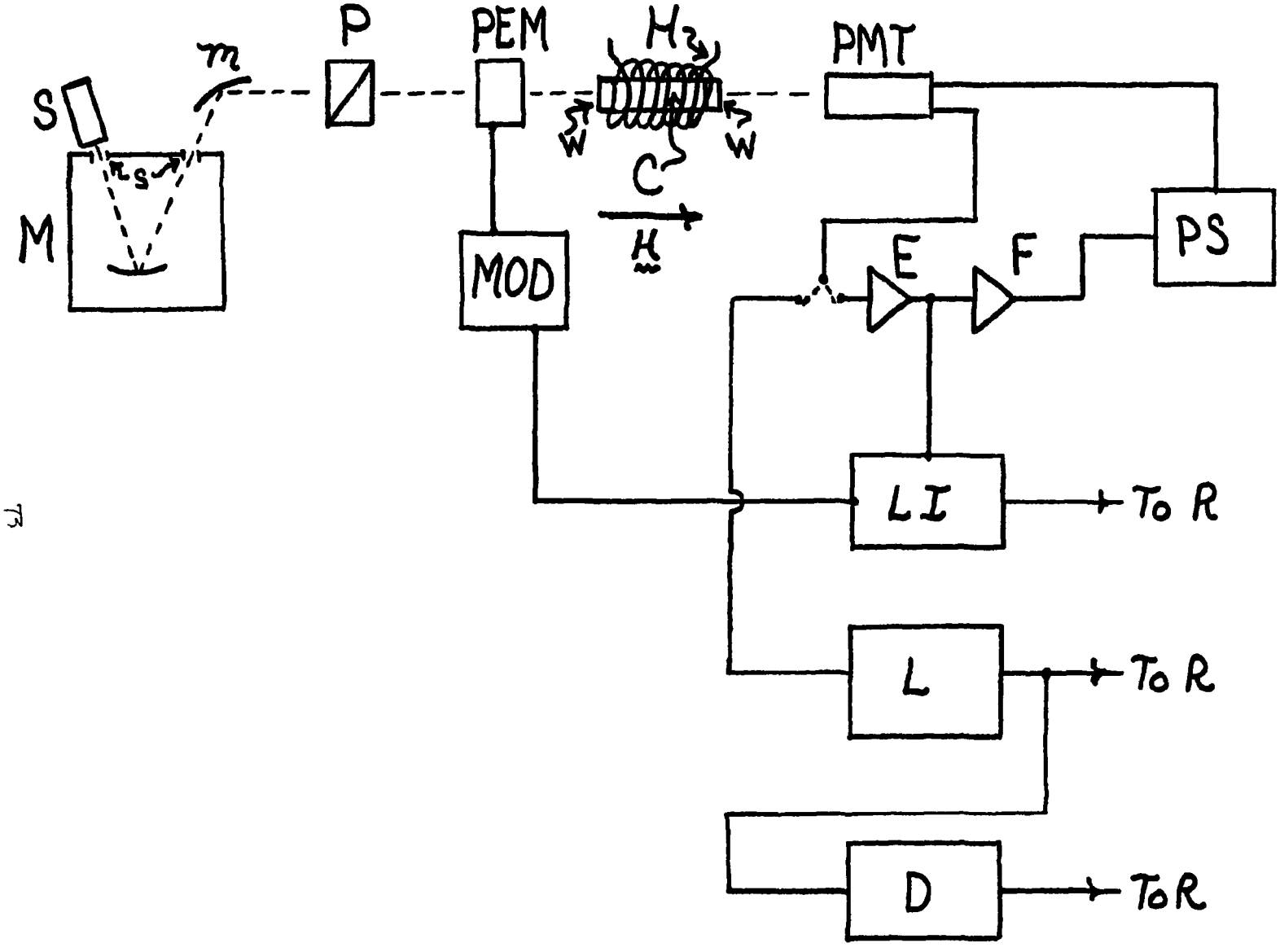

FIGURE 9

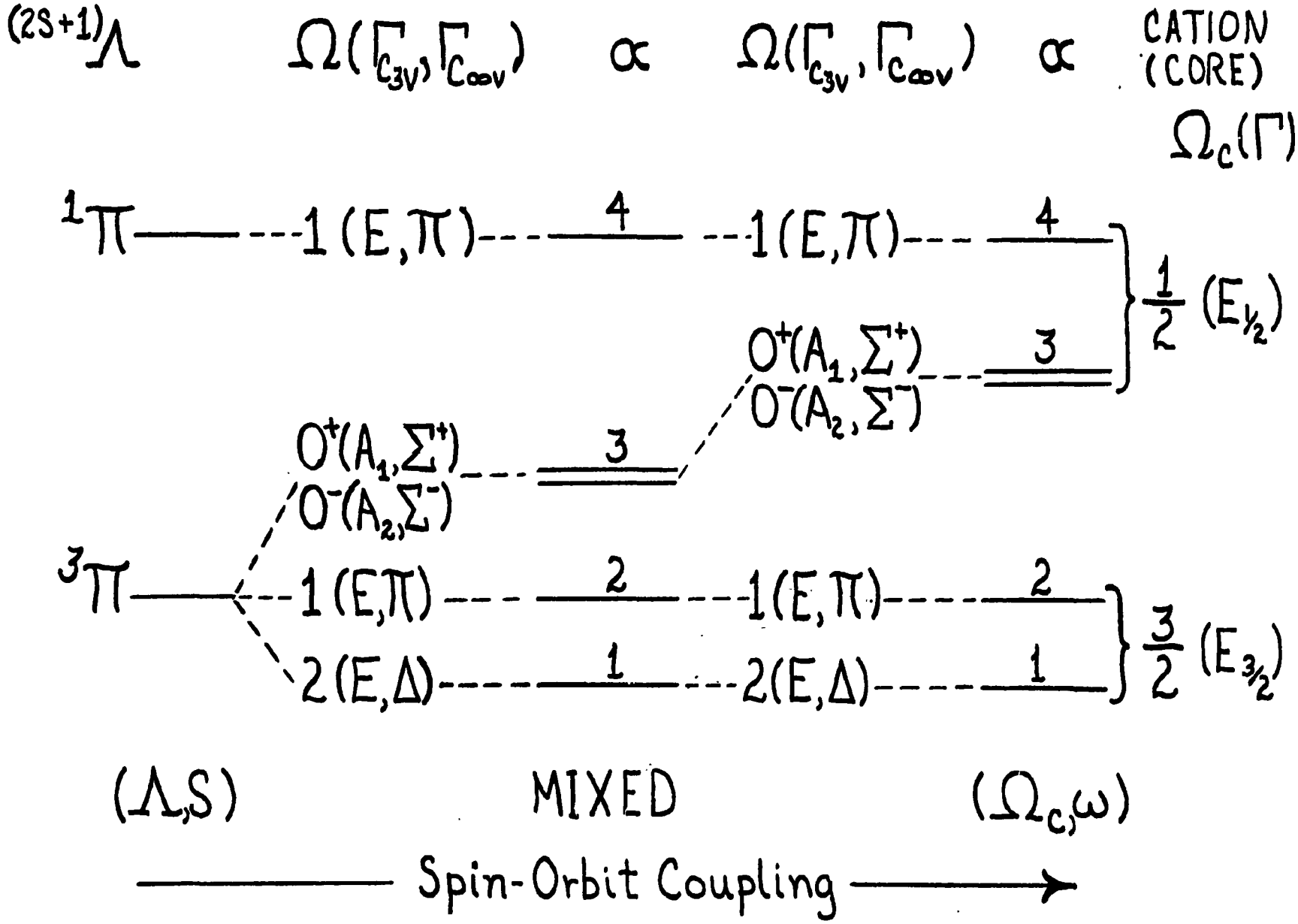
$^{(2S+1)}\Lambda$
$\Omega(\Gamma_{C_{3V}}, \Gamma_{C_{\infty v}})$
$\propto$
$\Omega(\Gamma_{C_{3V}}, \Gamma_{C_{\infty v}})$
$\propto$
CATION (CORE)
$\Omega_c(\Gamma)$
$^1\Pi$
$1(E,\Pi)$
4
$1(E,\Pi)$
4
$\frac{1}{2}(E_{1/2})$
$0^+(A_1,\Sigma^+)$
$0^-(A_2,\Sigma^-)$
3
$0^+(A_1,\Sigma^+)$
$0^-(A_2,\Sigma^-)$
3
$^3\Pi$
$1(E,\Pi)$
2
$1(E,\Pi)$
2
$2(E,\Delta)$
1
$2(E,\Delta)$
1
$\frac{3}{2}(E_{3/2})$
(Λ,S)
MIXED
(Ω_c,ω)
Spin-Orbit Coupling

FIGURE 10

The purpose of the present work is to present the magnetic-circular-dichroism (MCD) spectrum of MeI in the region of the first s-Rydberg transitions (ca. 1700Å-2000Å). It will be shown that these results lead to an unambiguous assignment of the origin bands and of many vibrational progression members.

Two of the physical properties obtainable from absorption spectroscopy, namely transition dipole (electric) moment and transition energy, can lead to estimations of the strength of spin-orbit interaction in the excited states. The electric-dipole selection rules in the (Λ,S)-limit are $\Delta\Lambda = 0 \pm 1$ ($\Sigma^+ \leftrightarrow \Sigma^-$), $\Delta S = 0$ and $\Delta\Sigma = 0$; therefore, in this limit, only the $^1\Sigma^+ \rightarrow {}^1\Pi_1$ transition is allowed. As spin-orbit interaction increases, the selection rule becomes $\Delta\Omega = 0, \pm 1$ ($\Sigma^+ \leftrightarrow \Sigma^-$); therefore, the $\Sigma^+ \rightarrow \Delta(^3\Pi_2)$ and $\Sigma^- (^3\Pi_0)$ transitions remain electric-dipole forbidden. In light of these considerations, it has been concluded[5] that hydrogen iodide lies in the strong spin-orbit coupling limit and that Ω is the only well-defined electronic quantum number. As a result, the azimuthal-angular (ϕ) dependent wave function may be expressed as

$$\Phi(\phi) = e^{\pm i\Omega\phi} \qquad ---(1)$$

Electronic angular momentum and magnetic moment (μ_e) constitute other properties of interest. The angular momentum, $\vec{\Omega} = \pm \hbar\Omega\vec{\epsilon}_3$ (where $\vec{\epsilon}_3$ is the unit vector in the molecular symmetry axis), is invariant to spin-orbit coupling strength. However, μ_e is sensitive to such changes, in a manner analogous to that of the Landé g value in atoms. In the present work, μ_e is calculated in the (Λ,S)-limit as

$$|\mu_e| = |\Lambda + 2\Sigma|\mu_B \qquad ---(2)$$

where μ_B is the Bohr magneton.

In considerations of CH_3I, one must also include the effects of a C_{3v} electrostatic potential on the linear-molecule basis. In terms of perturbation theory, this potential mixes states with different values of Ω. Thus, the integer nature of Ω is destroyed in first order and a new "quantum number", which is referred to as the electronic coriolis parameter ζ_e, is introduced. Furthermore, the only well-defined quantum number associated with axial angular momentum is a resultant of molecular rotational and electronic motions. However, since the electronic axial magnetic moment, when present, is much larger than that of the rotational motion, the magnetic moment of a C_{3v} molecule in a degenate state reflects ζ_e.

The C_{3v} potential also alters the relative absorption intensities: Many transitions, forbidden in HI, are theoretically allowed in CH_3I. Those transitions which, in the linear (Δ,S)-basis, are spatially forbidden (i.e., $\Delta\Lambda \neq 0,\pm 1$) but not spin forbidden, should exhibit a first-order intensity change due to the C_{3v} perturbation. Those $C_{\infty v}$ transitions which are spin-forbidden in the (Λ,S)-limit and also dipole forbidden in strong-coupling limit, should exhibit only second (and higher) order intensity effects. An example of this latter effect is the transition to State 1. This transition is forbidden in the (Λ,S)-limit ($\Delta S \neq 0$) and in the strong-coupling limit ($\Delta\Omega = \pm 2$). It is known experimentally that this transition is exceedingly weak (i.e., effectively forbidden); consequently, second-order effects can be inferred to be negligible. Indeed, the smallness of these intensity effects is generally regarded as sufficient justification for considering the Rydberg states of CH_3I in the $C_{\infty v}$ linear molecule basis. A synopsis of notations is given in Table 3.

TABLE 3

NOTATIONS AND ENERGIES

STATE INDEX[a] α	EXCITED-STATE DESIGNATION			TRANSITION ENERGY
	C_{3v} (Ω_c,ω)-COUPLING	$C_{\infty v}$ (Λ,S)-COUPLING	Ω	(ORIGIN IN cm^{-1})
0	A_1	$^1\Sigma^+$	0	$\equiv 0$
1	E	$^3\Pi_2$	2	49,230
2	E	$^3\Pi_1$	1	49,710
3	A_1,A_2	$^3\Pi_{0^\pm}$	0	54,040
4	E	$^1\Pi_1$	1	54,625

[a]Note that $\alpha = 0$ refers to the ground state.

The specific objectives of the MCD investigations are:

i) Determination of the magnetic moments of the excited states 1 through 4. A comparison of the experimental values of μ with their theoretical counterparts should provide a definitive test of the existing assignments. This is especially important in the cases of transitions $0 \rightarrow 1$ and $0 \rightarrow 3$. An extremely weak band has recently been assigned as $0 \rightarrow 1$, the basis for the assignment being the extrapolation of a presumed progression of vibronically-allowed transitions back to an origin. The transition $0 \rightarrow 3$, which was likewise assigned, is even more uncertain than the $0 \rightarrow 1$ assignment.

ii) The MCD band associated with a transition to a vibronic level should serve as an unambiguous indicator of that state (i.e., 1,2,3 or 4) which functions as the electronic origin for the vibronic band in question. This is an important capability because the vibrational progressions built on the different electronic origins are extensively overlapped in CH_3I.

iii) Some vibronic absorption bands of CH_3I have been assigned to e vibrational excitation of certain of the states 1 through 4. If this be the case, it follows that the e vibrational levels of states 1, 2 and 4, which are also of E symmetry, should exhibit a Jahn-Teller splitting. Consequently, the MCD spectrum should determine the component(s) responsible for the absorption intensity.

EXPERIMENTAL: A schematic diagram of the experimental apparatus is given in Figure 9. The optics are essentially those described by Allen, Schnepp, and Pearson.

The spectrum was measured with a McPherson-225 1m VUV monochromator. A Hinteregger hydrogen discharge lamp served as the radiation source. The

grating, ruled at 600 g/mm, had a reciprocal linear dispersion of 16.6Å/mm. Set widths ranged from 80-150μ. resulting in a resolution of 1.4-2.5Å.

The super-conducting magnet was operated at 4.2°K and maintained a magnetic-field strength of $\sim$ 4Tesla. The photomultiplier tube (EMI 9635 QB, quartz-faced) permitted measurement to 1550Å without concomitant use of scintillators. The electronics associated with initial treatment of the phototube current (i.e., electrometer, log amplifier, differentiator, and filter) were homemade.

The power supply was programmable: Feed-back from the filter maintained the phototube anode current so constant that the feed-back network exhibited a minimal response to frequencies greater than 1 kHz. Therefore, no high-frequency component (e.g., the 50 kHz modulator frequency) of the phototube current was either attenuated or amplified.

The CH_3I (J. T. Baker, reagent grade) was purified by vacuum-freeze-thaw cyclic techniques immediately before introduction into the sample cell. This cell was a vapor flow-cell which was operable at constant cell pressures ranging from 5×10^{-2} to 1Torr. The cell was constructed of non-magnetic stainless steel and was equipped with either LiF or CaF_2 optical windows. It was observed that CaF_2 produced a considerably larger "empty-cell" MCD spectrum than did LiF. However, after subtraction of baselines, either set of windows produced identical sample MCD spectra.

ANALYTICAL ASPECTS: EXPRESSIONS FOR THE ANALYSIS OF AN MCD SPECTRUM. The analysis of an MCD spectrum requires a relationship between the intrinsic molecular magnetic properties and the MCD spectrum. This relationship is a function of the external-magnetic-field strength and the zero-field absorption parameters. The basis of the relationship is two-fold:

---A potential-energy effect attributable to the presence of a magnetic dipole (u_e) in an external magnetic field. This effect produces an energy shift and/or an intensity change of the absorption band.

---A direct field effect which alters the transition moments (and, hence, the absorption intensities) because of field-induced changes in the molecular structure.

General mathematical expressions descriptive of these effects are available. The following derivation of the relationships between the MCD spectrum, the absorbance, the field strength and the intrinsic molecular properties is directed toward the specific objectives of this work.

Certain qualifications and assumptions are inherent in the ensuing derivation. These are:

---The equations apply only to linear or symmetric top molecules.

---The electronic ground state is presumed to be totally symmetric (i.e., it possesses neither electronic angular momentum nor magnetic moment).

---The gas sample is presumed to be isotropically oriented. It is noteworthy, in this connection, that ground-state magnetic moments arising from rotational motion can induce anisotropy.

We distinguish between right circularly polarized light (rcp, or +) and left circularly polarized light (lcp, or -) by the angular-momentum projection (on the propagation vector) associated with the specific polarization. That is, rcp and lcp possess resultant angular momenta of $+\hbar\vec{k}(m_j = +1)$ and $-\hbar\vec{k}(m_j = -1)$, respectively. In addition, the time-dependent electric field associated with rcp (+) and lcp (-) radiation is

$$\vec{E}_{\pm}(t) = \frac{E}{\sqrt{2}} \vec{i} \sin \omega t \mp \vec{j} \cos \omega t \qquad ---(3)$$

where $\vec{i}$ and $\vec{j}$ are unit vectors, orthogonal to each other and to the radiation-propagation vector, $\vec{k}$; where ω is the angular frequency of the radiation; and where E is the scalar field.

THE POTENTIAL-ENERGY EFFECT. A magnetic dipole moment $\vec{\mu}$ in an external magnetic field H has a potential energy, $U = -\vec{\mu} \cdot \vec{H}$. As a result, two distinct terms occur in the MCD expression. One term, attributable to the resultant magnetic moment of the ground state, produces an anisotropic orientation of the ground-state molecules. We assume that this effect is negligible in CH_3I. The second term will occur only when the electronic transition is accompanied by a change in angular momentum. Such a change can occur in CH_3I only when the excited electronic state is degenerate. In order to describe this latter effect, we will first consider an anisotropic sample in which all molecules are oriented with their unique axes parallel to $\vec{k}$. Thereafter, we will remove this restriction and determine the average-overspace effect for an isotropically-oriented sample.

The case $\theta = 0$: Consider the primitive parallel orientation. The potential energy of the excited state after absorption of r.c.p. light is $-\mu_e H$, where the scalar μ_e, the magnitude of the excited-state magnetic dipole moment, and the scalar H are defined as

$$\mu_e \equiv \frac{\vec{\mu}_e \cdot \vec{\Omega}_e}{|\vec{\Omega}_e|} \qquad ---(4)$$

where $\vec{\Omega}_e$ is the resultant electronic angular momentum, and where

$$H \equiv |\vec{H}|$$

It is evident from Fig. 9 that H is positive with respect to $\vec{k}$. Thus, the band resulting from absorption of rcp light is energetically shifted by $-\mu_e H$. We assume that this shift is a "rigid shift" (i.e., that the original band shape is retained). Conversely, for lcp light, the shift is $+\mu_e H$.

Within the confines of the "rigid shift" assumption, the absorbance induced by either rcp or lcp light of energy $\bar{\nu}_0$ in the presence of the field is related to the zero field absorbance as

$$A^{H}_{\pm,\theta=0}(\bar{\nu}_0) = \frac{\bar{\nu}_0}{\bar{\nu}_0 \pm \mu_e H} A^{0}_{\theta=0}(\bar{\nu}_0 \pm \mu_e H) \qquad ---(5)$$

where correction has been made for the inherent energy dependence of absorbance. The absorbance notation used in Eq. 5 and elsewhere in the text is elaborated in Table 4.

Assuming that $A^{0}_{\theta=0}(\bar{\nu}_0 \pm \mu_e H)/(\bar{\nu}_0 \pm \mu_e H)$ can be expressed as a Taylor expansion about $A^{0}_{\theta=0}(\bar{\nu}_0)/\bar{\nu}_0$, we find

$$\frac{A^{0}_{\theta=0}(\bar{\nu}_0 \pm \mu_e H)}{\bar{\nu}_0 \pm \mu_e H} = \frac{A^{0}_{\theta=0}(\bar{\nu}_0)}{\bar{\nu}_0} \pm \mu_e H \left[\frac{d\left(A^{0}_{\theta=0}(\bar{\nu})/\bar{\nu}\right)}{d\bar{\nu}}\right]_{\bar{\nu}_0} + \frac{\mu_e^2 H^2}{2}\left[\frac{d^2\left(A^{0}_{\theta=0}(\bar{\nu})/\bar{\nu}\right)}{d\bar{\nu}^2}\right]_{\bar{\nu}_0} \pm \cdots \qquad ---(6)$$

As a result, Eq. 5 may be rewritten as

$$A^{H}_{\pm,\theta=0}(\bar{\nu}_0) = A^{0}_{\theta=0}(\bar{\nu}_0) \pm \mu_e H\left\{\left[\frac{dA^{0}_{\theta=0}(\bar{\nu})}{d\bar{\nu}}\right]_{\bar{\nu}_0} - \frac{A^{0}_{\theta=0}(\bar{\nu}_0)}{\bar{\nu}_0}\right\} + \cdots \qquad ---(7)$$

It is not usually necessary to retain terms other than those which are linear

TABLE 4. Absorbance Symbols and Definitions

SYMBOL	DEFINITION
$A^{\circ}_{\Theta}(\bar{\nu})$	Zero-field absorbance at energy $\bar{\nu}$ for a sample in which all molecules are oriented with their figure axes at angle Θ with respect to the radiation-propagation vector, $\vec{k}$.
$A^{\circ}_{\Theta=0}(\bar{\nu})$	Special case of $A^{\circ}_{\Theta}(\bar{\nu})$ when $\Theta = 0$.
$A^{O}(\bar{\nu})$	Zero-field absorbance at energy $\bar{\nu}$ for an isotropically-oriented sample.
$A^{H}_{\pm,\Theta}(\bar{\nu})$	Field-on absorbance at energy $\bar{\nu}$, using either right (+) or left (-) circularly polarized light, for a sample in which all molecules are oriented at Θ with respect to $\vec{k}$.
$A^{H}_{\pm,\Theta=0}(\bar{\nu})$	Special case of $A^{H}_{\pm,\Theta}(\bar{\nu})$ when $\Theta = 0$.
$A^{H}_{\pm}(\bar{\nu})$	Field-on absorbance at energy $\bar{\nu}$ for an isotropically-oriented sample.

in field strength. Therefore, the truncated version of Eq. 7 which is linear in H is considered to be a good approximation to the potential-energy effect.

The Case of an Arbitrary Fixed θ: An equally specific orientation is that in which all sample molecules have their unique axes oriented at an angle Θ with respect to H. The effective intensity $|E'_{\pm}|^2$ directed along the unique figure axis when rcp or lcp light of intensity $|E_{\pm}|^2$ is propagated along H can be expressed as a sum of rcp and lcp light

$$|E'_{\pm}|^2_{\theta} = \frac{1}{4}\left\{(1+\cos\theta)^2 |E_{\pm}|^2 + (1-\cos\theta)^2 |E_{\mp}|^2\right\} \qquad ---(8)$$

where the intensity magnitudes $|E_{\pm}|^2$ and $|E_{\mp}|^2$ are equal, the subscripts denoting only the sense of polarization. In other words, the effective intensity at orientation θ for rcp light is designated $|E'_{+}|^2_{\theta}$. This can be considered to be a sum of two beams: A rcp beam of intensity $(1 + \cos)^2/4$ times that of the original beam and a lcp beam of intensity $(1 - \cos\theta)^2/4$ times that of the original beam.

These intensity factors may now be used as scaling parameters to determine $A^0_{\theta}(\bar{\nu}_0)$ relative to $A^0_{\theta=0}(\bar{\nu}_0)$. Consequently, we find

$$A^0_{\pm,\theta}(\bar{\nu}_0) = \frac{1}{4}\left\{(1+\cos\theta)^2 A^0_{\pm,\theta=0}(\bar{\nu}_0) + (1-\cos\theta)^2 A^0_{\mp,\theta=0}(\bar{\nu}_0)\right\}$$
$$= \frac{1}{2}(1+\cos^2\theta) A^0_{\theta=0}(\bar{\nu}_0) \qquad ---(9)$$

The "±" subscripts on the zero-field absorbances are physically irrelevant since, if the sample is not optically active, there is no difference in absorbance of rcp or lcp light in the absence of the field.

$$A^0_{\pm,\theta=0}(\bar{\nu}_0) = A^0_{\mp,\theta=0}(\bar{\nu}_0) = A^0_{\theta=0}(\bar{\nu}_0)$$

$$A^0_{\pm,\theta}(\bar{\nu}_0) = A^0_{\theta}(\bar{\nu}_0)$$

From Eq's. 7 and 8, the "field-on" absorbance of a sample oriented at θ is

$$A^{H}_{\pm,\theta}(\bar{\nu}_o) = \frac{1}{4}\left\{(1+\cos\theta)^2 A^{H}_{\pm,\theta=0}(\bar{\nu}_o) + (1-\cos\theta)^2 A^{H}_{\mp,\theta=0}(\bar{\nu}_o)\right\}$$

$$= \frac{(1+\cos\theta)^2}{4}\left\{A^{o}_{\theta=0}(\bar{\nu}_o) \pm \mu_e H\cos\theta\left[\left(\frac{dA^{o}_{\theta=0}(\bar{\nu})}{d\bar{\nu}}\right)_{\bar{\nu}_o} - \frac{A^{o}_{\theta=0}(\bar{\nu}_o)}{\bar{\nu}_o}\right]\right\}$$

$$+ \frac{(1-\cos\theta)^2}{4}\left\{A^{o}_{\theta=0}(\bar{\nu}_o) \mp \mu_e H\cos\theta\left[\left(\frac{dA^{o}_{\theta=0}(\bar{\nu})}{d\bar{\nu}}\right)_{\bar{\nu}_o} - \frac{A^{o}_{\theta=0}(\bar{\nu}_o)}{\bar{\nu}_o}\right]\right\}$$

$$= \frac{(1+\cos^2\theta)}{2} A^{o}_{\theta=0}(\bar{\nu}_o)$$

$$\pm (\cos^2\theta)\mu_e H\left\{\left(\frac{dA^{o}_{\theta=0}(\bar{\nu})}{d\bar{\nu}}\right)_{\bar{\nu}_o} - \frac{A^{o}_{\theta=0}(\bar{\nu}_o)}{\bar{\nu}_o}\right\} \quad ---(10)$$

<u>The Case of Isotropic Orientation</u>: For the case of isotropic orientation (gas-phase sample), the contribution of those molecules which are oriented at angle θ to the overall zero-field absorbance is

$$\frac{A^{o}_{\theta}(\bar{\nu}_o)\sin\theta\, d\theta}{\int_0^{\pi/2}\sin\theta\, d\theta}$$

It follows from Eq. 9 that the isotropic absorption is

$$A^{o}(\bar{\nu}_o) = \int_0^{\pi/2} A^{o}_{\theta}(\bar{\nu}_o)\sin\theta\, d\theta \Big/ \int_0^{\pi/2}\sin\theta\, d\theta$$

$$= \frac{A^{o}_{\theta=0}(\bar{\nu}_o)}{2}\int_0^{\pi/2}(1+\cos^2\theta)\sin\theta\, d\theta$$

$$= \frac{2}{3} A^{o}_{\theta=0}(\bar{\nu}_o) \quad ---(11)$$

The "field-on" expression follows, in similar fashion, from Eq. 10 and is

$$A^H_{\pm}(\bar{\nu}_0) = \int_0^{\pi/2} A^H_{\pm,\theta}(\bar{\nu}_0) \sin\theta \, d\theta \Big/ \int_0^{\pi/2} \sin\theta \, d\theta$$

$$= \frac{2}{3} A^0_{\theta=0}(\bar{\nu}_0) \pm \frac{\mu_e H}{3} \left\{ \left[\frac{dA^0_{\theta=0}(\bar{\nu})}{d\bar{\nu}} \right]_{\bar{\nu}_0} - \frac{A^0_{\theta=0}(\bar{\nu}_0)}{\bar{\nu}_0} \right\}$$

However, since (Eq. 11)

$$A^0_{\theta=0}(\bar{\nu}_0) = 3/2 \, A^0(\bar{\nu}_0),$$

we finally obtain

$$A^H_{\pm}(\bar{\nu}_0) = A^0(\bar{\nu}_0) \pm \frac{\mu_e H}{2} \left\{ \left[\frac{dA^0(\bar{\nu})}{d\bar{\nu}} \right]_{\bar{\nu}_0} - \frac{A^0(\bar{\nu}_0)}{\bar{\nu}_0} \right\} \qquad ---(12)$$

Eq. 12 refers to an isotropic sample. It relates the absorbance of right or left circularly polarized light (energy $\bar{\nu}_0$) in a magnetic field which is parallel to the propagation vector of the light to (i), quantities which can be measured in the absence of the field; (ii) magnetic field strength; and (iii) the electronic magnetic moment of the excited state. Therefore, Eq. 12 permits determination of the intrinsic molecular quantity μ_e.

In practice, the quantity measured is the absorbance difference between right and left circular polarization. This spectrum can be expressed approximately as

$$\Delta A^H(\bar{\nu}_0) \equiv A^H_-(\bar{\nu}_0) - A^H_+(\bar{\nu}_0) = -\mu_e H \left\{ \left[\frac{dA^0(\bar{\nu})}{d\bar{\nu}} \right]_{\bar{\nu}_0} - \frac{A^0(\bar{\nu}_0)}{\bar{\nu}_0} \right\} \qquad ---(13)$$

The average value of $\left[\frac{dA^0(\nu)}{d\bar{\nu}}\right] \bar{\nu}_0 / \frac{A^0(\bar{\nu}_0)}{\bar{\nu}_0}$ is approximately $\bar{\nu}_0/\Gamma$, where Γ is the half-width of the absorption band. Thus, for $\Gamma \approx 100$ cm^{-1} and $\bar{\nu}_0 \approx 5 \times 10^4$ cm^{-1} (i.e., for values which typify the s-Rydberg bands of CH_3I),

it is a good approximation to neglect $A^{O}(\bar{\nu}_0)/\bar{\nu}_0$. The $\Delta A^{H}(\bar{\nu}_0)$ term due to the potential energy effect may then be expected to exhibit the shape of the first energy derivative of the zero-field absorption band. This linear-field, derivative-shaped dependence is referred to as the $\mathcal{A}$ term.

THE DIRECT-FIELD EFFECT. This effect is also linear in H. However, it is generally much smaller than the potential-energy effect. It arises from an alteration of the molecular electronic structure produced by the magnetic field. The term which describes this MCD effect is known as the term. It arises from the fact that the alteration of structure produces a concomitant change of electric dipole transition moments and, hence, of absorption intensities.

In a perturbation-theory format, the first-order correction to the energy produces a splitting of doubly degenerate states and gives rise to the term. In contrast, the term derives from the first-order correction to the wavefunction and, hence, it is more complicated than the $\mathcal{A}$ term. It has been shown that the $\mathcal{B}$ term introduces a correction to Eq. 13 that is linear in both field strength and absorbance. Furthermore, the effect occurs for transitions which involve both degenerate and non-degenerate states.

A knowledge of $\mathcal{B}$ terms is not a primary concern of this work. However, in the data analysis, it is necessary to consider the direct-field effect in order to determine the $\mathcal{A}$ term accurately. The $\mathcal{B}$ term, therefore, is treated as a parameter and Eq. 13 is altered to read

$$\Delta A^{H}(\bar{\nu}_0) = -\mu_e H\left\{\left[\frac{dA^{\circ}(\bar{\nu})}{d\bar{\nu}}\right]_{\bar{\nu}_0} - \frac{A^{\circ}(\bar{\nu}_0)}{\bar{\nu}_0}\right\} + \mathcal{B}HA^{\circ}(\bar{\nu}_0)$$

$$\cong -\mu_e H\left[\frac{dA^{\circ}(\bar{\nu})}{d\bar{\nu}}\right]_{\bar{\nu}_0} + \mathcal{B}HA^{\circ}(\bar{\nu}_0) \qquad ---(14)$$

ANALYSIS TECHNIQUE. Moment analyses of the bands in the spectrum of CH_3I were performed in order to evaluate μ_e and $\mathcal{B}$. This procedure involves an integration of the MCD and the absorption bands and, via Eq. 14 yields

$$M_1 \equiv \int_{\bar{\nu}_1}^{\bar{\nu}_2} \Delta A^H(\bar{\nu})\, d\bar{\nu} = -\mu_e H \int_{\bar{\nu}_1}^{\bar{\nu}_2} \left[\frac{dA^o(\bar{\nu})}{d\bar{\nu}}\right] d\bar{\nu} + \mathcal{B}H \int_{\bar{\nu}_1}^{\bar{\nu}_2} A^o(\bar{\nu})\, d\bar{\nu}$$

$$= \mu_e H \left[A^o(\bar{\nu}_1) - A^o(\bar{\nu}_2)\right] + \mathcal{B}H \int_{\bar{\nu}_1}^{\bar{\nu}_2} A^o(\bar{\nu})\, d\bar{\nu} \quad \text{---(15a)}$$

and

$$M_2 \equiv \int_{\bar{\nu}_2}^{\bar{\nu}_3} \Delta A^H(\bar{\nu})\, d\bar{\nu} = \mu_e H \left[A^o(\bar{\nu}_2) - A^o(\bar{\nu}_3)\right] + \mathcal{B}H \int_{\bar{\nu}_2}^{\bar{\nu}_3} A^o(\bar{\nu})\, d\bar{\nu} \quad \text{---(15b)}$$

These linear equations may be solved for μ_e and $\mathcal{B}$. This technique is applicable to isolated bands (i.e., when the total absorbance between the limits $\bar{\nu}_1$ and $\bar{\nu}_3$ is attributable to one electronic transition).

In situations where the overlapping of absorption bands introduced uncertainties into the moment analysis technique, two other tactics, both involving a comparison of $[dA^o(\bar{\nu})/d\bar{\nu}]$ and $\Delta A^H(\bar{\nu})/[dA^o(\bar{\nu})/d\bar{\nu}]$ for the band maximum of interest with the same ratio at the maximum of an isolated band for which a good moment analysis was feasible. This tactic which, in essence, is merely a simple scaling technique was found to be quite accurate. The second tactic was employed when the overlapping of bands was so extensive that even the ratio-comparison technique proved useless. In these cases, a qualitative comparison of the MCD and the derivative spectra sufficed to determine the existence of an $\mathcal{A}$ term and, if it existed, its sign. No attempt to extract further information was made in such cases.

VIBRATIONAL CONSIDERATIONS. A primary objective of this work is the MCD analysis of transitions to vibrationally excited Rydberg states. We have found it convenient to categorize such transitions into two general areas:

FRANCK-CONDON-ALLOWED TRANSITIONS. Progressions in an a_1 vibrational mode which are built on the electric-dipole-allowed electronic origins $0 \rightarrow 2$ and $0 \rightarrow 4$ are viewed in terms of the Franck-Condon principle. Since, in this approximation, the electric-dipole operator operates only on the electronic part of the total wavefunction, the same intensity distribution factors (Franck-Condon factors) will appear in both the absorption and MCD spectra. Therefore, the evaluation of μ_e for any a_1 vibrational member should yield a value identical to that of the origin band.

FRANCK-CONDON-FORBIDDEN TRANSITIONS. Singly excited vibrations of type e (i.e., ν_4, ν_5, and ν_6) occur in conjunction with all electronic origins $0 \rightarrow 1$, 2, 3, and 4. Since the Franck-Condon factor for such transitions is identically zero, it is clear that vibronic coupling (i.e., Born-Oppenheimer breakdown) must be invoked. These transitions are subdivided, for convenience, into three distinct categories:

Allowed Electronic Transition: The vibronic states arising from an electronic state of E symmetry and a singly excited $\underline{e}$ vibration are $E \otimes \underline{e} = \underline{a_1}, \underline{a_2}, \underline{e}$. For electronic states 2 and 4, which transform as E and to which transitions from the ground state are allowed, the $\underline{e}$ vibronic component can obtain allowedness by intrastate mixing with the Franck-Condon allowed levels. This, of course, is the Jahn-Teller effect.

Consequently, if the vibronic perturbation is small, the magnetic moment of the excited $\underline{e}$ vibronic state should be identical to that of the parent E state. Therefore, if a vibronic band is perpendicular (i.e., the $\underline{e}$ component), the MCD band should exhibit an $\mathcal{A}$ term of the same magnitude as that of the origin. However, the sign of the $\mathcal{A}$ term is governed by the mixing (i.e., vibronic) state because it is "through" this state that the transition occurs. Consequently, if the angular momenta of the parent and mixing states are

parallel, the $\mathcal{A}_0$ term should possess the same sign as that of the origin; if antiparallel, the signs should be opposite.

Transitions to the $\underline{a_1}$ vibronic components are parallel. Consequently, the corresponding MCD bands will not exhibit any $\mathcal{A}_0$ terms.

Forbidden Electronic Transitions: Degenerate $\underline{e}$ vibrations also couple to the $0 \rightarrow 1$ origin band which, apparently, is electric-dipole-forbidden. The vibronic coupling aspects of this problem mimic those of the above section except that no Jahn-Teller coupling is possible because of the forbiddenness of the $0 \rightarrow 1$ electronic transition. Therefore, intensity may only be borrowed by means of coupling with other electronic states. Arguments concerning the magnitude and the sign of the resulting $\mathcal{A}_0$ term mimic those of the preceeding section with respect to both the $\underline{e}$ and $\underline{a_1}$ vibronic components.

Transitions to Excited Electronic States of a_1 and a_2 Symmetry: This last case concerns the appearance of $\underline{e}$ vibrational activity in transitions to non-degenerate electronic states. A case in point is the $0 \rightarrow 3$ transition. Since the vibronic symmetry is, of necessity, E, intensity borrowing from transitions to E states is required. Thus, though the absorption band is of perpendicular type, the vibronic transition should exhibit no $\mathcal{A}_0$ term simply because the parent electronic state possesses no angular momentum.

RESULTS

The absorption $[A^{O}(\bar{\nu})]$, derivative $[dA^{O}(\bar{\nu})/d\bar{\nu}]$, and MCD $[\Delta A^{H}(\bar{\nu})]$ spectra of gas-phase CH_3I at three sample pressures are shown in Figures 11-13. Derivative spectra are cited with respect to wavelength (λ) rather than energy ($\bar{\nu}$) because of the characteristics of the differentiator circuit. However, since only semi-quantitative comparisons between MCD and derivative spectra are required, the λ-derivatives suffice.

Results are tabulated in Table 5. The values of μ_e are cited, relative to the origin band of the vibronic transition in question, as the absolute numbers $|\mu_e$ (vibrational band)$/\mu_e$ (origin band)$|$. The derivative dependence is also cited as positive, negative, or zero relative tc that of the appropriate origin band. The relative moments, as indicated in the footnotes, were obtained either by the rigorous analysis specified in Eq. 14 or by a comparison of the MCD and derivative spectra as discussed in the Section on Analysis Technique. We now present a breif description of each band system.

BAND SYSTEM 1: The electronic origin of this progression is assigned as the C_{3v} counterpart of the $\Omega = 2 \leftarrow \Omega = 0$ transition which is forbidden in the linear molecule. This assignment is supported by the fact that all members of the band system contain singly-excited modes and that they are, in general, more intense than the origin band at 49,230 cm^{-1}. The MCD bands of all observed members exhibit a positive derivative dependence and yield essentially the same value of μ_e as does the origin band 1. This behavior (see Section on Forbidden Electronic Transitions) is precisely that expected.

BAND SYSTEM 2: The origin, at 49,710 cm^{-1}, is assigned as the C_{3v} counterpart of the lower-energy, allowed $\Omega = 1 \leftarrow \Omega = 0$ transition of the linear molecule. The MCD bands of all a_1 vibrationally-excited members exhibit a positive derivative dependence. They yield essentially equal

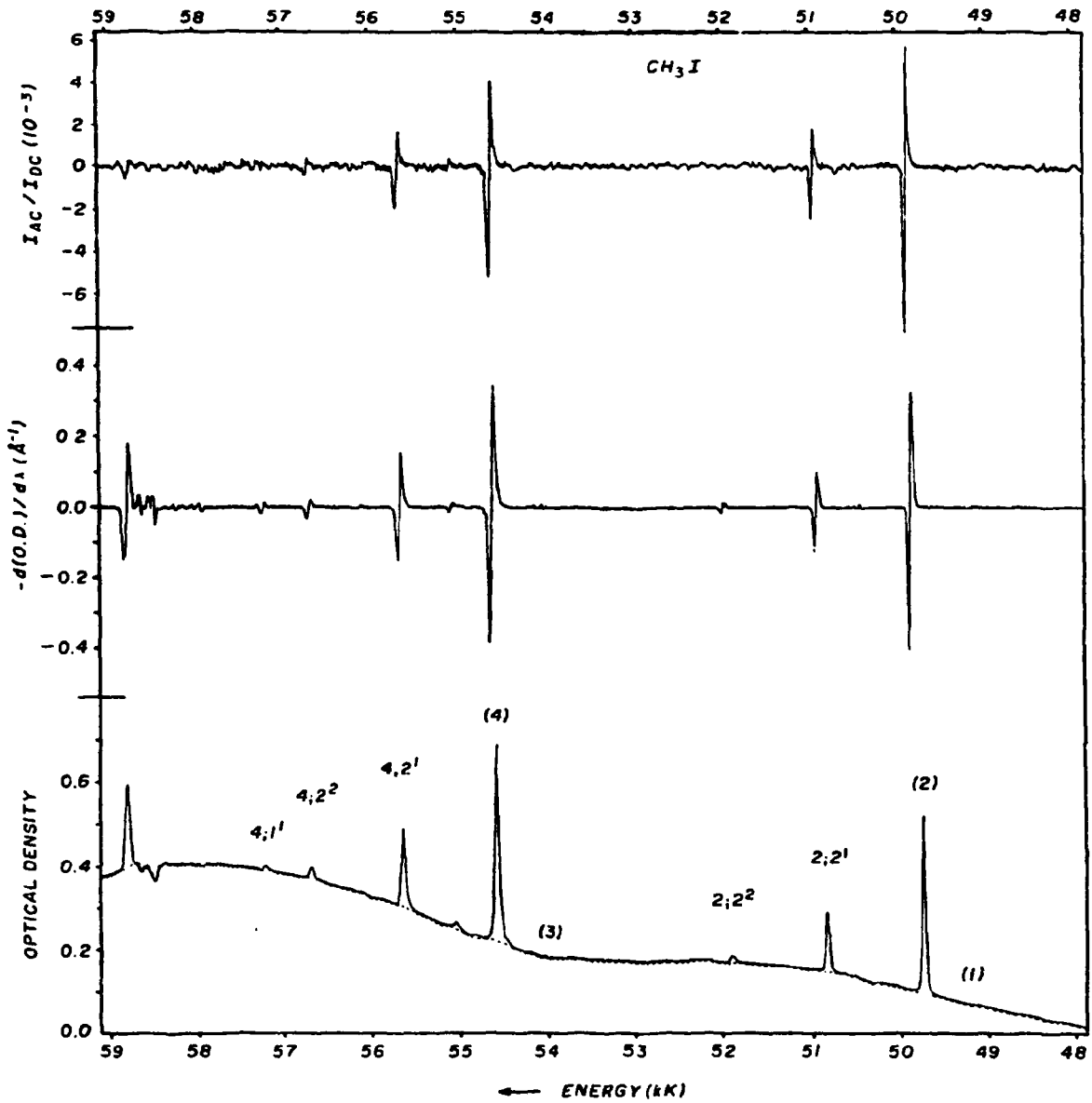
59 58 57 56 55 54 53 52 51 50 49 48
CH_3I
I_{AC}/I_{DC} (10^{-3})
6 4 2 0 -2 -4 -6
-d(O.D.)/dλ ($\AA^{-1}$)
0.4 0.2 0.0 -0.2 -0.4
OPTICAL DENSITY
0.6 0.4 0.2 0.0
(4)
4,2^1
4;2^2
4;1^1
(2)
2;2^1
2;2^2
(3)
(1)
ENERGY (kK)

FIGURE 11

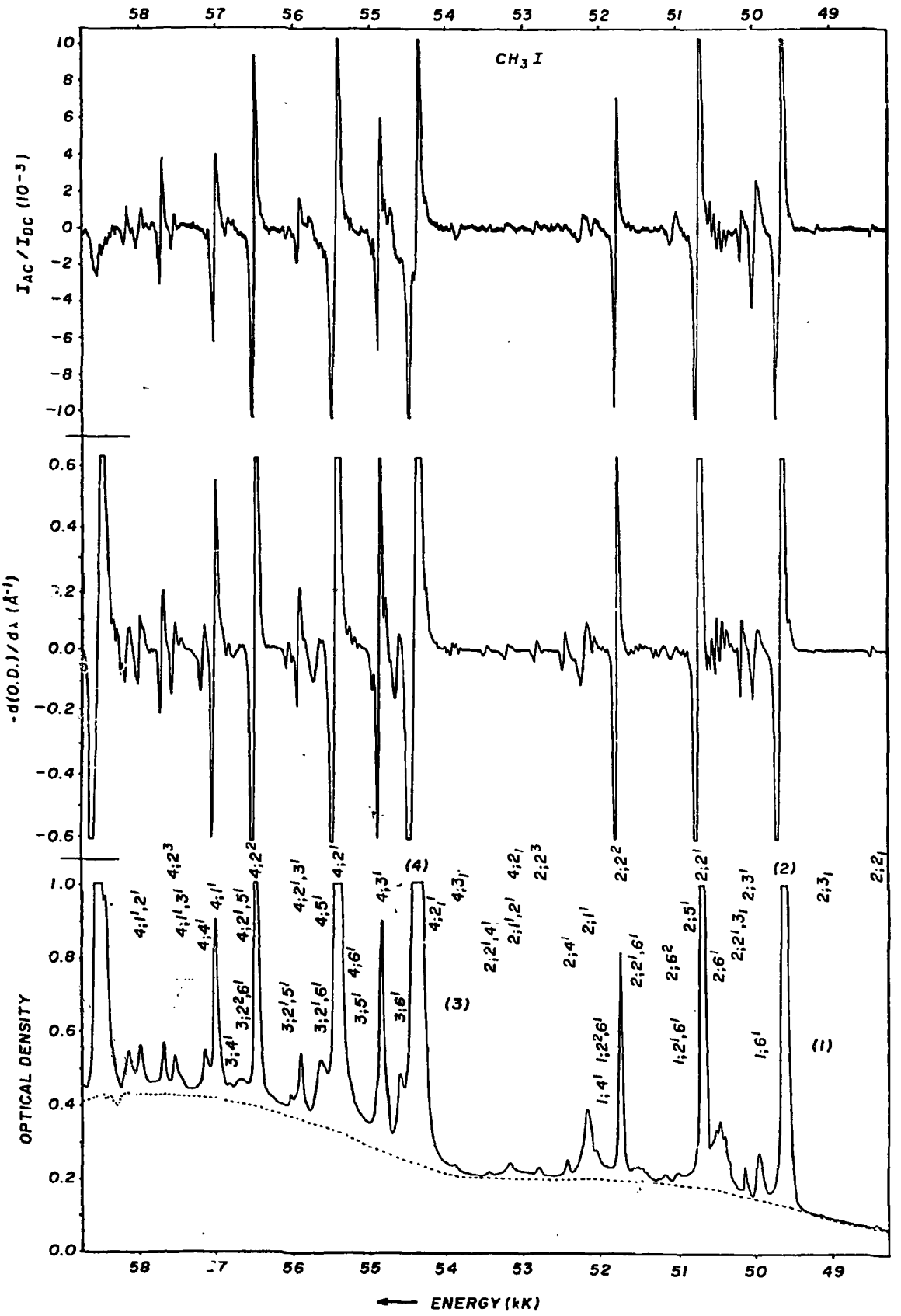
58 57 56 55 54 53 52 51 50 49
CH_3I
I_{AC}/I_{DC} (10^{-3})
10 8 6 4 2 0 -2 -4 -6 -8 -10
-d(O.D.)/dλ ($Å^{-1}$)
0.6 0.4 0.2 0.0 -0.2 -0.4 -0.6
OPTICAL DENSITY
1.0 0.8 0.6 0.4 0.2 0.0
4;1¹,2¹ 4;1¹,3¹ 4;2³ 4;4¹ 4;1¹ 3;4¹ 3;2²,6¹ 4;2¹,5¹ 4;2² 3;2¹,5¹ 4;2¹,3¹ 3;2¹,6¹ 4;5¹ 4;2¹ 4;6¹ 3;5¹ 4;3¹ 3;6¹ (4) 4;2¹ 4;3¹ (3) 2;2¹,4¹ 2;1¹,2¹ 4;2₁ 2;2³ 2;4¹ 2;1¹ 1;4¹ 1;2²,6¹ 2;2¹,6¹ 2;2² 1;2¹,6¹ 2;6² 2;5¹ 2;2¹ 2;6¹ 2;2¹,3₁ 2;3¹ 1;6¹ (2) 2;3₁ (1) 2;2₁
58 57 56 55 54 53 52 51 50 49
← ENERGY (kK)

FIGURE 12

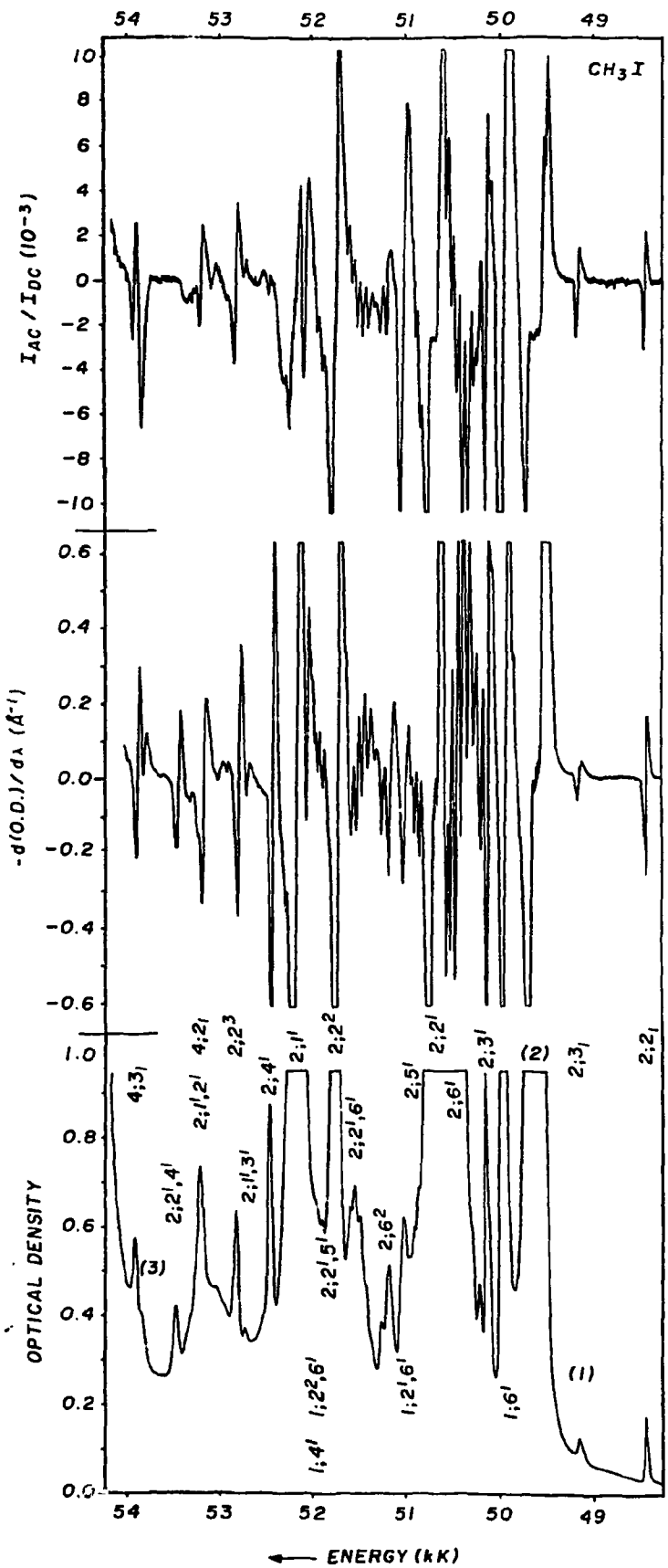
54
53
52
51
50
49
CH3I
IAC / IDC (10-3)
-d(O.D.)/dλ (Å-1)
OPTICAL DENSITY
4;3₁
2;2¹,4¹
2;1¹,2¹
4;2₁
2;2³
2;1¹,3¹
2;4¹
2;1¹
2;2²
2;2¹,5¹
2;2¹,6¹
2;6²
1;4¹
1;2²,6¹
1;2¹,6¹
2;5¹
2;2¹
2;6¹
2;3¹
1;6¹
(2)
2;3₁
(1)
2;2₁
(3)
ENERGY (kK)

FIGURE 13

TABLE 5.

AN MCD ANALYSIS OF THE FIRST s-RYDBERG STATES OF METHYL IODIDE

ASSIGNMENT	ENERGY (cm^{-1})	DERIVATIVE DEPENDENCE[a]	RELATIVE[a] $\lvert\mu_e\rvert$
		BAND SYSTEM 1	
1	49,220	+	1.00
$1;6^1$	49,965	+	$1.02 \pm .05$
$1;2^1,6^1$	51,115	+	1.01[b]
$1;2^2,6^1$ $1;4^1$	51,205	+	0.95[b]
		BAND SYSTEM 2	
$2;2_1$	48,460	+	$0.97 \pm .01$
$2;2_1^1$	49,550	+	c
2	49,710	+	1.00
$2;3^1$	50,195	+	$1.26 \pm .30$
$2;6^1$	50,545	-	$0.89 \pm .10$
$2;2^1$	50,800	+	$1.02 \pm .09$
$2;5^1$	50,940	d	d
$2;6^2$	51,300	+	e
$2;2^1,6^1$	51,640	-	0.92[b]
$2;2^2$	51,890	+	1.00[b]
$2;2^1,5^1$	52,020	-	c
$2;1^1$	52,340	+	1.11[b]
$2;4^1$	52,595	0	---
$2;1^1,3^1$	52,865	+	c
$2;2^3$	52,975	+	
$2;1^1,2^1$	53,375	+	c
$2;2^1,4^1$	53,650	0	---

TABLE 5 (continued)

ASSIGNMENT	ENERGY (cm^{-1})	DERIVATIVE DEPENDENCE[a]	RELATIVE[a] $\lvert\mu_e\rvert$
		BAND SYSTEM 3	
(3)	54,035	0	---
$3;6^1$	54,840	?	---
$3;2^1,6^1$	55,920	0	---
$3;2^2,6^1$	57,020	?	---
$3;2^1,5^1$	56,330	e	e
$3;4^1$	57,020	e	e
		BAND SYSTEM 4	
$4;3_1$	54,100	+	1.02[b]
$4;2_1^1$	54,450	+	c
(4)	54,625	+	1.00
$4;^1$	55,095	+	$0.99 \pm .05$
$4;6^1$	55,450	-	~ 1
$4;2^1$	55,707	+	$1.05 \pm .05$
$4;5^1$	55,920	-	c
$4;2^1,3^1$	56,195	+	~ 1
$4;2^2$	56,780	+	~ 1
$4;2^1,5^1$	57,020	-	c
$4;1^1$	57,300	+	~ 1
$4;4^1$	57,450	0	---
$4;1^1,3^1$	57,770	+	c
$4;2^3$	57,855	+	c
$4;1^1,2^1$	58,320	+	c

[a]Relative to the origin.

[b]Determined by comparison of $\Delta A^H(\bar{\nu})$ and $dA^O(\bar{\nu})/d\lambda$.

[c]This band is extensively overlapped and cannot be treated quantitatively. However, it appears to have approximately the same relative intensity as the origin band.

[d]The MCD band cannot be resolved.

[e]There is a derivative dependence of the same sign and size as the origin of band system 2.

values of μ_e. The value of μ_e for the $2;3^1$ band appears to be somewhat large; however, this vibrational feature also contains the intense $2;6^1$ band -- and this overlapping produces a large uncertainty in μ_e.

MCD bands corresponding to the excitation of e modes are observed. Transitions to singly-excited e vibrations are symmetry forbidden and, as discussed earlier, vibronic coupling is almost certainly responsible for their occurence. All bands assigned to single excitation of ν_5 and ν_6 possess a negative derivative dependence and exhibit values of $|\mu_e|$ which are equal to that of the origin. The value of $|\mu_e|$ for the $2;6^1$ band was obtained by Eq. (14); all others were obtained from a comparison of derivative and MCD spectra.

Only one doubly-excited ν_6 mode, namely $2;6^2$, has been assigned previously. This band exhibits a positive derivative dependence, and a value of μ_e equal to that of the origin.

The ν_4 vibrational mode is responsible for two of the observed bands. The MCD bands exhibit no derivative dependence; hence, there is no $\mathcal{A}$ term present and the active vibronic component must be a_1.

BAND SYSTEM 3: The origin of this band system is very weak and appears merely as a shoulder on the low-energy side of the more intense $4;3_1$ band. The MCD of this origin possesses no derivative dependence. However, a large absorbance-dependence $\mathcal{B}$ term is observed. This is in keeping with the assignment $\Omega = 0 \leftarrow \Omega = 0$ of the linear molecule. The $\mathcal{B}$ term indicates that the origin lies at $54{,}035 \pm 10$ cm^{-1}.

As in progression 1, all bands, other than the origin, contain e vibrational excitations and all of these are more intense than the origin band. Five vibrationally-excited members have been assigned; each of these is discussed breifly in the following:

---The $3;6^1$ band (54,840 cm^{-1}) is overlapped by the much more intense origin band 4. The MCD band is also obscured by this same origin band and it is difficult to determine whether or not it exhibits any derivative dependence. It appears that the band consists only of a $\mathcal{B}$ term of the same sign as that of origin 3.

---The above conjecture is confirmed by the MCD of the $3;2^1,6^1$ band. In this instance, the absence of any derivative dependence is quite definite.

---The $3;2^2,6^1$ band, like the $3;6^1$ band exhibits an uninformative MCD band shape.

---The $3;2^1,5^1$ band exhibits a derivative dependence of the same sign and size as the bands associated with $\underline{a_1}$ vibrational excitation in progression 2. The same observation applies to the $3;4^1$ band.

BAND SYSTEM 4: This band system, with origin at 54,625 cm^{-1}, resembles band system 2 quite closely in both its absorption and MCD profiles. As can be observed from Table II, all vibronic bands which consist solely of $\underline{a_1}$ mode excitations possess a positive derivative dependence and the observed values of $|\mu_e|$ are all essentially identical.

The bands which contain ν_5 excitations show a negative derivative dependence and the values of $|\mu_e|$ appear to be identical to that of the origin band. The single member assigned to the ν_4 vibration (i.e., $4;4^1$) has no derivative dependence.

NON-s-RYDBERG ASSIGNMENTS: Several bands which occur at the high-energy end of the 6s-Rydberg region have been assigned to p-Rydberg electron configurations.

The highest-energy, internal absorption which appears in Figures 11 and 12 has an associated MCD band which displays no derivative dependence. Of the four approximately equally intense bands on the lower-energy side of this

intense band, the first (lowest energy) and third have been assigned previously to band system 4. The second of these four bands displays a MCD intensity which, when compared with the members of band system 4, indicates a magnetic moment which is least twice that of the $\alpha = 4$ origin. The highest-energy band of these four however, appears to belong to band system 4. The shape of this MCD band, however, is somewhat strange when compared with the derivative. It is much narrower and, for this reason, it is thought that a detailed analysis will reveal the presence of two or more near-degenerate transitions.

DISCUSSION

The fundamental motivations of this work were (1) to verify prior electronic assignments by an experimental determination of the magnetic moments of the various states; (2) to validate the assignments of vibrational-progression members; and (3) to determine the symmetries of the Franck-Condon-forbidden vibronic states. The following discussion concerns each of these objectives in turn.

ELECTRONIC ASSIGNMENTS. The validity of the origin band assignments for states 2 and 4 has been established by investigations of relative absorption intensities and term values and by comparative studies of the CH_3I and HI spectra. However, the assignment of the origin bands for states 1 and 3 has posed a problem because of their extremely low intensity and the presence of hot bands, associated with states 2 and 4, are more or less coincidence with them.

Comparison of the relative magnetic moment ratio of states 1, 2, 3 and 4 of 1:0.33:0:0.27 with that calculated from Eq. 2, namely 1:0.33:0:0.33, is excellent. The fact that no A term is observed for state 3 is in accord with the lack of electronic angular momentum of this state.

Two primary effects contribute to departure of the actual magnetic moment ratio from that calculated for a (Λ,S)-coupled, linear molecule. The first, spin-orbit coupling, occurs in the linear and C_{3v} systems. The second, the Coriolis effect, occurs only in the C_{3v} system. The close correlation of theory, in the guise of Eq. 2, with experiment suggests that the C_{3v} perturbation is not significant and that the assignments for the origins 1, 2, 3 and 4 are quite secure.

VIBRATIONAL SERIES ASSIGNMENTS. All MCD bands which have been assigned to

Franck-Condon-allowed transitions exhibit positive $\mathcal{A}$ terms (i.e., positive with respect to the $\mathcal{A}$ term of the origin). They also have values of μ_e which are essentially equal to that of the appropriate origin band. Hence, this work verifies the origin assignments.

For the Franck-Condon-forbidden transitions of band system 1 and singly-excited ν_5 and ν_6 modes of band systems 2 and 4, the MCD bands have the same values of μ_e as those of the appropriate origin bands. Hence, once again the previous origin assignments are substantiated.

The MCD bands assigned to single-excitation of the ν_4 mode in band systems 2 and 4 exhibit no apparent $\mathcal{A}$ terms. This observation is consistent with the assignment of a vibronically-allowed transition since one of the three vibronic components of this state is of $\underline{a_1}$ symmetry.

The band assigned as $2;6^2$ has a positive $\mathcal{A}$ term, unlike all single excitations of ν_6 modes which are joined to origin 2. Since $\underline{e} \otimes \underline{e} \supset \underline{a_1}$, this transition is Franck-Condon allowed. However, a non-zero Franck-Condon factor implies a difference of the ν_6 force constants in states 0 and 2. The frequency of the vibration in state 0 is 880 cm^{-1}, and in state 2, 835 cm^{-1}. Thus, we calculate the Franck-Condon intensity ratio $I(2;6^2)/I(2)$ to be $\sim 0.5\%$. The reported value, which is in excellent agreement, is 1%.

The $2;2^1,3^1$ member is predicted to coincide with the $2;6^2$ member. Since the relative intensities of the $2;2^1$ and $2;3^1$ members are 0.65/0.02, the intensity of the $2;2^1,3^1$ band is expected to be $\sim 1.3\%$ that of origin band 2. This calculated intensity, in conjunction with the MCD spectrum, leads to the inference that the 51300 cm^{-1} band is due to a superposition of both the $2;6^2$ and $2;2^1,3^1$ transitions.

As noted, the MCD data for those features of band system 3 which were assigned as vibronically-allowed transitions in the singly-excited ν_6 mode were difficult to analyze. The $3;2^1,6^1$ band, however, does not exhibit an $\mathcal{A}$ term. As a result, we have assumed that the $3;6^1$ and $3;2^2,6^1$ bands likewise

have no $dA^0(\tilde{\nu})/d\tilde{\nu}$ dependence: The antisymmetric part of these vibrational functions is, after all, identical to that of the $3;2^1,6^1$ band.

The bands assigned to singly-excited ν_4 and ν_5 modes in state 3 possess $\mathcal{A}$ terms. Therefore, one is tempted to discount the existing assignments since the parent electronic state, $^3\Pi_0$ ($\Omega = 0$), has no angular momentum and should not exhibit an $\mathcal{A}$ type MCD signature. However, the same (linear molecule) electron configuration which yields the A_1 state also produces an A_2 state and the transition $0(A_1) \rightarrow 3(A_2)$ is strictly dipole-forbidden. The spatial parts of the $3(A_1)$ and $3(A_2)$ states differ in their ϕ-dependent parts: The A_1 state arises from the symmetric combination of the originally degenerate $C_{\infty v}$ functions whereas the A_2 state arises from the antisymmetric combination. Both transitions $0(A_1) \rightarrow 3(A_1)$ and $0(A_1) \rightarrow 3(A_2)$, when combined vibronically with a single e excitation, become vibronically allowed. It is conceivable that a combination of the $\mathcal{B}$ terms of the near-degenerate A_1 and A_2 excited-state pair could produce a derivative-shaped MCD band (i.e., a pseudo-$\mathcal{A}$ term). A further investigation of this possibility is underway.

VIBRONIC COUPLING. An e vibrational level of states 1, 2 or 4, all of which transform as E in C_{3v} will exhibit a Jahn-Teller splitting into three components e, a_1 and a_2. One should observe transitions to either or both of the a_1 or e components.

State 1: The origin band of the $0 \rightarrow 1$ transition of the linear molecule is forbidden. In CH_3I, it is extremely weak and all the vibrational members observed contain singly-excited e vibrations. In addition, all of these bands are more intense than origin. Therefore, vibronic coupling of state 1 with other electronic states is inferred to be mechanism through which intensity is conferred on zero-order transitions that are both electric-dipole and Franck-Condon forbidden.

The presence of $\mathcal{A}$ terms indicates that the transition occurs to $\underline{e}$ components in each case. The equality of μ_e for the origin band with μ_e for all band system members implies that transition intensity to the $\underline{a_1}$ components is negligible. The sign of the $\mathcal{A}$ terms indicates that the state(s) responsible for the absorption intensity has angular momentum vectors parallel to that of state 1.

The transitions $0 \rightarrow 2$ and $0 \rightarrow 4$ are the only strongly-allowed perpendicular excitations in the vicinity of $0 \rightarrow 1$. It is assumed, therefore, that the vibronic interaction responsible for the intensity of the $0 \rightarrow 1$ band system is stolen from $0 \rightarrow 2$ and $0 \rightarrow 4$. Since these states combine with state 1 in a parallel manner, it follows that the angular function of Eq. 2, $e^{+i\phi}$, of states 2 and 4 couples with the $e^{+i2\phi}$ function of state 1, whereas, $e^{-i\phi}$ couples with $e^{-i2\phi}$.

In summary, it is inferred that the observed vibronic states of band system 1 (i) are of $\underline{e}$ symmetry; (ii), gain transition intensity via mixing with states 2 and 4; and (iii), mix electronically with states 2 and 4 in a parallel manner. The resulting conclusion concerning the vibronic coupling is that the effective ϕ dependent, electronic perturbation Hamiltonian has the form $e^{i\phi} \pm e^{-i\phi}$ and that it leads to an effective symmetry reduction $C_{3v} \rightarrow C_s$.

States 2 and 4: Since transitions to electronic states 2 and 4 are electric-dipole allowed even in the linear molecule, the vibronic transitions which terminate on singly-excited $\underline{e}$ modes are merely Franck-Condon forbidden. Therefore, transition intensity may be induced in the $\underline{e}$ vibronic components by simple Jahn-Teller coupling. The presence of an $\mathcal{A}$ term in the MCD spectrum of these excitations and the values of μ_e relative to the origin band indicate that the vibronically-allowed transitions associated with ν_5 and ν_6 modes terminate on the $\underline{e}$ Jahn-Teller component. The relative signs

of the $\mathcal{A}$ terms suggest that the state(s) responsible for the transition intensity has (have) have their angular momentum vectors anti-parallel to those of the zero-order states 2 and 4.

It is concluded that the zero-order functions, $\Phi(\phi)$, namely $e^{i\phi}$ and $e^{-i\phi}$, mix, respectively, with $e^{-i\phi}$ and $e^{i\phi}$ functions. Consequently, the effective vibronic Hamiltonian must be of the form $e^{i2\phi} \pm e^{-i2\phi}$ and be the first harmonic of the effective potential inferred for state 2.

The MCD bands of all transitions assigned to singly-excited ν_4 modes exhibit no $\mathcal{A}$ terms. Therefore, these transitions terminate on the $\underline{a_1}$ component of the vibronic manifold and coupling with an allowed $\underline{a_1}$ electronic state, possibly the state associated with the highest-energy band in Figs. 11 and 12, is required. The lack of intensity in the $\underline{e}$ component implies a vibronic Hamiltonian whose electronic part possesses a relatively small weighting coefficient for the $e^{\pm i2\phi}$ term. In contrast, the observation of the $\underline{a_1}$ component implies that the weighting coefficient of an $e^{i\phi} \pm e^{-i\phi}$ term is relatively largely.

CONCLUSION

This investigation demonstrates the utility of the MCD technique in the study of Rydberg transitions. The previous assignments of electronic-transition origins have been verified, and the assignments of vibrational band members have been elaborated. Vibronically-induced transitions were investigated and the symmetries of the corresponding excited states were deduced: In each case of vibronic interaction, only one component was observed though two were symmetry allowed.

This work suggests several problems on which MCD can provide significant experimental information. These include spin-orbit interaction, vibronic coupling, and the relationship between the electronic singular momentum of a linear molecule and that of a symmetric top. Work on these topics is presently underway.

IV. PHOTOELECTRON SPECTROSCOPIC (UPS) STUDIES

IV. PHOTOELECTRON SPECTROSCOPIC (PES) STUDIES

The items of Section II.A which refer to photoelectron spectroscopic studies are:

134, 137, 138, 139, 140, 145, 149, 150, 156, 159, 165, 166 and 168.

Approximately 25% of all the work performed was of a photoelectron spectroscopic nature. Despite the fact that the studies were very varied, they can be synopsized in only a few categories.

A. PES OF DICARBONYLS

(See items 134, 137, 138, 139, 140, 149, 156, 157, 159)

The carbonyl group is one of the more important functional groups in chemistry. As a result, we have invested considerable work in an effort to determine the manner in which carbonyl groups interact among themselves and with other functional groups.

A "simple dicarbonyl compound" is defined as one which contains neither heteroatoms (other than two oxygens) nor carbon-carbon unsaturation. The two highest-occupied MO's of simple dicarbonyls consist predominantly of linear combinations of the two oxygen non-bonding 2p atomic orbitals, n_1 and n_2. For symmetrical dicarbonyls, the symmetry-adapted, semi-localized functions are

$$n_+ = \frac{1}{\sqrt{2}}(n_1+n_2)$$

$$n_- = \frac{1}{\sqrt{2}}(n_1-n_2)$$

where the subscripts +/- refer to phasing. These functions, $n_{+/-}$ are degenerate in a zeroth-order approximation.

For non-symmetrical dicarbonyls, they are

$$n_+ = an_1 + bn_2$$

$$n_- = cn_1 - dn_2$$

where, in the absence of overlap of n_1 and n_2, $b = \sqrt{1-a^2}$, $c = b$ and $d = a$. These functions are non-degenerate even in zeroth-order.

The purpose of this work is to develop criteria for the assignment of the non-bonding MO's of dicarbonyls. This is accomplished by collecting UPS data for a large number of dicarbonyls and noting regularities in them. It is found that relevant assignment criteria can be derived directly from the following investigations.

---The nature of the interactions which lift the zero-order degeneracy of the n_+ and n_- MO's: The magnitude of interaction as a function of carbonyl separation is experimentally determinable. One merely obtains an average value of $|I(n_+) - I(n_-)| \equiv \Delta\bar{n}$ for fixed carbonyl separations and notes that this average is quite representative of the splitting Δn found in all such compounds.

---The magnitude of this splitting as a function of the separation of the two carbonyl centers: The energetic order of n_+ and n_- is usually obtained by MO computations. No attempt at any greater generality exists.

---The energetic order of the n_+ and n_- MO's which results from the splitting: The removal of the n_+/n_- degeneracy is accomplished, on a theoretical level, by through-bond mixing with skeletal σ orbitals. Since these σ orbitals are more tightly bound than the n orbitals, these interactions always destabilize the n MO's.

---The Franck-Condon band shapes of the n_+/n_- ionization bands: The

ionization of an electron from a skeletally delocalized π orbital should produce a geometry change. Thus, the adiabatic and vertical transition for such an ionization event should be quite different and the resulting band shape might well be broad and Gaussian. The removal of an electron from a skeletally non-delocalized n orbital should produce little geometry change of the cationic state. Therefore, the adiabatic and vertical transitions might well be coincident. If only approximately coincident, the intensity of such a band will drop less sharply to higher energies, generating a band shape which we refer to as "blue degraded". For somewhat obvious reasons, we refer to the ionization event of gaussian band shape as $I(n^{\sigma})$ and to the blue-degraded event as $I(n^{o})$.

(i) α-DICARBONYLS

α-Dicarbonyls exhibit the largest interactions. The magnitude of the interaction is thought to be independent of the dihedral angle between the carbonyl units: Figure 1 is a schematic of the interaction model. An unspecified cis-α-dicarbonyl is pictured, although the same results obtain for all dihedral angles, including the cis and trans conformations.

The σ bond between the carbonyls and the bonds peripheral to the carbonyls are the only ones which will interact strongly with the n MO's. Furthermore, symmetry considerations indicate that only the n_+ MO will be affected. Hence, we use the labelling n_+^{σ}, where the superscript σ suggests that the $I(n_+^{\sigma})$ event should possess a gaussian band shape. The non-interacted orbital is denoted n_-^{o} and should exhibit a blue-degraded $I(n_-^{o})$ band shape. Therefore, the predicted MO order is

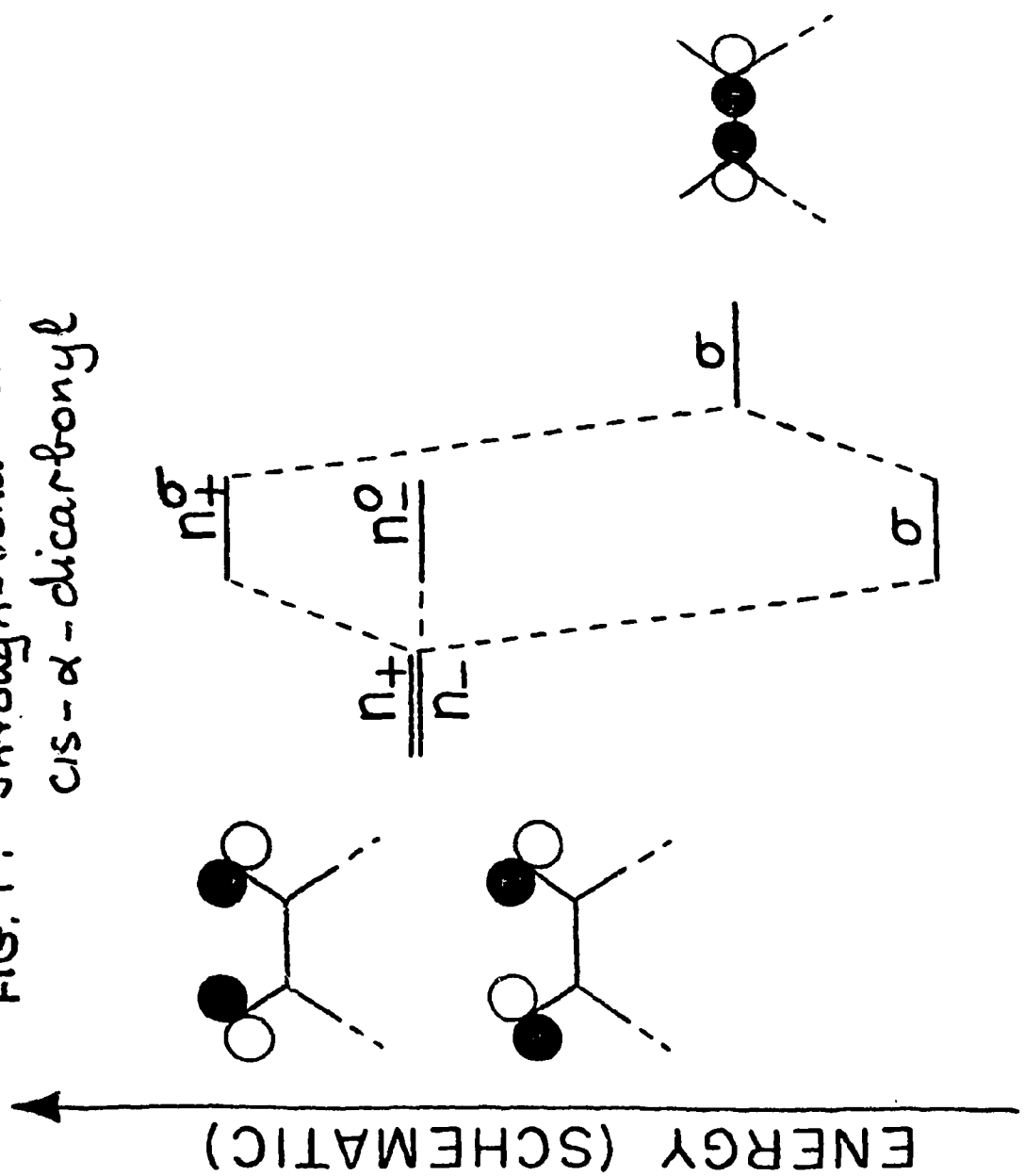
FIG. 1 : Through-bond interaction in a cis-4-dicarbonyl
ENERGY (SCHEMATIC)
n+σ
n°
n+
n−
σ
σ

$n_+^\sigma > n_-^o$ and the expected band shape characteristics are gaussian and blue-degraded, respectively.

The MO diagrams, as obtained by CNDO/s for the simplest α-dicarbonyl, namely trans-glyoxal, are shown in Figure 2. The observed n orbital ionization bands are also shown in Figure 2. The LCAO coefficients of Figure 2 clearly demonstrate the dominance of σ mixing in the n_+ MO and its near absence in the n_- MO. Figure 2 exemplifies all points presented in our discussion of α-dicarbonyls.

The vertical ionization energies for the two n MO's of 34 α-dicarbonyls are listed in Table 1 along with the difference, Δn, between them. The data show that, although $I(n_+)$ and $I(n_-)$ vary widely for different molecules, $\Delta\bar{n}$ is relatively constant. In fact, for the first 26 compounds listed, it is found that $\Delta\bar{n} = 1.9 \pm 0.15$eV (mean and standard deviation). This constancy is emphasized in Figure 3.

(ii) β-DICARBONYLS

The through-bond interactions in β-dicarbonyls are mediated by two intervening σ bonds. Calculations suggest that $n_-^\sigma > n_+^o$ by 0.8eV. The same MO order and similar energetic splittings are obtained for all conformations, except those for which direct overlap between the two lone pairs is significant. In this latter case, the MO order is unchanged but $\Delta\bar{n}$ increases.

Table 2 lists the vertical ionization energies and the values of $\Delta\bar{n}$ for β-dicarbonyls. The behavior of $\Delta\bar{n}$ for these molecules is shown in Figure 4. Several observations are appropriate:

---$\Delta\bar{n}$ is considerably smaller for β-dicarbonyls than for α-dicarbonyls.

---The $\Delta\bar{n}$ values for formylurea and acetylurea are slightly larger than

FIG 2: trans-Glyoxal

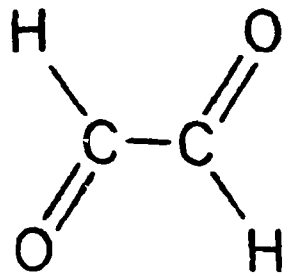

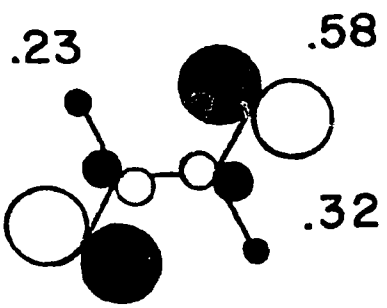

n_+^{σ}

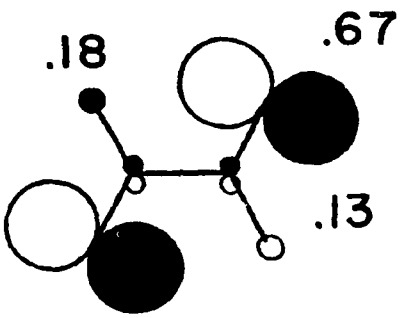

n_-^{o}

TABLE 1

VERTICAL IONIZATION ENERGIES (eV)

FOR THE NON-BONDING MO's OF α-DICARBONYLS.

The difference $\Delta\bar{n}$ is defined as $\Delta\bar{n} \equiv |I_{(n_+)} - I_{(n_-)}|$

NUMBER INDEX	COMPOUND	$I_{(n_+)}$	$I_{(n_-)}$	$\Delta\bar{n}$
1	HCOCOH	10.52	12.19	1.67
2	$CH_3COCOCH_3$	9.55	11.46	1.91
3	$CH_3COCOOH$	10.42	12.42	2.00
4	$CH_3COCOOCH_3$	9.88	11.66	1.78
5	$CH_3COCONH_2$	9.71	11.48	1.77
6	$HOCOCONH_2$	10.51	12.40	1.89
7	$C_2H_3OCOCONH_2$	9.85	11.73	1.88
8	$C_2H_3OCOCON(CH_3)_2$	9.31	11.09	1.78
9	$H_2NCOCONH_2$	9.80	11.72	1.92
10	HOCOCOOH	11.20	13.25	2.05
11	ClCOCOCl	11.26	13.42	2.16
12	$C_2H_5OCOCOCl$	10.77	12.76	1.99
13	$(CH_3)HNCOCONH(CH_3)$	9.33	11.20	1.87
14	$(CH_3)_2NCOCON(CH_3)_2$	∿9.0	10.49	∿1.49
15	1,2-cyclobutanedione	9.58	11.70	2.12
16	[4.4.2]propella-11,12-dione	8.65	10.4	1.75
17	[4.4.2]propell-3-ene-11,12-dione	8.60	10.5	1.9
18	[4.4.2]propella-3,8-diene-11,12-dione	8.70	∿10.7	∿2.0

TABLE 1 (cont.)

NUMBER INDEX	COMPOUND	$I_{(n_+)}$	$I_{(n_-)}$	$\Delta\bar{n}$
19	3,3,7,7-tetramethyl-1,2-cycloheptanedione	8.70	10.60	1.90
20	3,3,7,7-tetramethyl-5-oxa-1,2-cycloheptanedione	8.90	10.90	2.0
21	3,3,7,7-tetramethyl-7-thia-1,2-cycloheptanedione	8.75	10.65	1.90
22	3,3-dimethylindanedione	8.7	10.8	2.1
23	diphenylglyoxal	9.1	11.1	2.0
24	Camphorquinone (3,7,7-trimethyl-bicyclo[2.2.1]hept-2,3-dione)	8.71	10.46	1.75
25	Bicyclo[2.2.1]hept-2,3-dione	9.00	10.85	1.85
26	7,7-cyclopropylbicyclo [2.2.1]hept-2,3-dione	8.75	∿10.7	∿1.95
27	Tetrafluoro-1,2-cyclobutanedione	10.45	13.04	2.59
28	Bicyclo[2.2.1]hept-5-ene-2,3-dione	8.73	11.17	2.44
29	5-methylbicyclo[2.2.1]hept-5-ene-2,3-dione	8.50	10.90	2.40
30	7,7-dimethylbicyclo[2.2.1] hept-5-ene-2,3-dione	8.50	10.80	2.30
31	7,7-cyclopentylbicyclo[2.2.1] hept-5-ene-2,3-dione	8.45	10.75	2.30
32	7,7-cyclopropylbicyclo[2.2.1] hept-5-ene-2,3-dione	8.50	∿10.95	∿2.45
33	7-isopropenylbicyclo[2.2.1] hept-5-ene-2,3-dione	8.30	10.90	2.60
34	7-oxabicyclo[2.2.1] hept-5-ene-2,3-dione	8.95	11.55	2.60

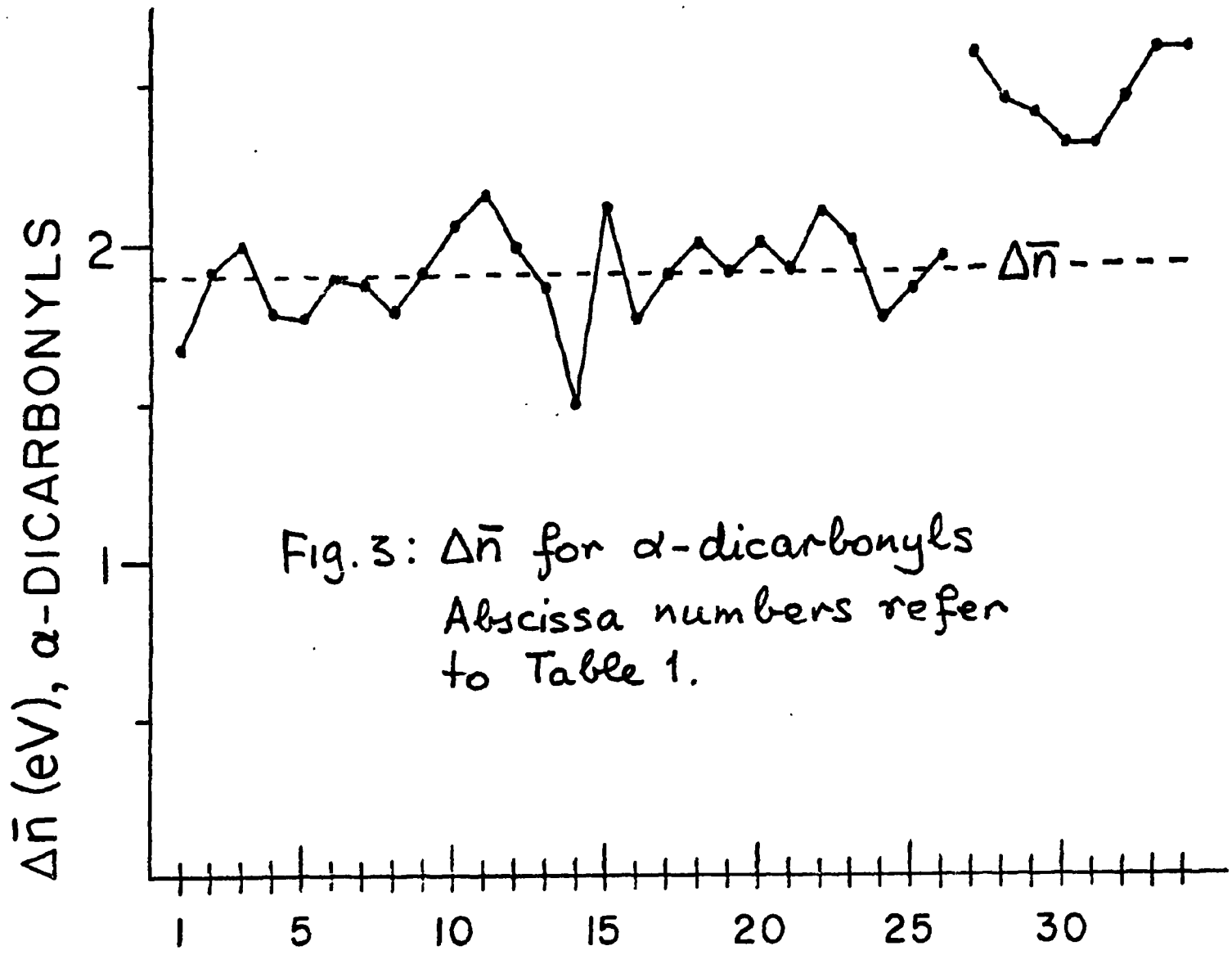

Fig. 3: $\Delta\bar{n}$ for α-dicarbonyls
Abscissa numbers refer
to Table 1.

TABLE 2

VERTICAL IONIZATION ENERGIES (eV)

FOR THE NON-BONDING MO's OF β-DICARBONYLS.

The difference $\Delta\bar{n}$ is defined as $\Delta\bar{n} \equiv |I_{(n_-)} - I_{(n_+)}|$

NUMBER INDEX	MOLECULE	$I_{(n_-)}$	$I_{(n_+)}$	$\Delta\bar{n}$
1	2,2-dimethyl-1,3-propanedial	9.8	10.5	0.7
2	2,4-pentanedione	∿9.6	10.15	∿0.55
3	3-methyl-2,4-pentanedione	9.43	10.05	0.62
4	3,3-dimethyl-2,4-pentanedione	9.30	9.86	0.56
5	formylurea	∿10.6	11.35	∿0.75
6	acethylurea	∿10.3	11.1	∿0.8
7	1,3-cyclopentanedione	9.53	10.40	0.87
8	2-methyl-1,3-cyclopentanedione	9.40	10.18	0.78
9	2,2-dimethyl-1,3-cyclopentanedione	9.34	10.05	0.71
10	succinic anhydride	10.80	11.61	0.81
11	maleic anhydride	11.10	11.95	0.85
12	succinimide	∿10.1	∿10.8	∿0.7
13	N-methylsuccinimide	∿10.0	10.71	∿0.71
14	1,3-cyclohexanedione	9.60	10.04	0.44
15	2-methyl-1,3-cyclohexanedione	9.48	9.81	0.33
16	2-isopropyl-1,3-cyclohexanedione	9.29	9.61	0.32
17	2-t-butyl-1,3-cyclohexanedione	9.15	9.62	0.47

TABLE 2(cont.)

NUMBER INDEX	MOLECULE	$I_{(n_-)}$	$I_{(n_+)}$	$\bar{\Delta n}$
18	glutaric anhydride	10.58	11.17	0.59
19	glutarimide	10.05	∿10.5	∿0.45
20	dihydrouracil	∿10.1	11.0	∿0.9
21	uracil	10.13	11.0	0.87
22	thymine	10.05	10.88	0.83
23	1,3-dimethyluracil	9.70	10.55	0.85
24	2,2,4,4-tetramethyl-1,3-cyclobutanedione	9.53	8.80	0.73

Fig.4 : $\Delta\bar{n}$ for β-dicarbonyls
Abscissa numbers refer to Table 2

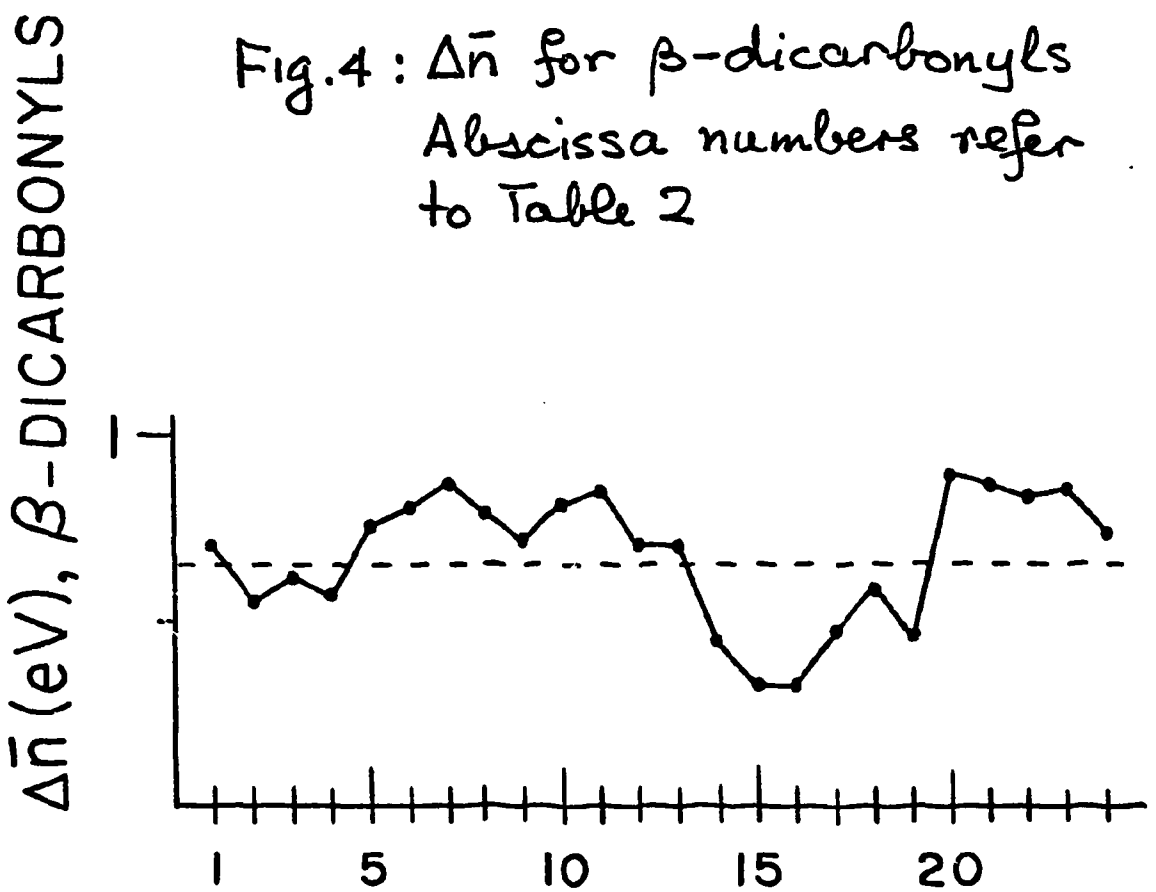

those for the simple acyclic dicarbonyls.

---The value of $\Delta\bar{n}$ for the 5-membered-ring cyclic molecules is 0.8 ± 0.1eV and is quite constant.

---Values of $\Delta\bar{n}$ for the symmetrical 6-membered-ring cyclic molecules (numbers 14 through 19 of Table 2) are generally less than for other compounds of Table 2.

We now rationalize the observed I(n) band shapes of non-coaxial β-dicarbonyls. It is empirically clear that the n_-^σ MO must be significantly more skeletally involved than n_+^o: The directed carbon-carbon bonds of n_-^σ contribute significantly to bonding between the carbonyls and, therefore, ejection of an electron from n_-^σ should produce a geometry change in the σ structure between the carbonyls and generate a gaussian UPS band. In n_+^o, the bonds between the carbonyls are not directed; in fact, the atomic orbital on carbon two (C_2) is so directed that it is effectively non-bonding (i.e., there is little overlap with the AO's on C_1 and C_3). Ejection of an electron from n_+^o, therefore, should produce a negligible effect on the skeletal geometry and cause $I(n_+^o)$ to be blue-degraded.

(iii) γ-DICARBONYLS

UPS data exist only for eight such molecules. These data are listed in Table 3 and the $\Delta\bar{n}$ values are plotted in Figure 5. Second, the carbonyl groups in all eight of these molecules are coaxial. As for β-dicarbonyls, coaxial carbonyl groups are found to invert the n MO order obtained for non-coaxial γ-dicarbonyls.

(iv) δ-DICARBONYLS

CNDO/s calculations on 1,5-pentanedial yield $n_-^\sigma > n_+^o$, just as in

TABLE 3

VERTICAL IONIZATION ENERGIES (eV)

FOR THE NON-BONDING MO's OF γ-DICARBONYLS.

The difference $\Delta\bar{n}$ is defined as $\Delta\bar{n} \equiv |I_{(n_+)} - I_{(n_-)}|$

NUMBER INDEX	MOLECULE	$I_{(n_-)}$	$I_{(n_+)}$	$\Delta\bar{n}$
1	1,4-cyclohexanedione	9.65	∿9.85	∿0.2
2	1,4-benzoquinone	9.99	10.29	0.30
3	2-methyl-1,4-benzoquinone	9.78	10.17	0.39
4	2,5-dimethyl-1,4-benzoquinone	9.60	∿10.05	∿0.45
5	tetramethyl-1,4-benzoquinone	9.25	9.75	0.50
6	tetrachloro-1,4-benzoquinone	9.90	∿10.1	∿0.2
7	2,3-dichloro-5,6-dicyano-1,4-benzoquinone	10.58	10.76	0.18
8	tetrafluoro-1,4-benzoquinone	11.21	10.96	0.25

non-coaxial β-dicarbonyls. Computed $\Delta\bar{n}$ values for several molecular conformations are effectively constant at ∿0.4eV.

The UPS data for three δ-dicarbonyls are listed in Table 4 and the $\Delta\bar{n}$ values are plotted in Figure 5. Since only three compounds are listed in Table 4, the results can hardly be considered general. However, in view of the nature of the molecules being investigated, it does not seem likely that this list will be appreciably lengthened in the near future.

(v) CONCLUSIONS

The conclusions for this work are:

---The through-bond nature of dicarbonyl interactions is confirmed. Through-space interactions are also observed: These are most clearly exemplified by entries 27 through 34 in Table 1.

---The magnitude of the through-bond dicarbonyl interaction as a function of the spatial separation of the carbonyl groups is summarized in Table 5. The interaction, as measured by $\Delta\bar{n}$, decreases rapidly with increasing carbonyl separation. The concept of an average interaction energy, gauged by $\Delta\bar{\bar{n}}$, possesses considerable validity.

---The energetic order of the non-bonding MO's of dicarbonyls can be synopsized by dividing them into two classes: Those in which the carbonyl groups are coaxial, and those in which they are not. Figure 6 provides a schematic of the results obtained.

---UPS band shape differences are rationalized. This is accomplished by noting that the form of the n MO's between the carbonyls controls the band shape tendencies. The gaussian band always derives from the n MO

TABLE 4

VERTICAL IONIZATION ENERGIES (eV)

FOR THE NON-BONDING MO's OF δ-DICARBONYLS.

The difference $\Delta\bar{n}$ is defined as $\Delta\bar{n} \equiv |I_{(n_+)} - I_{(n_-)}|$

NUMBER INDEX	MOLECULE	$I_{(n_-)}$	$I_{(n_+)}$	$\Delta\bar{n}$
1	1,3-diacetylazulene	∿9.1	∿9.1	∿0
2	cis-bicyclo[3.3.0] octane-3,7-dione	9.45	9.78	0.33
3	4,6,8-trimethyl-1,3-diacetylazulene	8.4	8.75	0.35

Fig.5: $\Delta\bar{n}$ for γ- and δ-dicarbonyls
Abscissa numbers for the γ-case refer to Table 3, and for the δ-case to Table 4

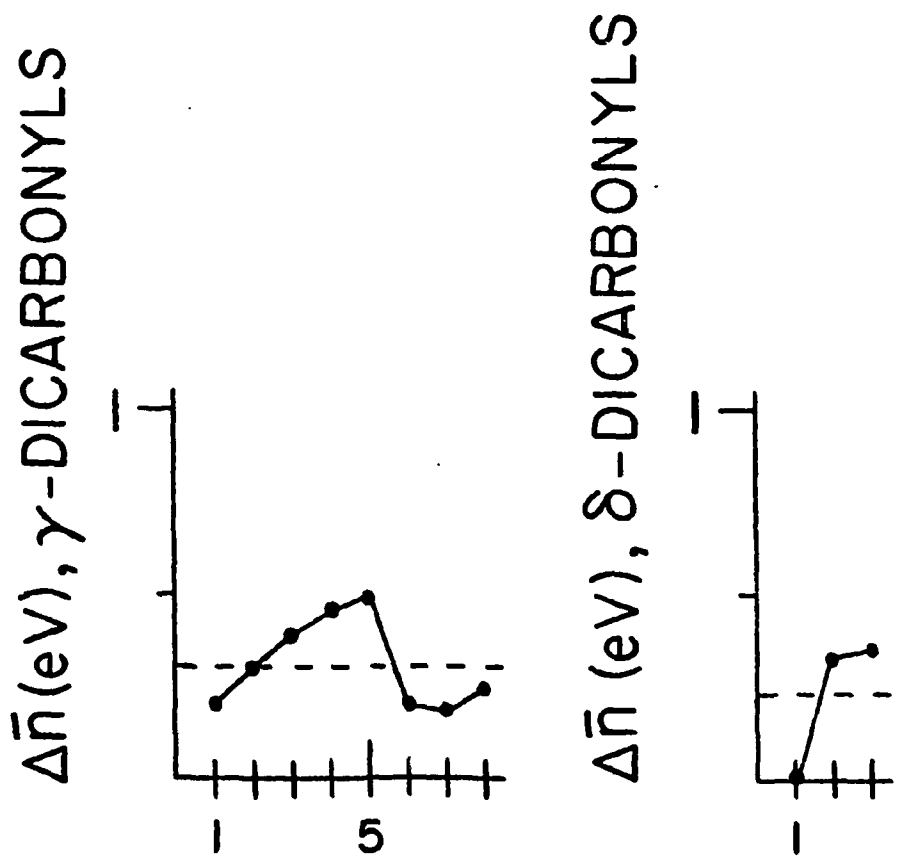

TABLE 5

MEAN VALUES OF $\Delta\bar{n}$ AND STANDARD DEVIATION (RMS)

FOR α,β AND γ-DICARBONYLS. ALL VALUES ARE IN eV.

	$\Delta\bar{n}$	Standard Deviation
α-dicarbonyls	1.9	0.15
β-dicarbonyls	0.65	0.17
γ-dicarbonyls	0.3	0.13
δ-dicarbonyls	(0.23)	---

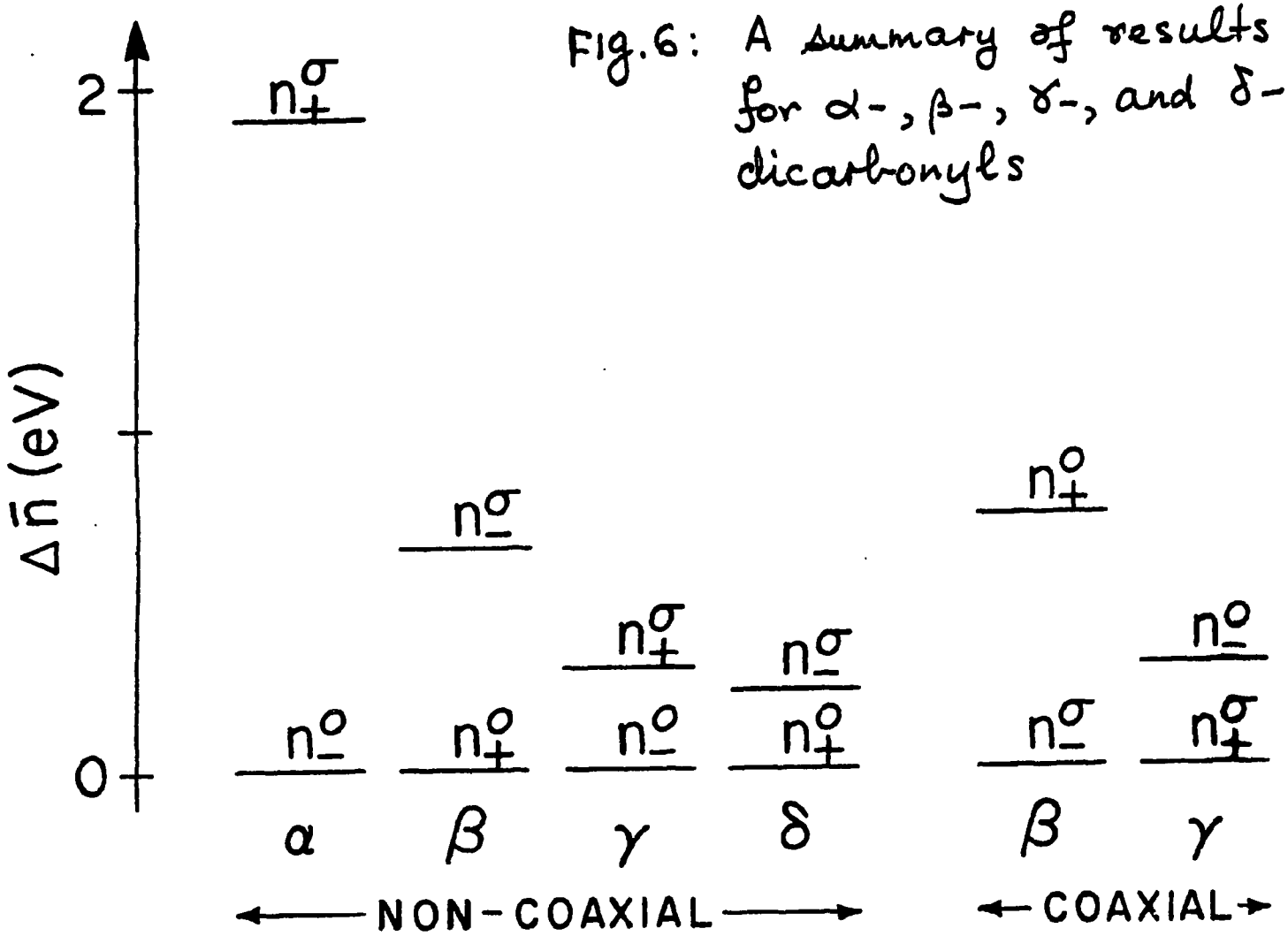

Fig.6: A summary of results for α-, β-, γ-, and δ-dicarbonyls

with directed σ bonds, while the blue-degraded band always arises from the n MO in which the skeletal σ orbital between the carbonyls are effectively non-bonding.

---The gaussian shaped UPS band lies at lower ionization energy in non-coaxial dicarbonyls, and the blue-degraded band lies at lower ionization energy in coaxial dicarbonyls.

B. BIOLOGICAL CONSIDERATIONS

Ultraviolet photoelectron spectroscopy (UPS) has had enormous impact on chemistry. It is assured that it will have comparable influence on molecular biology. The reasons are straightforward: First, the UPS measurement technique is simple and direct; second, a great deal of interpretive ease is guaranteed by Koopmans' theorem, and, third, because of Koopmans' theorem, the UPS data relate in a straightforward way to a very basic electronic structure concept, namely the canonical molecular orbital.

Koopmans' theorem consists of two parts. The first part is a simple energy equivalence $I(k) = -\varepsilon(k,SCF)$ which equates the kth ionization limit to the negative of the kth spin-orbital energy. The second, and more important part is a selection rule which states that the only events of significant probability are those which depopulate individual spin-orbitals. Put another way, this rule states that "shake-up" and "shake-off" events are improbable. Consequently, the mapping of UPS events onto the filled valence spin-orbital set is isomorphic. If spin-orbital coupling is negligible (i.e., $\xi < 20meV$), this isomorphism simplifies further and refers now to the MO (and not MSO) set.

The majority of all UPS works are implicitly based on this isomorphism. Usually, such works generate a set of empirical numbers (UPS data) and a set of theoretical numbers (a quantum chemical scheme), and invoke the Koopmans' energy equivalence as the sole exemplar of the isomorphism. Such a mapping technique is inadequate. First, the quantum chemical scheme is usually algorithmic and not of HF-SCF quality; second, the Koopmans' energy equivalence, because of correlation and relaxation neglects, is probably accurate only to 1 or 2eV; and, third, the mapping is best vested in a comparison of the empirical cationic charge density (more specifically, the charge density of the positive hole) with that of the canonical HF-SCF MO from which charge has been removed in the ionization event. Indeed, one could wax cynical and assert, with much truth, that our trust in the verity of Koopmans' theorem stems not so much from the existence of a great deal of corroborative data as from a dearth of contrary evidences.

Despite this, it must be admitted that considerable UPS experience now exists; that Koopmans' theorem, in both its aspects, appears to be highly valid; that the expertise pertinent to the recognition of non-Koopmans' situations does exist; and that the net result has been a most concrete vindication of the orbital concept and an accretion of information on the electronic structure of molecules. Unfortunately since the UPS technique involves gas phase measurements, almost all of this experience refers to small, non-polar (or weakly-polar) molecules. Little or no data is available for the large polar molecules which constitute the majority type in the biological regime: These molecules usually decompose at temperature considerably lower than those required for gasification.

(i) EXPERIMENTAL

The gas pressures required for UPS measurements have a lower limit of $\sim$1um($\sim 10^{-3}$ mm Hg). It has been found that many biological materials which decompose readily in the ambient atmospheric environment do not do so (or, at least, do not do so quite as readily) in high vacuum. The general procedure which we have followed is based on the availability of the heated sample probe. It consists of a slow heating rate of $\sim 1^{\circ}$C/minute until the sample pressure is $\sim$1um. The spectrum is then recorded and its constancy in time checked. A number of decomposition indicators exist. These may be as obvious as inspection of the sample for change of color or charring; as definitive as mass spectrometry; or as sensitive as the UPS spectrum itself to slight contamination by a variety of small but rather probable decomposition products. Indeed, the instrumental sensitivity to contaminants is such that little difficulty is experienced in defining either the optimum temperature range or the decomposition products which appear when the upper limits are exceeded. Of course, spectra cannot be obtained for those materials (e.g., Vitamin K_1, protoporphyrin IX dimethyl ester, etc.) which decompose before pressures of $\sim 1\mu$ are achieved.

The spectra reported here were obtained on a Perkin-Elmer PS-18 photoelectron spectrometer. The sample area was capable of sustaining temperatures as high as 350°C to within $\pm 2^{\circ}$C. Normal resolution ($\sim$20meV) degrades for T $\geq 140^{\circ}$ and, at 300°C, is 75-100meV. Our experience suggests that the great majority of small to medium-sized biological molecules (vide infra) will yield to such measurements.

(ii) BEYOND UPS

The restriction to gas phase studies is irksome. If such studies were feasible in the solid state, the decomposition attendant to heating could be avoided and molecular size or complexity would not be a limiting factor. It is our opinion that X-ray fluorescence and Auger spectroscopy provide pertinent techniques for this purpose. A schematization of the UPS and X-ray fluorescence experiments is shown in Figure 7. It is clear that both processes contain similar information, that of X-ray fluorescence being greater since it also provides a physical (as opposed to chemical) means of assessing MO shapes and their AO compositions. The Auger process is complementary to X-ray fluorescence; it also contains similar information, and is intense where X-ray fluorescence is minimal (e.g., carbon and oxygen compounds) and weak where X-ray fluorescence is intense (i.e., the heavier elements).

(iii) A SMATTERING OF RESULTS

a. THE DNA/RNA BASES. The low-energy UPS region of the five DNA/RNA bases are shown in Figure 8. The spectra exhibit considerable detail: For example, I(2) and I(4) of uracil and thymine possess distinct vibronic structure.

Detailed discussion of these spectra are available elsewhere. Hence, we will be brief. The nature of the ionization events may be determined by chemical mapping techniques. For example, an ionization event which removes charge from a -C=C- unsaturation region will be very sensitive to methyl substitution at this site, but relatively insensitive to such substitution at sites far removed from this region. Similarly, methyl substitution of an amine group will have a large effect on the ionization event which removes a π electron from an orbital with large amplitude

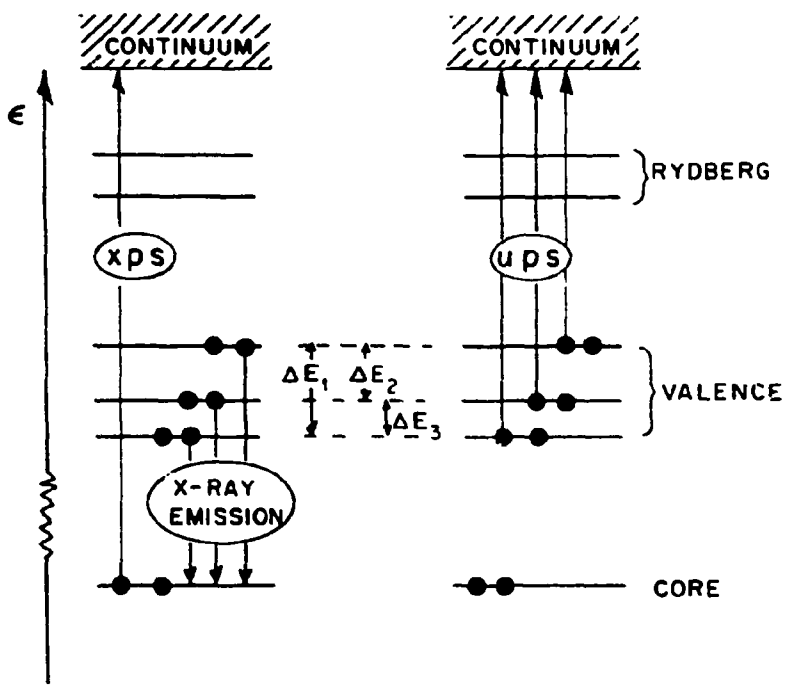

Figure 7. A comparison of UPS and X-ray fluorescence events in an orbital format.

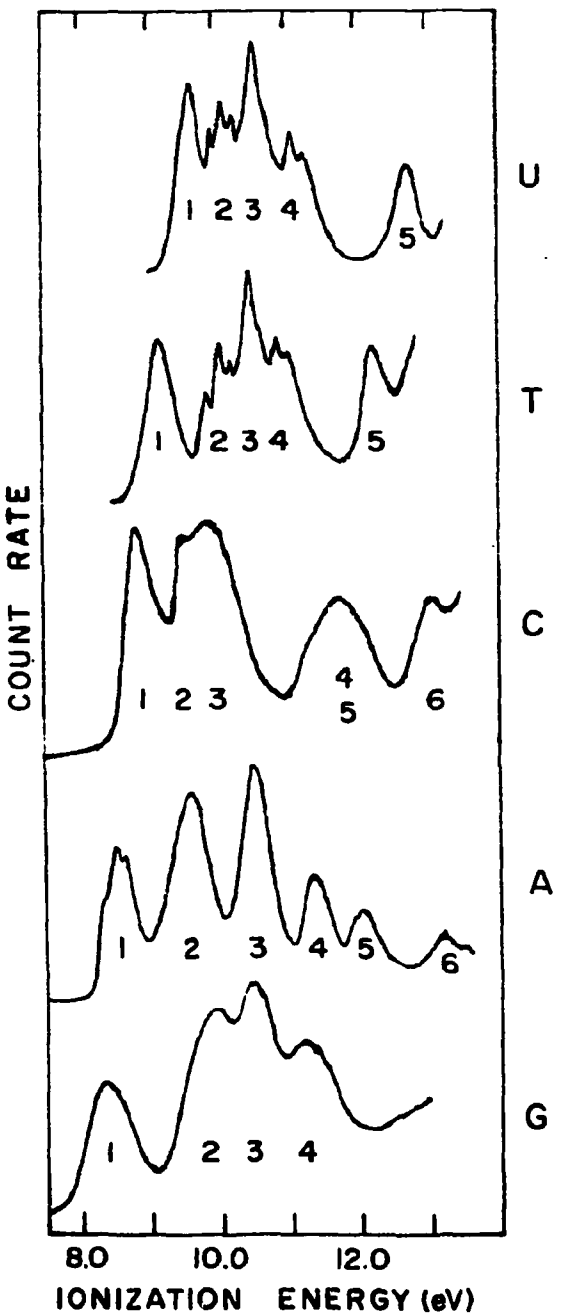

Figure 8. Photoelectron spectra of uracil (U), thymine (T), cytosine (C), adenine (A) and guanine (G) in the low-energy range. Ionization events are numbered serially in order of increasing energy.

on this group, and little or no effect on one which removes an n electron from a carbonyl oxygen. By such means, the ionization event identifications of Figure 9 have been established.

It is well to emphasize that Figure 9 contains more empirical information on the electronic structure of the DNA/RNA bases than the totality of that previously available. And Figure 9 does not exhaust the empirical data base! Indeed, the chemical mapping ploy enables one to distinguish the π-ionization events as $\pi(NH_2)$, $\pi(-C=C-)$, $\pi(-C=O)$, etc. and the n ionization events as n_+ or n_-, where the notation which is either bracketed or subscripted carries information on both the symmetry and spatial distribution of charge in the cationic state (i.e., in the vacated canonical MO). It is precisely this sort of information which is required in order to elicit the isomorphism between the UPS data and SCF-MO results: One simply compares chemically-mapped charge density distributions with MO SCF charge densities and allows adequate variance in the equivalence $I(k) = -\varepsilon(k,SCF)$ to take account of charge reorganization and electron correlation deficiencies.

b. THE PULLMAN k-INDEXING. The UPS data, via the frontier MO approximation, provide information on a great diversity of biological phenomena. For example, the lowest-energy $I(\pi)$ event contains information on relative π-electron donor efficiencies (e.g., the abilities to interrelate, to complex, or to react) and the lowest-energy I(n) event makes very specific reference to hydrogen-bonding abilities. These topics have been discussed in admirable fashion by Pullman. Unfortunately, not being possessed of any UPS data, Pullman was forced to calculate the quantities of interest. Thus, he used a simple Hückel approach to obtain the Koopmans' equivalent of $I(\pi)$, namely $\varepsilon(\pi)$. According to

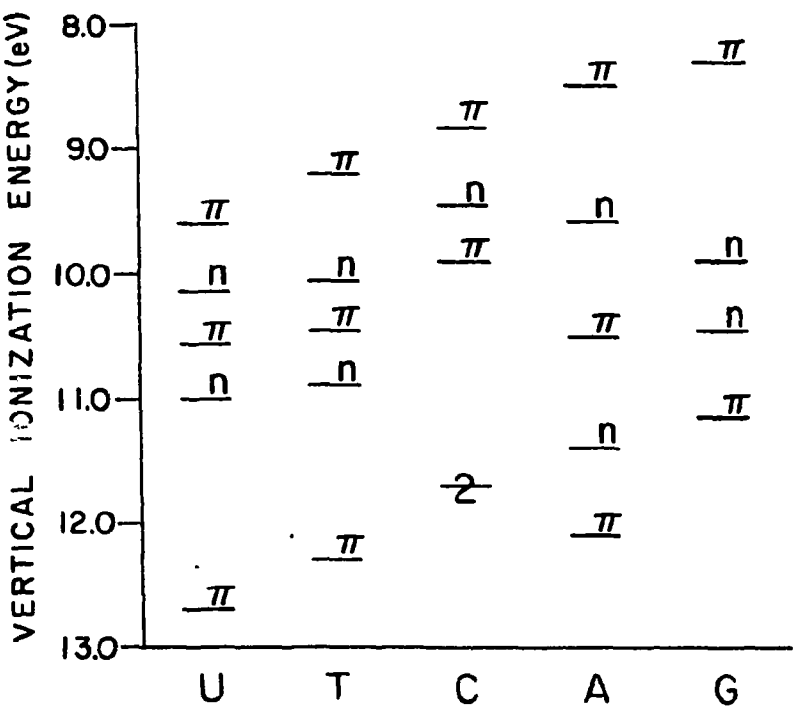

Figure 9. Plot of the vertical ionization energies and MO assignments of the four or five highest occupied MO's for uracil (U), thymine (T), cytosine (C), adenine (A) and guanine (G).

Pullman, the π donor ability is encapsuled in the coefficient k of $\epsilon(\pi) = \alpha + k\beta$ where α and β are average Coulomb and exchange integrals for a large range of heteroatomic biologicals. Hence, it is of interest to evaluate the relevance of the Pullman indexing.

A plot of $I(\pi)$ versus the Pullman k coefficient is shown in Figure 10 for a series of biologicals as well as, for reference, a set of simple hydrocarbons. Several observations are pertinent:

---First, despite some scatter, the biomolecule regression line constitutes a remarkable vindication of the Pullman attitudes.

---Second, as expected, the biomolecule regression line lies considerably higher than that of the aromatic hydrocarbons.

---Third, although $I(1)$ is of π-type in most instances, it is of n-type in barbituric acid (and, possibly, nicotinic acid and nicotinamide). In these instances, frontier MO considerations based on the supposition $I(1) = I(\pi)$ are wrong.

---Fourth, these data provide direct measures of absolute (and relative) electron donor abilities. Such knowledge is at the heart of biochemical processes.

---Fifth, although UPS data do not directly speak to the subject of electron affinities, these data, in conjunction with N → V spectroscopic information, do lead to facile extraction of electron affinity information.

c. ELECTRON DONOR SCALING. In order to emphasize the relevance to electron donating abilities, we present in Figure 11 the experimental counterpart of a theoretical scaling first given by Pullman. This scaling is a graphic rendition of the power of the UPS technique.

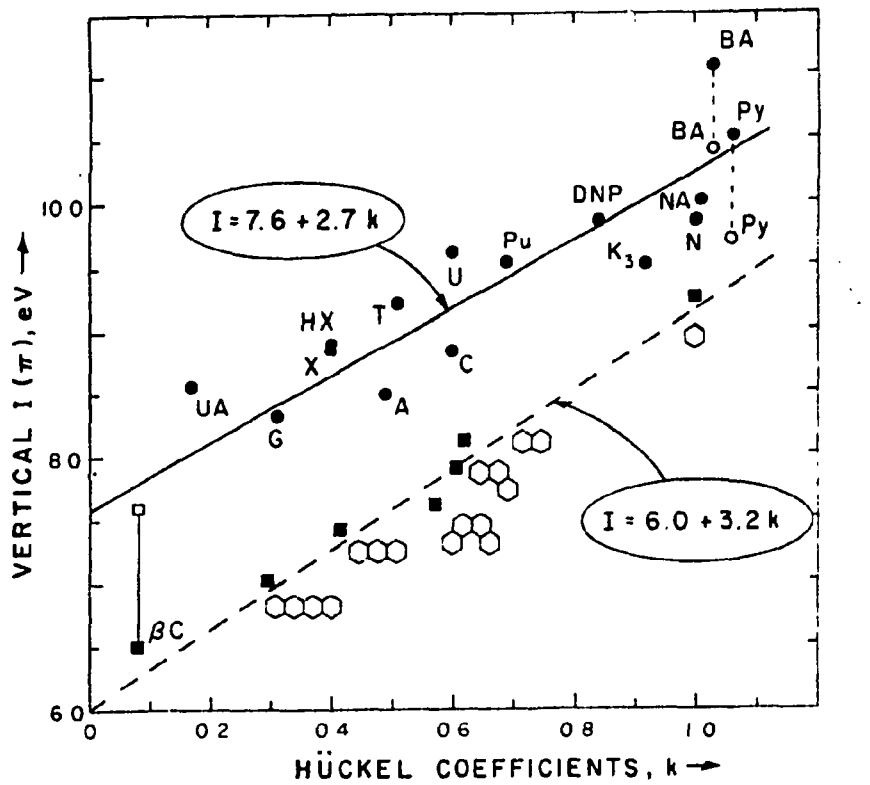

Figure 10. A plot of I(π, vertical) versus the Hückel coefficient, k. The symbolism is βC:β-carotene; UA:uric acid; G:guanine, X:xanthine; HX:hypoxanthine; A:adenine; T: thymine; C:cytosine; U:uracil; Pu:purine; DNP:2,4-dinitrophenol; K_3:vitamin K_3; N: nicotinic acid; NA:nicotinamide; BA:barbituric acid; Py:pyrimidine. The solid circles denote I(π, vertical); the open circles denote I(n, vertical). For βC the open square and the solid square denote I(π, vertical) and I(π, adiabatic), respectively.

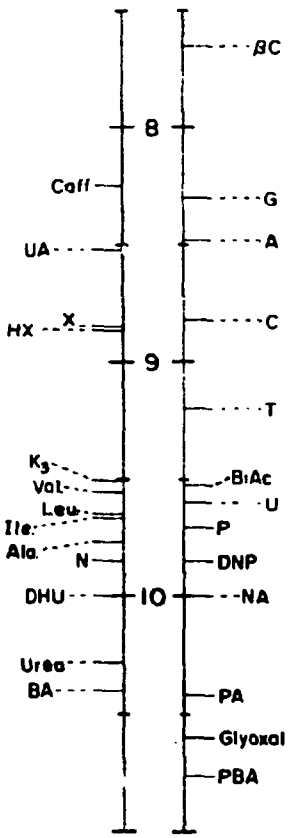

Figure 11. An absolute electron-donor ability (or basicity) scale for a variety of biologicals -- an experimental counterpart to a computational scaling by the Pullmans. The center scale is vertical ionization energy (eV) for the lowest ionization event. The symbolism is that of Figure 10 with the additions Caff:caffeine; BiAc:biacetyl; Val:ℓ-valine; Leu:ℓ-leucine; Ile:ℓ-isoleucine; Ala:ℓ-alanine; P:pyruvamide; DHU:dihydrouracil; PA:pyruvic acid; PBA:parabanic acid.

(iv) CONCLUSION

The application of UPS to biology is in its infancy. Further development of the technique, within UPS restrictions, will proceed along two lines: The ability to work at P < 1μm, which will decrease T and, hence, the possibility of decomposition; and the use of substitution devices (such as methylation or trimethylsilylation) which will render many involatiles volatile.

The UPS technique, being limited to gas phase studies, must be superceded by others which are pertinent to the solid state and which can extract similar information. The primary replacement techniques, all presently in development, are:

---X-ray fluorescence spectroscopy (particularly for molecules containing heavier elements)

---Auger spectroscopy (particularly for molecules consisting of C, O, N and H)

---ESCA, when adequate resolution is attainable at high electron kinetic energies.

In our opinion, it is these latter techniques, which are not limited by molecule size or volatility, which will provide the most potent probes for the electronic structure of larger biomolecules (e.g., nucleotides, steroids, etc.).

In the meantime, even with UPS, there is much that must be done.

C. UPS OF 1,4-BENZOQUINONES

(See item 159)

The UPS of the 1,4-benzoquinones has been investigated by four sets of authors who have arrived at very different sets of assignments. The

core of the problem appears to lie in a breakdown of the Koopmans' theorem in these systems. Hence, the resolution of the problem lies in one of two directions: Either the assignments must be made on the basis of totally-empirical considerations or calculations which press beyond the Koopmans' level must be performed. We have chosen the former route, placing our confidence in the small perturbations engendered by innocuous substituents such as methyl effects or in the rather large effects of fluorine substituents on the σ-ionization events.

The net result has been a very clear-cut set of UPS assignments, a set so heavily invested in empirical considerations that it is no longer arguable and which also agrees with preliminary calculations that do not invoke Koopmans' theorem.

D. UPS OF AZULENES

The UPS of ∿20 azulenes have been obtained and assigned. The reason for interest in these systems was totally involved with their very excellent electron-donor properties.

V. INORGANIC SALTS

V. INORGANIC SALTS

The items of Section II.A which refer to these studies are 147, 155 and 178.

A. COLORS OF POST-TRANSITION METAL SALTS

(See item 178)

The colors of post-transition metal salts have been interpreted as an external spin-orbit coupling effect in which the metal ion relaxes spin-forbiddenness in the anion. The purpose of this work is to develop a configuration approach to such spin-orbit mixing problems.

(i) THE CONFIGURATION MODEL

The zero-order configuration wavefunctions are constructed from four MO functions: The LUMO and HOMO of the metal ion, φ_m, and φ_m, respectively; and the LUMO and HOMO of the anion, φ_a, and φ_a, respectively. These configurations are diagrammed in Figure 1 and elaborated in Table 1.

The transition of interest is $^3\psi_{A*} \leftarrow {}^1\psi_0$. This transition is anion-localized and is responsible for the color of post-transition metals. In order for it to acquire transition probability, it must mix with singlet $\leftarrow$ singlet, $S_i \leftarrow S_0$ transitions. Consequently, we write the spin-orbit corrected $^3\Psi_{A*}$ function as

$$^3\Psi_{A*} = {}^3\psi_{A*} + C_1\ {}^1\psi_0 + C_2\ {}^1\psi_{A*} + C_3\ {}^1\psi_{M*} + C_4\ {}^1\psi_{CT} + C_5\ {}^1\psi_{RCT} \qquad ---1$$

where

$$C_i(i = 1,2,3,4\&5) = \langle {}^1\psi_i | \mathcal{H}' | {}^3\psi_{A*} \rangle / [E_i^0 - E^0({}^3A*)] \qquad ---2$$

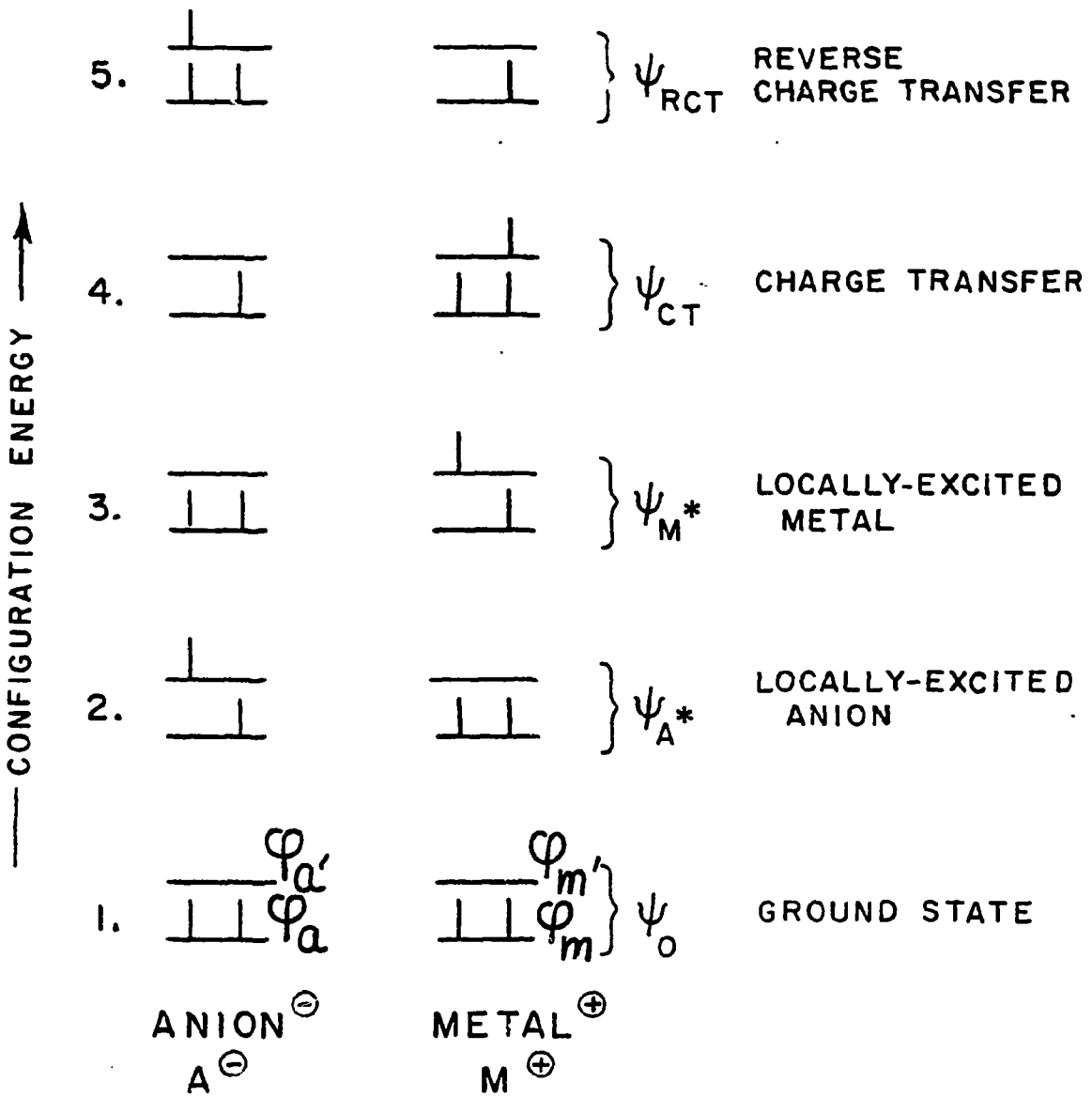
5.
4.
3.
2.
1.
ψ_{RCT}
REVERSE CHARGE TRANSFER
ψ_{CT}
CHARGE TRANSFER
ψ_{M^*}
LOCALLY-EXCITED METAL
ψ_{A^*}
LOCALLY-EXCITED ANION
$\varphi_{a'}$
φ_a
$\varphi_{m'}$
φ_m
ψ_0
GROUND STATE
CONFIGURATION ENERGY
ANION $\ominus$
$A^\ominus$
METAL $\oplus$
$M^\oplus$

FIGURE 1

TABLE 1

CONFIGURATION WAVEFUNCTIONS

CONFIGURATION	SINGLETS ($M_S = 0$)	TRIPLETS	M_S
GROUND STATE ψ_0	$\lvert\varphi_a\bar{\varphi}_a\varphi_m\bar{\varphi}_m\rvert$	- - -	
LOCALLY EXCITED ANION ψ_{A^*}	$\frac{1}{\sqrt{2}}(\lvert\varphi_a\bar{\varphi}_a,\varphi_m\bar{\varphi}_m\rvert + \lvert\varphi_a,\bar{\varphi}_a\varphi_m\bar{\varphi}_m\rvert)$	$\lvert\varphi_a\varphi_a,\varphi_m\bar{\varphi}_m\rvert$	1
		$\lvert\bar{\varphi}_a\bar{\varphi}_a,\varphi_m\bar{\varphi}_m\rvert$	-1
		$\frac{1}{\sqrt{2}}(\lvert\varphi_a\bar{\varphi}_a,\varphi_m\bar{\varphi}_m\rvert - \lvert\varphi_a,\bar{\varphi}_a\varphi_m\bar{\varphi}_m\rvert)$	0
LOCALLY EXCITED METAL ψ_{M^*}	$\frac{1}{\sqrt{2}}(\lvert\varphi_a\bar{\varphi}_a\varphi_m\bar{\varphi}_m,\rvert + \lvert\varphi_a\bar{\varphi}_a\varphi_m,\bar{\varphi}_m\rvert)$	$\lvert\varphi_a\bar{\varphi}_a\varphi_m\varphi_m,\rvert$	1
		$\lvert\varphi_a\bar{\varphi}_a\bar{\varphi}_m,\bar{\varphi}_m\rvert$	-1
		$\frac{1}{\sqrt{2}}(\lvert\varphi_a\bar{\varphi}_a\varphi_m\bar{\varphi}_m,\rvert - \lvert\varphi_a\bar{\varphi}_a\varphi_m,\bar{\varphi}_m\rvert)$	0
CHARGE-TRANSFER ψ_{CT}	$\frac{1}{\sqrt{2}}(\lvert\varphi_a\bar{\varphi}_m,\varphi_m\bar{\varphi}_m\rvert + \lvert\varphi_m,\bar{\varphi}_a\varphi_m\bar{\varphi}_m\rvert)$	$\lvert\varphi_a\varphi_m,\varphi_m\bar{\varphi}_m\rvert$	1
		$\lvert\bar{\varphi}_a\bar{\varphi}_m,\varphi_m\bar{\varphi}_m\rvert$	-1
		$\frac{1}{\sqrt{2}}(\lvert\varphi_a\bar{\varphi}_m,\varphi_m\bar{\varphi}_m\rvert - \lvert\varphi_m,\bar{\varphi}_a\varphi_m\bar{\varphi}_m\rvert)$	0
REVERSE CHARGE-TRANSFER ψ_{RCT}	$\frac{1}{\sqrt{2}}(\lvert\varphi_a\bar{\varphi}_a\varphi_m\bar{\varphi}_a,\rvert + \lvert\varphi_a\bar{\varphi}_a\varphi_a,\bar{\varphi}_m\rvert)$	$\lvert\varphi_a\bar{\varphi}_a\varphi_a,\varphi_m\rvert$	1
		$\lvert\varphi_a\bar{\varphi}_a\bar{\varphi}_a,\bar{\varphi}_m\rvert$	-1
		$\frac{1}{\sqrt{2}}(\lvert\varphi_a\bar{\varphi}_a\varphi_m\bar{\varphi}_a,\rvert - \lvert\varphi_a\bar{\varphi}_a\varphi_a,\bar{\varphi}_m\rvert)$	0

where $\mathcal{H}'$ is the spin-orbit Hamiltonian and the superscript zero on the energies denotes the eigenvalues of the non-relativistic Hamiltonian. The spin-orbit-corrected ground state wavefunction is

$$^1\psi_0 = {}^1\psi_0 + C_6\,{}^3\psi_{A^*} + C_7\,{}^3\psi_{M^*} + C_8\,{}^3\psi_{CT} + C_9\,{}^3\psi_{RCT} \qquad ---3$$

The transition moment of interest, now given by $^3\psi_{A^*} \leftarrow {}^1\psi_0$, is, in first order

$$M = \sum_{i=1}^{5} C_i \langle {}^1\psi_i | \sum_j e\vec{r}_j | {}^1\psi_0 \rangle + \sum_{i=6}^{9} C_i \langle {}^3\psi_i | \sum_j e\vec{r}_j | {}^3\psi_{A^*} \rangle \qquad ---4$$

where C_i, i = 6, 7, 8 and 9, is given by

$$C_i \ (i = 6,7,8\&9) = \langle {}^3\psi_i | \mathcal{H}' | {}^1\psi_0 \rangle / (E_i^0 - E_0^0) \qquad ---5$$

The first term of Eq. 4 describes the mixing of singlet states into $^3\psi_{A^*}$ while the second describes the mixing of triplets into $^1\psi_0$.

The spin-orbit Hamiltonian may be approximated as a sum of one-electron parts

$$\mathcal{H}' = \frac{e^2}{2m^2c^2} \sum_{N,j} \frac{Z_N}{r_{jN}^3} \vec{\ell}_j \cdot \vec{s}_j = \sum_{N,j} \xi_N \vec{\ell}_j \cdot \vec{s}_j \qquad ---6$$

where the indices N and j run over atomic centers and electrons, respectively; $\vec{\ell}$ and $\vec{s}$ are orbital and spin angular momentum operators, respectively; and ξ is an empirical spin-orbit coupling constant for which values are available in the literature. The configurational expressions for M given in Eq. 4 may now be reduced to one-electron MO format. The results for the $M_S = 0$ components of the triplet states are given in Table 2.

(ii) RESULTS OF THE MODEL

Expressions 1, 2 and 6 do not contain any spin-orbit coupling on the

TABLE 2

TRANSITION DIPOLE MOMENT IN MO FORMAT

[$\mathcal{H}'_z$ component only]

COMPONENT	MO EXPRESSION[a]
1	$\dfrac{-\sqrt{2}\,\langle\varphi_a\|\mathcal{H}'_z\|\varphi_{a'}\rangle\,\langle\varphi_a\|\vec{r}\|\varphi_a\rangle}{E^0(^3A^*) - E_0^0}$
2	$\dfrac{-\sqrt{2}\,(\langle\varphi_a\|\mathcal{H}'_z\|\varphi_a\rangle - \langle\varphi_{a'}\|\mathcal{H}'_z\|\varphi_{a'}\rangle)\langle\varphi_a\|\vec{r}\|\varphi_{a'}\rangle}{E^0(^3A^*) - E^0(^1A^*)}$
3	0
4	$\dfrac{-\sqrt{2}\,\langle\varphi_{m'}\|\mathcal{H}'_z\|\varphi_{a'}\rangle\langle\varphi_a\|\vec{r}\|\varphi_{m'}\rangle}{E^0(^3A^*) - E^0(^1CT)}$
5	$\dfrac{-\sqrt{2}\,\langle\varphi_a\|\mathcal{H}'_z\|\varphi_m\rangle\langle\varphi_m\|\vec{r}\|\varphi_{a'}\rangle}{E^0(^3A^*) - E^0(^1RCT)}$
6	$\dfrac{-\sqrt{2}\,\langle\varphi_{a'}\|\mathcal{H}'_z\|\varphi_a\rangle(\langle\varphi_a\|\vec{r}\|\varphi_a\rangle + \langle\varphi_{a'}\|\vec{r}\|\varphi_{a'}\rangle)}{E_0^0 - E^0(^3A^*)}$
7	0
8	$\dfrac{-\sqrt{2}\,\langle\varphi_{m'}\|\mathcal{H}'_z\|\varphi_a\rangle\,\langle\varphi_{m'}\|\vec{r}\|\varphi_{a'}\rangle}{E_0^0 - E^0(^3CT)}$
9	$\dfrac{-\sqrt{2}\,\langle\varphi_{a'}\|\mathcal{H}'_z\|\varphi_m\rangle\,\langle\varphi_a\|\vec{r}\|\varphi_m\rangle}{E_0^0 - E^0(^3RCT)}$

metal center. Evaluation of these expressions indicates that they are small. In addition, it is clear that, being independent of the metal, they cannot account for the increase in spin-orbit coupling which is induced as the metal ion gets heavier. These expressions are totally unimportant in heavy-metal salts such as $Pb(NO_2)_2$ but very important in light-metal salts such as $NaNO_2$.

With the specification that $\ell_z = -i \frac{\partial}{\partial \phi}$, the sum of expressions 1 and 6 reduces to

$$\vec{M} = \sqrt{2} \langle \varphi_a' | \mathcal{H}_z' | \varphi_a \rangle (\vec{\mu}(^3A^*) - \vec{\mu}_0) / [E_0^0 - E^0(^3A^*)] \qquad ---7$$

which describes an intensity conferral on the $^3\Psi_{A^*} \leftarrow {}^1\Psi_0$ transition caused by the change of static dipole moment between the $^3\Psi_{A^*}$ and $^1\Psi_0$ states. This contribution is important only when the $T_1 \leftarrow S_0$ transition possesses significant charge-transfer character.

Expressions 3 and 7 are zero because $\vec{r}_i$, being a one-electron operator, cannot remove the orthogonality of the configuration wavefunctions which are involved. Thus, intensity cannot be borrowed from locally-excited metal states.

Expressions 4, 5, 8 and 9 are diagrammed in Figure 2. The transitions which contribute intensity are charge-transfer, and all of the spin-orbit integrals involve metal orbitals. Some of these integrals are quite large. Lastly, the energy denominators are also likely to be small. Indeed, the energy split of $^3\Psi_{A^*} - {}^1\Psi_{CT}$ can approach zero; thus we expect that expression 4 dominates the description of the $^3\Psi_{A^*} \leftarrow {}^1\Psi_0$ transition dipole moment.

(iii) COMPUTATIONS

The results of quantum chemical computations for $NaNO_2$ and $AgNa(NO_2)_2$ are given in Tables 3 and 4, where a brief comparison with experiment is

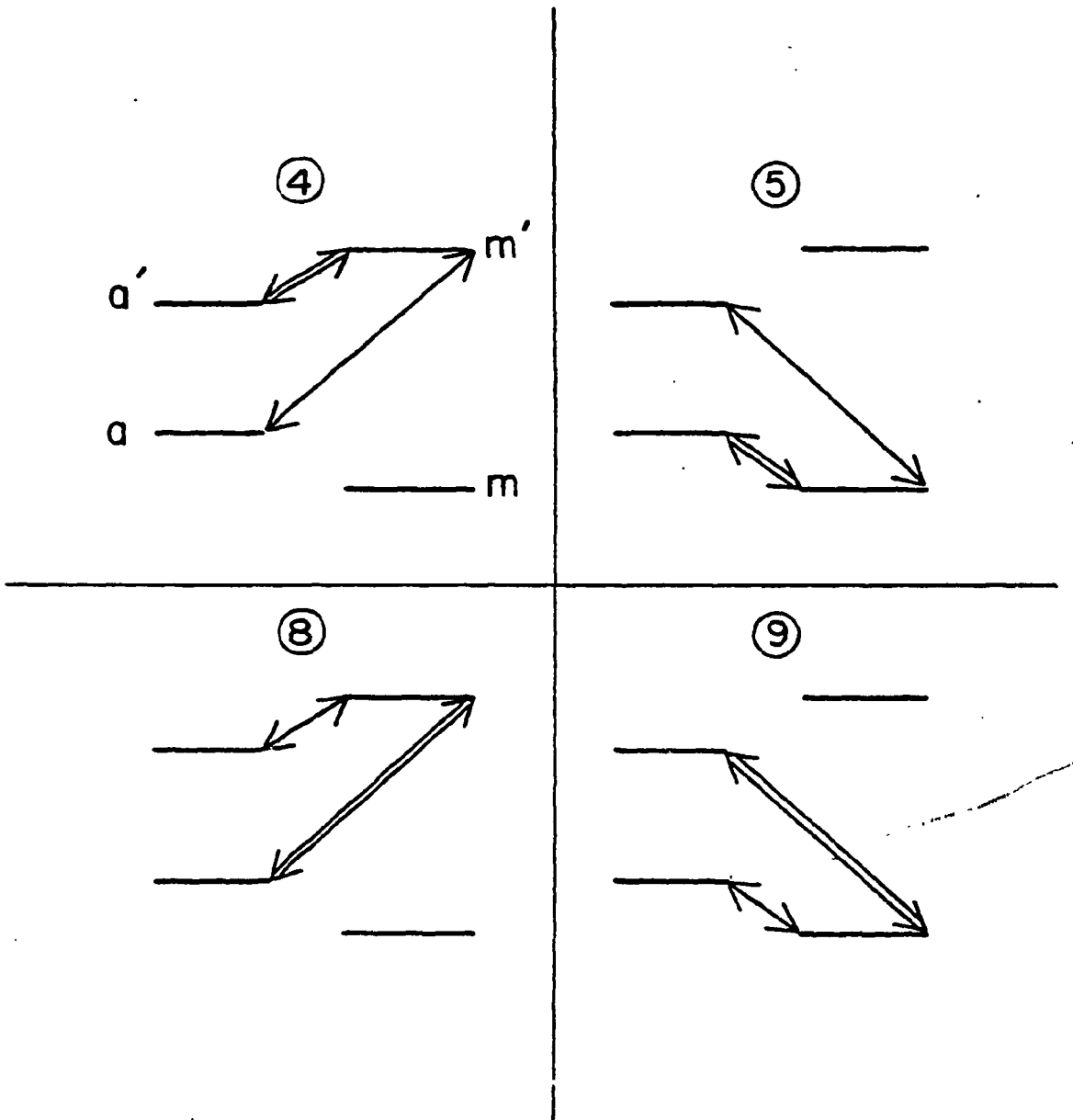

FIGURE 2

TABLE 3

CALCULATED TRANSITION PROBABILITIES FOR THE
$^3B_1 \leftrightarrow {}^1A_1$ EXCITATION OF $NaNO_2$

EXPRESSION	INTEGRAL	M y-POLARIZED	M z-POLARIZED
1	$\langle 2b_1 \vert \mathcal{H}_y' \vert 4a_1 \rangle \langle 2b_1 \vert \vec{r}_z \vert 2b_1 \rangle$	---	-6.139×10^{-4}
2	$\langle 4a_1 \vert \mathcal{H}_y' \vert 1b_1 \rangle \langle 1b_1 \vert \vec{r}_z \vert 2b_1 \rangle$	---	4.461×10^{-4}
2	$\langle 1a_2 \vert \mathcal{H}_z' \vert 4a_1 \rangle \langle 1a_2 \vert \vec{r}_y \vert 2b_1 \rangle$	1.259×10^{-4}	---
4	$\langle 2b_1 \vert \mathcal{H}_y' \vert 5a_1 \rangle \langle 4a_1 \vert \vec{r}_z \vert 5a_1 \rangle$	---	4.228×10^{-4}
4	$\langle 4b_2 \vert \mathcal{H}_z' \vert 2b_1 \rangle \langle 4a_1 \vert \vec{r}_y \vert 4b_2 \rangle$	4.012×10^{-4}	---
6	$\langle 2b_1 \vert \mathcal{H}_y' \vert 4a_1 \rangle \langle 2b_1 \vert \vec{r}_z \vert 2b_1 \rangle$	---	5.484×10^{-4}
6	$\langle 2b_1 \vert \mathcal{H}_z' \vert 2b_2 \rangle \langle 2b_2 \vert \vec{r}_y \vert 4a_1 \rangle$	-4.119×10^{-4}	---
6	$\langle 2b_1 \vert \mathcal{H}_z' \vert 3b_2 \rangle \langle 3b_2 \vert \vec{r}_y \vert 4a_1 \rangle$	9.219×10^{-4}	---
8	$\langle 4a_1 \vert \mathcal{H}_y' \vert 5a_1 \rangle \langle 2b_1 \vert \vec{r}_z \vert 5a_1 \rangle$	---	1.231×10^{-4}
	$\vec{M}$ =	1.037×10^{-3}	9.325×10^{-4}
	f =	2.593×10^{-7}	2.097×10^{-7}
	$f(obs)$ =	8×10^{-8}	~ 0

TABLE 4

CALCULATED TRANSITION DIPOLE MOMENTS FOR $AgNa(NO_2)_2$

Expression Number	Integral	Structure I	Structure II
4	$\frac{\langle 4a_1 \vert \mathcal{H}_y \vert 2b_1 \rangle \langle 3a_1 \vert r_z \vert 4a_1 \rangle}{E\ ^3A' - E\ ^1CT}$	9.217×10^{-3}	2.549×10^{-2}
5	$\frac{\langle 3a_1 \vert \mathcal{H}_y \vert 1b_1 \rangle \langle 1b_1 \vert r_z \vert 2b_1 \rangle}{E\ ^3A' - E\ ^1RCT}$	-1.662×10^{-3}	-3.178×10^{-3}
8	$\frac{\langle 3b_1 \vert \mathcal{H}_y \vert 3a_1 \rangle \langle 3b_1 \vert r_z \vert 2b_1 \rangle}{E_0 - E\ ^3CT}$	1.784×10^{-3}	-1.833×10^{-3}
9	$\frac{\langle 2b_1 \vert \mathcal{H}_y \vert 1a_1 \rangle \langle 3a_1 \vert r_z \vert 1a_1 \rangle}{E_0 - E\ ^3RCT}$	7.204×10^{-4}	1.740×10^{-3}
	$\vec{M}$ =	1.006×10^{-2}	2.222×10^{-2}
	f =	2.440×10^{-5}	1.190×10^{-4}
	$f(obs)$ =	1.1×10^{-4}	1.1×10^{-4}

also made. The following conclusions result:

---The agreement with experiment is excellent. It vindicates the suppositions used in constructing the model. The calculations suggest that the neglected contributions of Table 2, while not zero, are not major contributors of intensity.

---The effective spin-orbit coupling in the mixed silver salt originates in the 5p AO's of Ag.

---The intensity in the heavy-metal salts is stolen from high-probability, low-energy, charge-transfer transitions ($^1\Psi_{CT} \leftarrow {}^1\Psi_0$). This mechanism is much different from that operative in the alkali nitrites where higher energy $^1\Psi_{A^*} \leftarrow {}^1\Psi_0$ transitions are the dominant contributors.

---The model appears to be general for salts of the post-transition metals. Thus, we assert that the color properties of the post-transition metal salts are obtained by spin-orbit mixing with, and intensity-stealing from charge transfer transitions of anion → metal or, less probably, anion ← metal types.

B. ELECTRONIC STRUCTURE OF NCO^- AND NCS^- GROUPS

(See item 147)

This material was prepared for the lead chapter of "The Chemistry of Cyanate and Thiocyanate Groups", a volume in "Functional Groups", edited by S. Patai. The intent of the chapter was to evaluate the status of our knowledge of electronic structure for ground and excited states of these functionals.

(i) SUMMARY OF GROUND STATE CONSIDERATIONS

We have presented a simple unified description of the ground state electronic structure of cyanato and thiocyanato compounds. The MO description of the closed shell ground state is adequate to the task of

accounting for geometries, photoelectron and ESCA spectra, and the X-ray emission spectra and electronic absorption spectra of the photoionized cyanato and thiocyanato entities. The success achieved is directly attributable to Koopmans' theorem and to the MO concept (i.e., the supposition that each electron experiences only the average field produced by all the other electrons).

There remains hardly any doubt that the highest occupied MO in NCO^- and NCS^- is of π-symmetry; and that the next, whether σ or π, lies several electron volts to higher binding energies. These results also hold for covalently bonded NCO and NCS groups --- although there is, of course, some slight splitting due to the lowering of symmetry. Indeed, the constituent ground state orbitals of the NCO and NCS groups can be recognized even in such complex molecules as phenylisothiocyanate. Thus, it may be concluded that the cyanato and thiocyanato groups are true functional groups or, in a more spectroscopic language, true chromophores.

In a more jaundiced vein, there are a few other observations which we feel obliged to make. These are:

---There is a great need for much further experimental work. This work should include structure determinations of phenylisocyanate and phenylisothiocyanate; extensive photoelectron spectroscopic and ESCA investigations; and --- with high preference --- a systematic X-ray emission spectroscopic study of both salts and covalent compounds. These X-ray studies should include sulfur $K\beta$, carbon $K\alpha$, nitrogen $K\alpha$ and oxygen $K\alpha$ investigations at the highest attainable resolution.

---No particular need exists for any further semi-empirical computational works, unless they constitute an attempt to unify existing or, even better, new experimental data.

---Approximate means for "experimental" access to such quantities as orbital energies, LCAO coefficients, and even "atom charges" in a molecule do exist. However, any effort to attain high precision (i.e., several signigicant figures) intrudes on the theoretical difficulties already discussed. In other words, while the MO ideology can ensure a close relatedness of experiment and theory, this relatedness is fated to remain inexact and, at a certain limit, to be ill-defined.

(ii) SUMMARY OF EXCITED STATE CONSIDERATIONS

Our knowledge of excited states of cyanates and thiocyanates is in exceedingly poor repair. In order to be specific, we enumerate:

---The intravalence (N → V) assignments for the cyanates overlap to a considerable degree with the extravalence (N → R) assignments. Both sets of assignments cannot be simultaneously correct. The determination of the proper assignments demands the redetermination of vacuum ultraviolet (VUV) spectra of HNCO, C_2H_5NCO and NaNCO; the determination of VUV spectra of CH_3NCO and SiH_3NCO; and the use of independent assignment criteria such as are provided by MCD and ELD measurements.

---No VUV spectra of any thiocyanates appear to be available. These, of course, should be measured.

---The tellurocyanates and selenocyanates, if their spectra were available, could settle the question of N → R or N → V assignments in the cyanates.

---The behavior of the theoretical energy levels $^{(1,3)}\Sigma^+$, $^{(1,3)}\Sigma^-$ and $^{(1,3)}\Delta$ must be studied as a function of the parameters A, B, C, D, ξ_{np} and $\xi_{(n+1)p}$ (See Figure 3). Such studies would lead to predictions about the spectra of cyanates, thiocyanates, tellurocyanates and selenocyanates which might help in making definitive assignments for all of them.

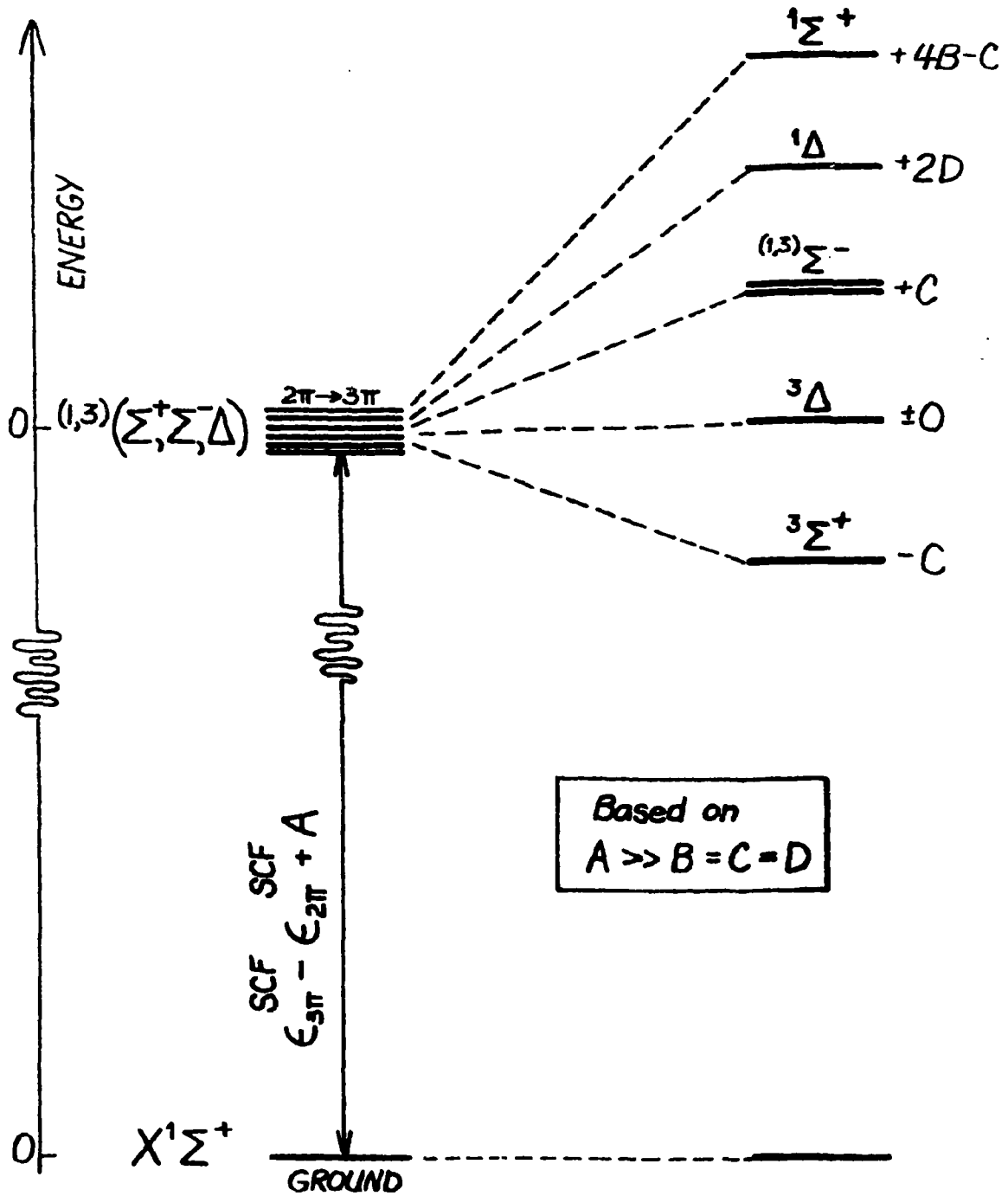
ENERGY
0
(1,3)(Σ+,Σ-,Δ)
2π→3π
0
X¹Σ+
GROUND
SCF SCF
ε3π − ε2π + A
¹Σ+
+4B-C
¹Δ
+2D
(1,3)Σ-
+C
³Δ
±0
³Σ+
-C
Based on
A >> B = C = D

FIGURE 3

---The luminescence studies are qualitative and require reinvestigation in order to establish the intrinsic nature of the luminescence, its polarization, and its dependence on matrix.

---The study of solvent effects on transition energies, intensities and polarizations must be extended in order to confirm or negate the Charge Transfer to Solvent (or CTTS) concept.

Despite the deficiencies implied above, a number of definitive statements can be made. These are:

---Cyanates and thiocyanates emit phosphorescence of $T_1 \rightarrow S_0$ nature. This phosphorescence is assigned as $^3\Sigma^+ \rightarrow X^1\Sigma^+$. The $^3\Sigma^+$ state may be characterized by a bent NCO or NCS group.

---Non-aryl cyanates and thiocyanates do not emit fluorescence of $S_1 \rightarrow S_0$ nature. It is probable that the density of states at the S_1 level is so high that $S_1 \rightarrow S_0$ emission cannot compete with the energy degradative events $S_1 \rightsquigarrow S_0$ or $S_1 \rightsquigarrow T_1$.

---The lower-energy $S_j \leftarrow S_0$ absorption region is dominated by the $^1\Delta \leftarrow X^1\Sigma^+$ and $^1\Sigma^- \leftarrow X^1\Sigma^+$ transitions (or their analogs in point groups of lower symmetry). Many, if not all, of these lower energy S_j states are characterized by a bent NCO or NCS grouping. The resulting spectra, as expected, are diffuse.

---The higher-energy $S_j \leftarrow S_0$ absorption region is dominated by $^1\Sigma^+ \leftarrow X^1\Sigma^+$ (or its analog in point groups of lower symmetry) and R $\leftarrow$ N transitions. The possible occurrence of $^1\Pi \leftarrow X^1\Sigma^+$ transitions (or analogs) in this region is debatable.

Theory and computation are in much better repair than is experiment. It is in the realm of experiment that the greatest amount of work is required.

C. TRIPLET STATES OF SOME INORGANIC ANIONS

(See item 155)

The triplet states of salts of the chlorite ion: $C\ell O_2^-$; the sulfate ion: $SO_4^=$; the tungstate ion: $WO_4^=$; and the molybdate ion: $MO_4^=$ have been detected. The experimental techniques used were absorption, phosphorescence and specular reflection at temperatures ranging from ∿300 to 2.8K. A sampling of data for molybdates is given in Table 5.

Data for the other anions are equally rough and a considerable deal of work will be required to establish the assignments.

TABLE 5

CHARACTERISTICS OF THE $S_0 \leftrightarrow T_1$ TRANSITION OF MOLYBDATE SALT

SALT	ABSORPTION		EMISSION		
	λ(max) [nm]	ε [ℓ/mol cm]	λ(max) Exc [nm]	λ(max) Em [nm]	τ_p [μsec]
Li_2MoO_4			328	610	10
Na_2MoO_4	330	1.5	325	611	880
$CaMoO_4$			305	508	220
$ZnMoO_4$			294	550	---
$SrMoO_4$			245	500	156
Ag_2MoO_4			290	370	---
$CdMoO_4$	315	14.0	337	535	230
Cs_2MoO_4			370	395	---
$BaMoO_4$			348	508	---
$PbMoO_4$	303	7	359	503	10
$Bi_2(MoO_4)_3$			308	560	---

VI. HIGHLY-POLAR MOLECULES

VI. HIGHLY-POLAR MOLECULES

The items of Section II.A concerned with this topic are

131, 133, 135, 136, 141, 147, 155 and 174.

Of these 131, 133, 135 and 136 were concerned with generation of the precision data required for the formulation of models. In specific, these items measured quantum yields of fluorescence and phosphorescence, luminescence decay constants, oscillator strengths and polarizations for the four {ortho, meta, para}-triads (a total of 12 molecules): fluorobenzonitriles, cyanoanilines, aminoacetophenones and cyanoanisoles. As a result, a detailed elaboration of rate constants, electronic states and the effects of polar substituents on them became available.

This work is still underway and preliminary data are available for a large number of polar entities. These data are collected in Tables 1 and 2. An example of absorption and luminescence spectra of the aminoacetophenones is given in Figures 1, 2 and 3, the luminescence spectra being of poor quality because of low quantum yields of emission.

The purpose of this work, however, was not to elaborate experimental details but rather to construct a model which would satisfy the demands of experiment. Such a model has evolved, although it still remains primitive.

A. A MODEL FOR POLAR MOLECULES

A schematic of the energy levels of D-ϕ-A molecules as a function of solvent polarity is given in Figure 4. On the left side of this Figure, phosphorescence is weak and fluorescence dominant; the ^1L_a-^1L_b separation is large, and the oscillator strengths $f(^1L_a \leftarrow {}^1\Gamma_1)$ and

TABLE 1

POLAR D-ϕ-A MOLECULES

ABSORPTION DATA (kK) IN VARIOUS SOLVENT MEDIA[a]

MOLECULE	ISOMER	$^1L_b \leftarrow {}^1A$			$^1L_a \leftarrow {}^1A$		
		Ethanol	MCH	3MP	Ethanol	MCH	3MP
Methylbenzoic Acid	o	35.97(m)	---	34.03(o)	---	---	42.37(m)
	m	37.17(m)	---	---	45.45(m)	---	---
	p	35.46(o)	---	---	42.37(m)	---	41.49(m)
Fluorobenzonitrile	o	35.59(o)	---	---	43.57(o)	---	---
	m	35.52(o)	---	---	43.67(o)	---	---
	p	36.54(o)	---	---	44.30(m)	---	---
Toluamide	p	35.71(sh)	---	35.71(o)	42.64(m)	---	43.29(m)
Chlorobenzonitrile	m	34.78(o)	---	---	42.92(o)	---	---
	p	35.56(o)	---	35.56(o)	42.46(m)	---	42.37(m)
Bromobenzonitrile	p	35.50(o)	---	35.50(o)	41.04(m)	---	41.07(m)
Methoxybenzoic Acid	m	33.90(m)	---	---	42.92(m)	---	---
	p	39.68(m)	---	36.04(o)	39.06(m)	---	39.53(m)

TABLE 1 (cont.)

MOLECULE	ISOMER	$^1L_b \leftarrow {}^1A$			$^1L_a \leftarrow {}^1A$		
		Ethanol	MCH	3MP	Ethanol	MCH	3MP
Cyanoanisole	o	33.90(m)	33.56(o)	---	42.02(o)	42.20(m)	---
	m	33.60(o)	33.70(o)	---	43.48(m)	42.02(o)	---
	p	35.34(o)	35.20(o)	---	40.15(m)	40.80(m)	---
Cyanophenol	o	33.67(m)	33.46(o)	---	42.37(o)	42.55(o)	---
	m	33.90(m)	33.83(o)	---	43.05(m)	42.79(o)	---
	p	35.34(o)	35.30(o)	35.40(o)	42.01(m)	41.67(m)	42.07(m)
Cyanoaniline	o	30.75(m)	31.86(m)	~30.44(o)	40.30(m)	41.06(m)	41.20(m)
	m	31.20(m)	32.26(m)	30.90(o)	39.70(m)	41.24(m)	41.20(m)
	p	---	33.06(o)	33.00(o)	36.20(m)	???	38.20(m)
Cyanophenoxide	p	---	---	---	36.50(m)	---	---
N,N-Dimethylcyanoaniline	p	---	---	---	34.60(m)	---	---
Methyl Aminobenzoate	o	29.51(m)	---	---	---	---	---
	m	31.35(m)	---	---	---	---	---
	p	33.61(sh)	33.61(sh)	33.67(sh)	34.36(m)	---	37.04(m)
Aminobenzoic Acid	p	---	---	---	34.48(m)	---	---

TABLE 1 (cont.)

MOLECULE	ISOMER	$^1L_b \leftarrow {}^1A$			$^1L_a \leftarrow {}^1A$		
		Ethanol	MCH	3MP	Ethanol	MCH	3MP
N-Methylaminobenzoic Acid	p	---	---	---	33.28(m)	34.01(m)	---
N,N-Dimethylaminobenzoic Acid	-	---	---	---	32.47(m)	32.51(m)	32.89(m)
Aminoacetophenone	o	27.40(m)	---	28.41(m)	38.80(m)	---	39.53(m)
	m	29.50(m)	---	30.77(m)	39.00(m)	---	40.82(m)
	p	---	---	~29.90(m)	---	---	---
Nitrophenol	p	---	---	---	31.95(m)	---	---
Nitroaniline	o	---	26.50(m)	---	---	37.00(m)	---
	m	---	28.70(m)	---	35.41(sh)	37.20(m)	---
	p	---	---	---	26.90(m)	31.00(m)	31.55(m)
N,N-Dimethylnitroaniline	p	---	---	---	25.80(m)	---	28.49(m)

[a]All energies refer to room temperature. (o) designates a band origin, (m) designates a band maxima, (sh) designates a shoulder. Compounds were purified by standard methods (distillation, crystallization, gas chromatography, volatilization and/or zone refining.

TABLE 2

EMISSION DATA FOR POLAR D-ϕ-A MOLECULES[a,b,c]

MOLECULE	ISOMER	SOLVENT	FLUORESCENCE	PHOSPHORESCENCE		Φ_P/Φ_F
			ENERGY (cm^{-1})	ENERGY (cm^{-1})	LIFETIME (s)	
Methylbenzoic Acid	o	EPA	---	27,780	1.2	>100
	m	EPA	---	29,710	2.7	>100
	p	EPA	---	30,300	1.7	>100
Fluorobenzonitrile	o	Ethanol	35,000	26,800	2.43	0.18
	m	Ethanol	34,900	26,600	2.60	0.15
	p	Ethanol	35,750	27,100	2.05	0.96
Toluamide	o	EPA	35,590	27,690	0.65	5.3
	m	EPA	34,360	26,870	2.55	6.6
	p	EPA	35,080	27,010	1.25	>100
Chlorobenzonitrile	o	EPA	34,250	25,970	0.38	10.6
	m	EPA	34,480	26,320	0.47	18.7
	p	EPA	34,250	25,840	0.15	16.8
Bromobenzonitrile	o	EPA	34,840(m)	25,970	1.25×10^{-2}	
	m	EPA	34,970(m)	26,320	1.05×10^{-2}	
	p	EPA	34,720(m)	25,770	4.9×10^{-3}	

TABLE 2 (cont.)

MOLECULE	ISOMER	SOLVENT	FLUORESCENCE	PHOSPHORESCENCE		Φ_P/Φ_F
			ENERGY (cm^{-1})	ENERGY (cm^{-1})	LIFETIME (s)	
Methoxybenzoic Acid	o	EPA	31,250	25,640	0.96	3.9
	m	EPA	31,250	26,320	2.68	1.7
	p	EPA	33,900	26,460	2.03	6.2
Cyanoanisole	o	Ethanol	33,200	26,000	1.4	0.42
	m	Ethanol	33,000	25,000	1.82	0.45
	p	Ethanol	~35,000-33,900(m)	26,320	1.59	1.01
Cyanophenol	o	EPA	32,050	26,320	2.48	1.31
	m	EPA	32,260	25,320	3.21	0.79
	p	EPA	33,900	26,320	2.63	1.51
Sulfanilamide	m	EPA	28,290(m)	22,320(m)	1.92	1.04
	p	EPA	31,500	25,640	1.22	5.16
Cyanoaniline	o	Ethanol	27,600(m)	24,300(m)	3.65	0.31
	m	Ethanol	27,500(m)	21,510(m)	2.65	0.054
	p	Ethanol	30,000(m)	24,500	2.45	0.73
N,N-Dimethylcyanoaniline	p	EPA	30,770	24,100	2.13	1.2
N,N-Diethylcyanoaniline	p	EPA	30,488	24,100	2	5.3

TABLE 2 (cont.)

MOLECULE	ISOMER	SOLVENT	FLUORESCENCE	PHOSPHORESCENCE		Φ_P/Φ_F
			ENERGY (cm^{-1})	ENERGY (cm^{-1})	LIFETIME (s)	
Methyl Aminobenzoate	o	EPA	27,000(m)	22,570(m)	2.45	<0.01
	m	EPA	25,500(m)	23,980(m)	2.4	0.15
	p	EPA	30,303(m)	24,380	1.8	0.20
Aminobenzoic Acid	p	EPA	31,060	24,040	2.1	0.15
N-Methylaminobenzoic Acid	p	EPA	29,630(m)	23,530	2.3	0.13
N,N-Dimethylaminobenzoic Acid	p	EPA	29,590(m)	23,810(m)	1.84	0.18
Aminoacetophenone	o	Ethanol	23,260(m)	22,000(m)	5.55×10^{-2}	0.14
	m	Ethanol	22,600(m)	20,000(m)	0.23	0.13
	p	Ethanol	28,300(m)	22,520(m)	0.72	1.3
Nitroaniline	o	EPA	20,000(m)	---	---	<0.01
	m	EPA	18,000(m)	---	---	<0.01
	p	EPA	---	18,100(m)	0.24	>100
N-Methylnitroaniline	p	EPA	23,260	19,610	0.23	19.3
N,N_Dimethylnitroaniline	p	EPA	22,730	19,230	0.22	2.8

TABLE 2 (cont.)

[a]All energies refer to 77°K. Quoted energies are for 0,0 bands except where marked by "(m)" which connotes a band maximum. The experimental error is approximately 50 cm^{-1}. The ratio of phosphorescence to fluorescence intensities is denoted by Φ_P/Φ_F and has been corrected for instrument parameters. The absence of any symbolism in a given data slot incidates our inability to measure the quantity in question.

[b]Compounds were purified by standard methods (distillation, crystallization, gas chromatography, volatilization and/or zone refining) until a constancy of luminescence parameters was achieved. All solvents were fluorometric grade and were non-emissive at the level of sensitivity needed in this work. Measurement procedures have been described elsewhere.

[c]Mesomeric, inductive and steric effects are undoubtedly operative to some extent in all of these systems. It seems reasonable that the relative importance of these effects in the different isomers varies as follows:

o : steric; inductive ≥ mesomeric
m : inductive only
p : mesomeric ≥ inductive

The energies of S_1 and T_1 states will depend on that particular mix of these effects which operates in the case of a given molecule. For example, in the chloro- and bromobenzonitriles, m is of highest T_1 and S_1 energy, presumably because only the inductive effect operates in this isomer. In a "stronger" DA system, where p possesses the highest T_1 and S_1 energies, we must, it seems, associate this happenstance with a dominant importance of the mesomeric effect in these cases.

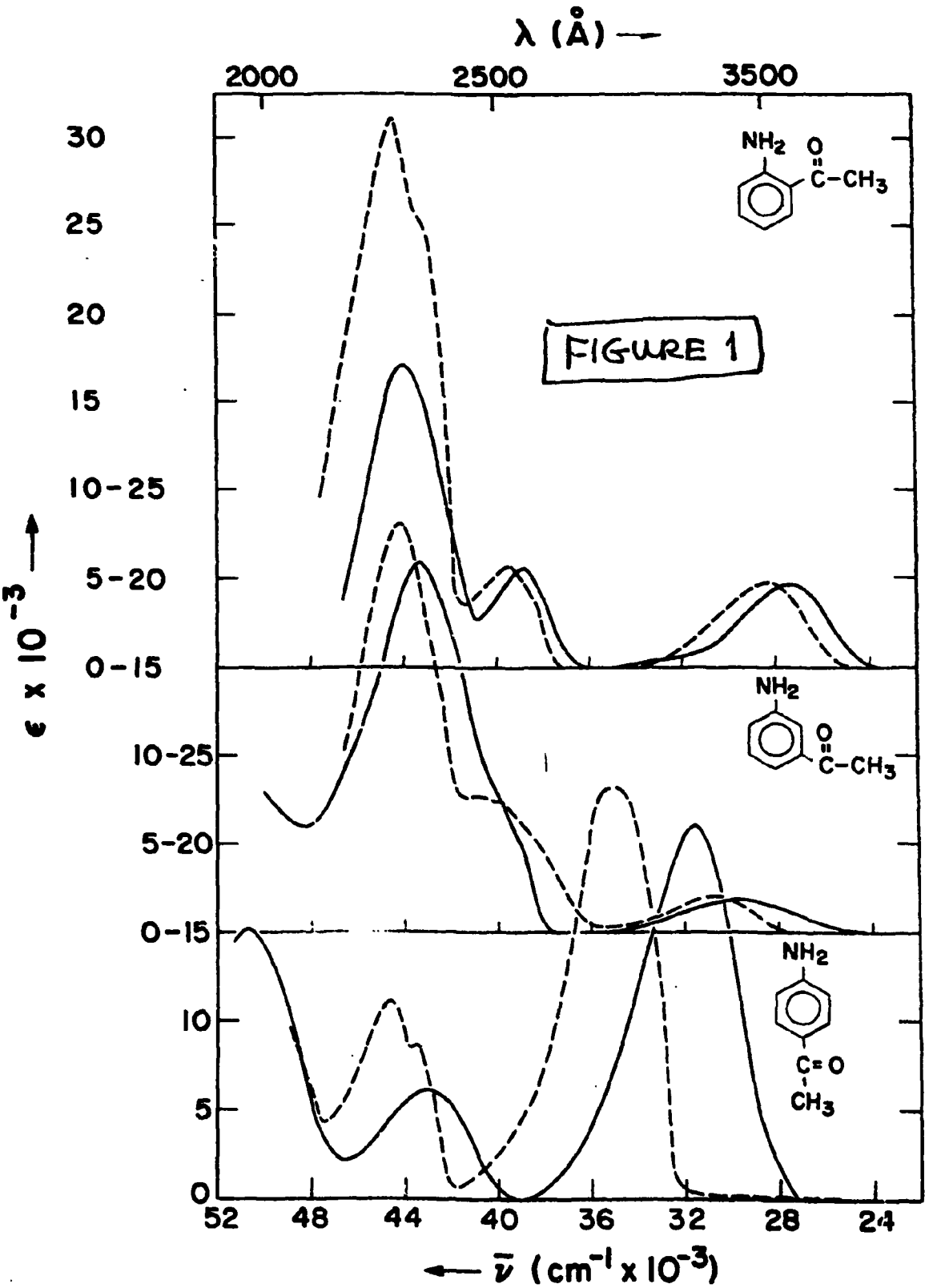

Figure 1. Absorption spectra of o, m-, and p-aminoacetophenones in ethanol (solid line) and 3-methylpentane (3MP, dashed line) at room temperature.

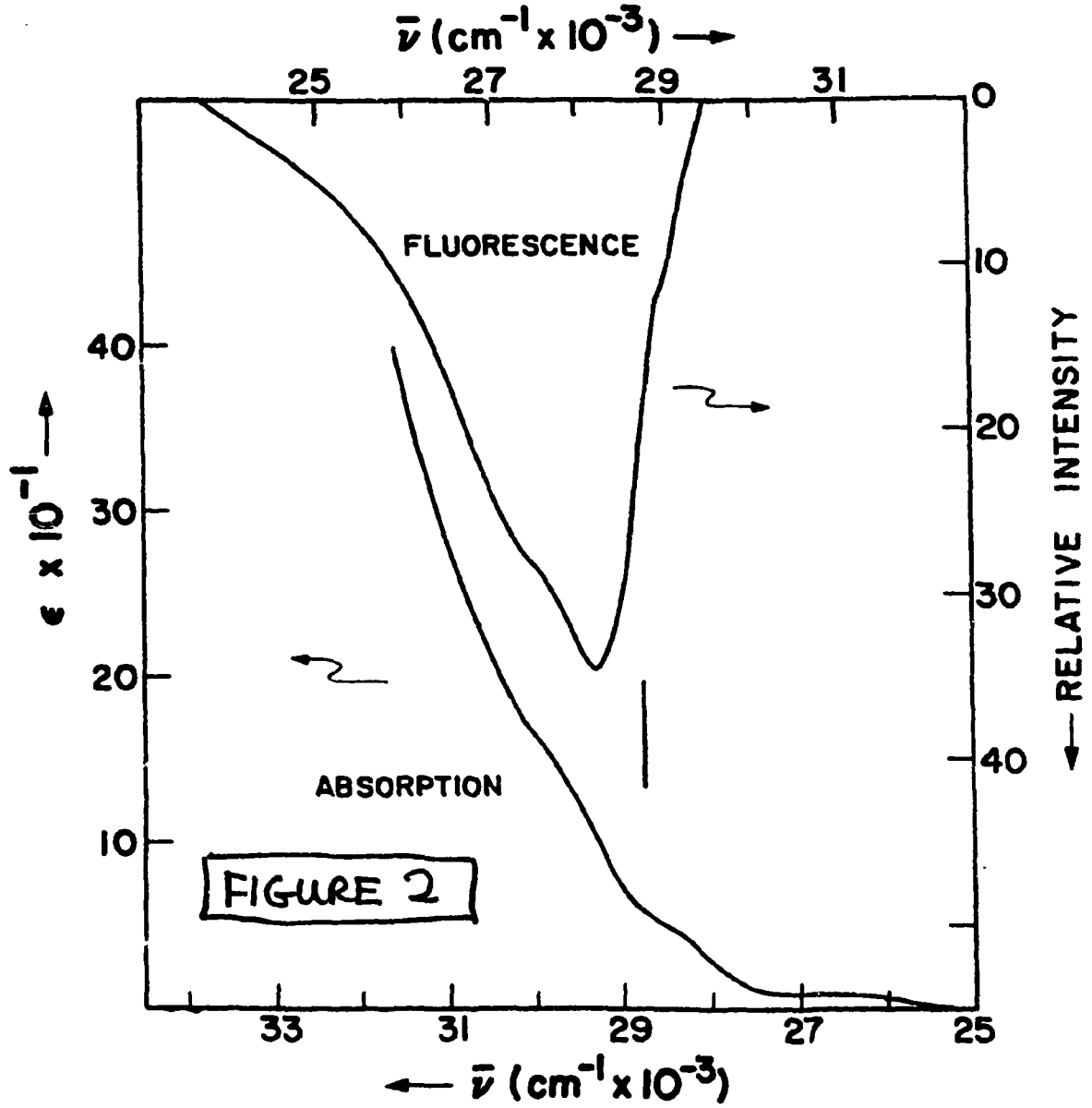

Figure 2. Fluorescence and absorption spectra of p-aminoacetophenone. The fluorescence refers to an ethanol medium at 77°K. Absorption refers to a 3MP medium at ∿300°K. The mirror plane position is indicated by a vertical line.

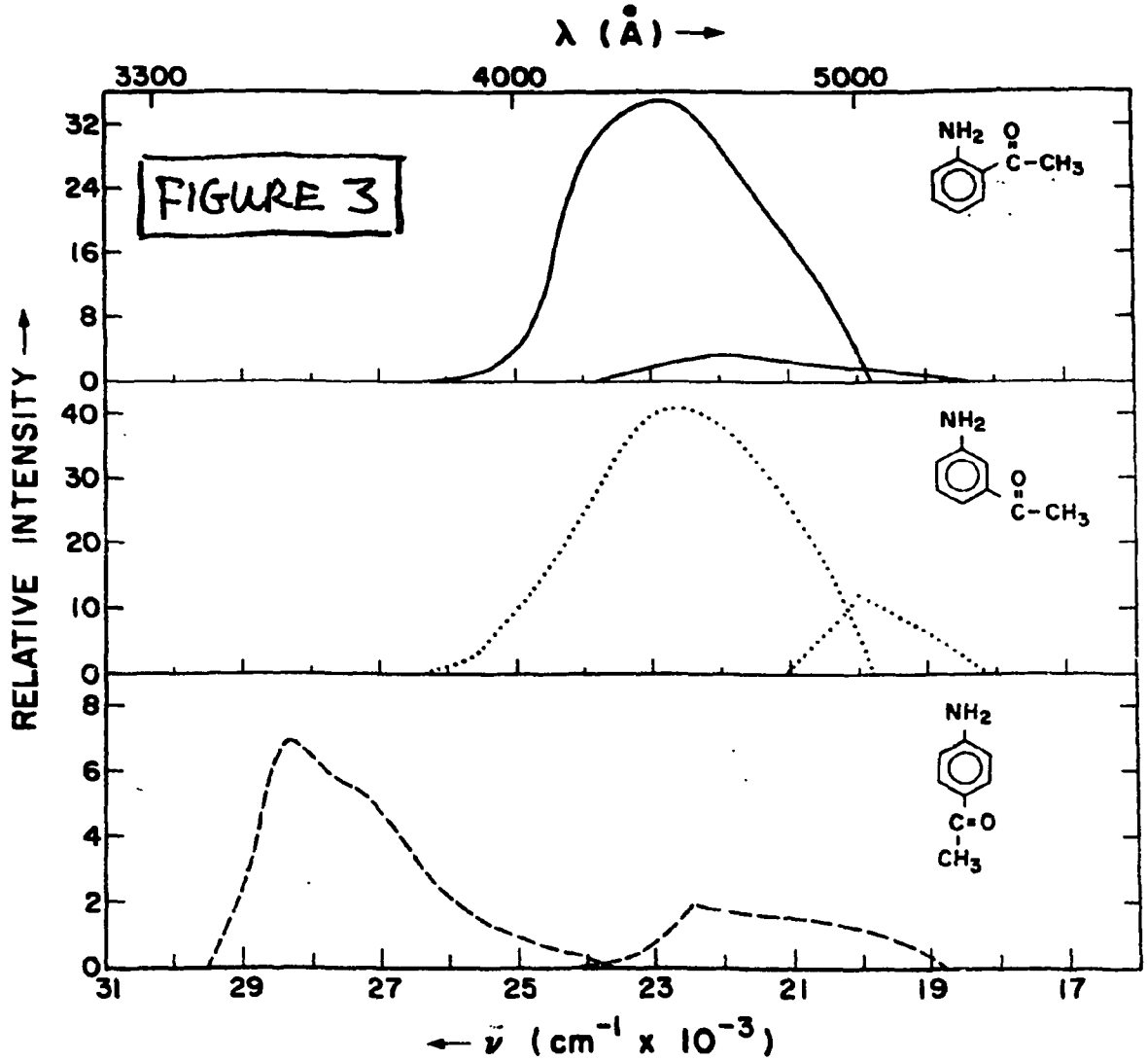

Figure 3. Total luminescence spectra of o-, m- and p-aminoacetophenones in an ethanol glass at 77°K. The spectra are corrected for all instrumental parameters.

FIGURE 4

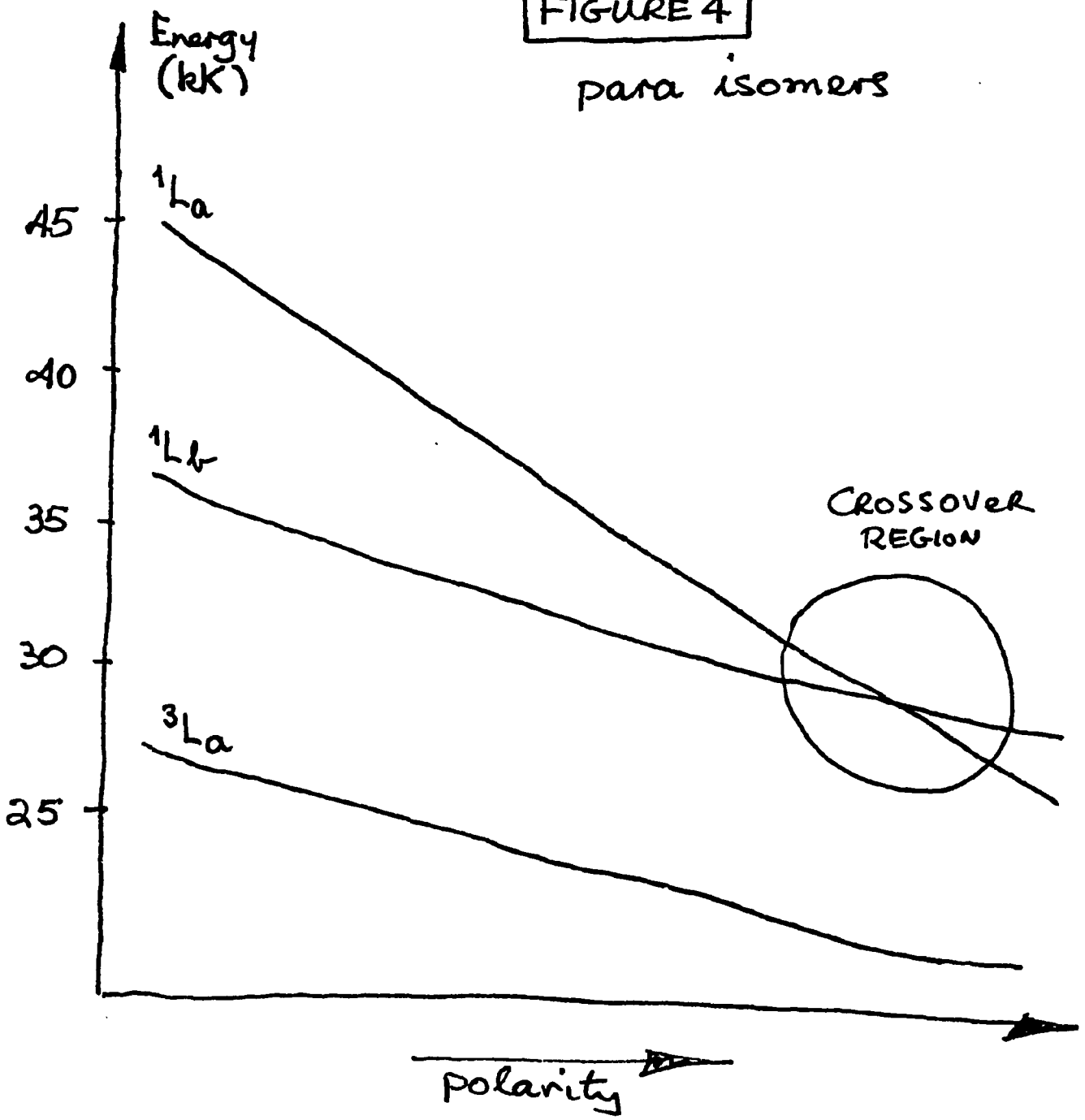

para isomers

$f(^1L_b \leftarrow {}^1\Gamma_1)$ are large and small, respectively. As one progresses to the right, the ratio $f(^1L_a \leftarrow {}^1\Gamma_1)/f(^1L_b \leftarrow {}^1\Gamma_1)$ increases and the ^1L_a-^1L_b splitting decreases. This situation persists up to the crossover region which occurs in the vicinity of nitroaniline. On the left of the crossover region, phosphorescence is weak or absent, fluorescence is dominant and the ^1L_b band is totally submerged beneath the stronger ^1L_a band.

The crossover region itself is of greatest interest. For example, a very innocent substitution, such as N-methylation of an amine group, can shift a molecule from left to right (i.e., from solely phosphorescent to solely fluorescent). Indeed, the sensitivity of the luminescence parameters in this region is so great that the same transformation can be accomplished by a change of solvent.

This model is supported experimentally and computationally. At the moment, we are studying luminescence parameters in the crossover region in an effort to understand the coupling of states which occurs here. Such studies lead us to conclude that the Platt substitutional model is far superior to the Nagakura-Murrell model in terms of explaining the results of both experiment and MO computations.

The behavior of the ortho- and meta-compounds is quite different. The ^1L_a-^1L_b separation tends to increase slightly with increasing polarity and, as a result, no crossover occurs. The $f(^1L_a \leftarrow {}^1\Gamma_1)/f(^1L_b \leftarrow {}^1\Gamma_1)$ ratio is close to unity under all circumstances and increases toward unity as polarity increases. Hence, these molecules behave normally: They usually exhibit both phosphorescence and fluorescence and the effects of innocent substitution or solvent changes are negligible. A diagram

illustrative of level dependencies is given in Figure 5.

It is clear that this work represents a large generalization of the area of polar molecules. It will shortly be prepared for publication.

FIGURE 5

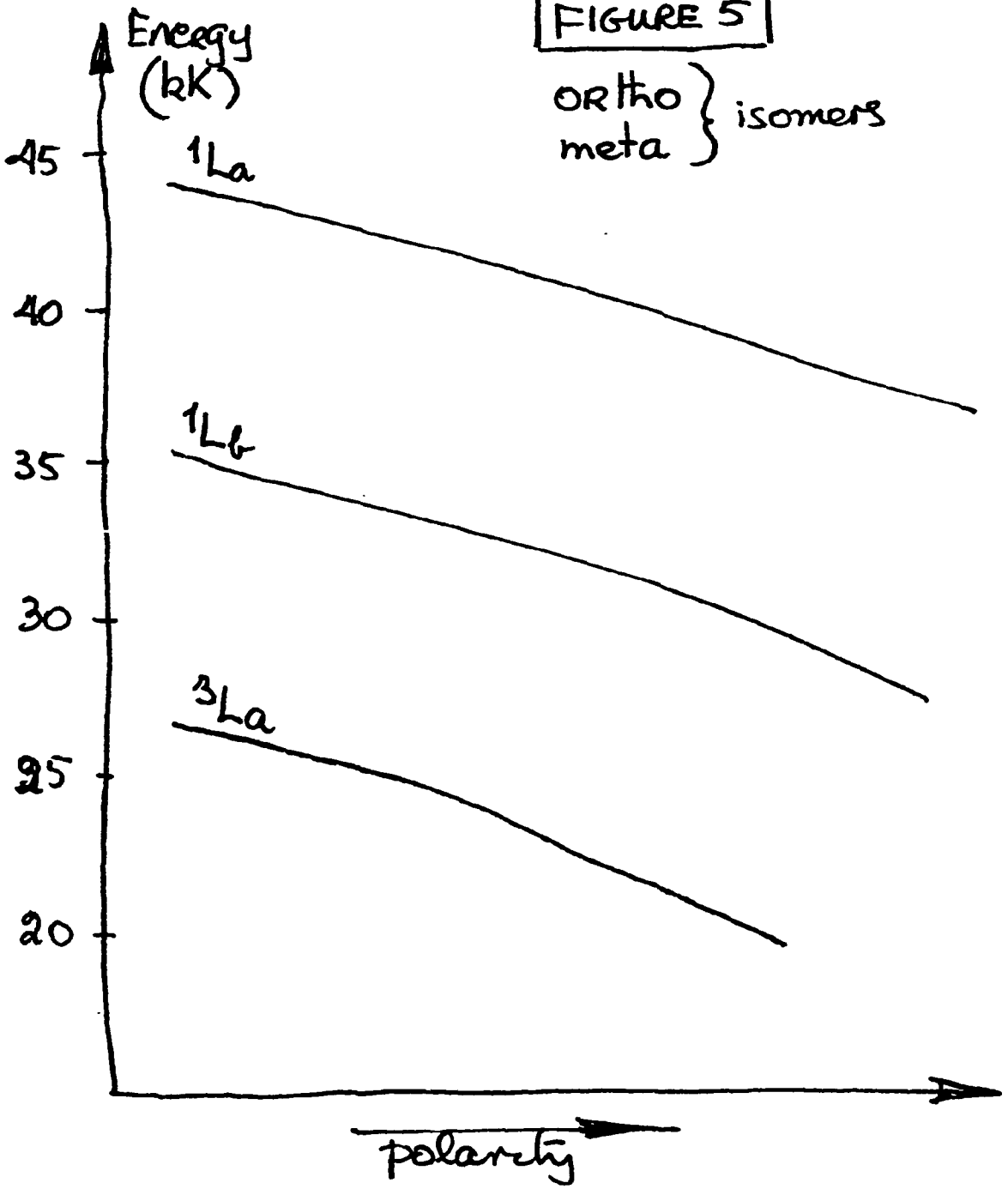
Energy (kK)
45
40
35
30
25
20
^1L_a
^1L_b
^3L_a
ortho
meta
isomers
polarity

VII. MOLECULAR GENETICS

VII. MOLECULAR GENETICS

(See item 167)

The only item of Section II.A concerned with this topic is 167.

A. INTRODUCTION

This report consists of a preliminary investigation into the application of abstract mathematics to molecular genetics. For our purpose we will consider molecular genetics to consist solely of the conceptual processes which comprise the biological information storage and retrieval system. No discussion of the complex physico-chemical interactions which underly the information system will be given except to the extent necessary to define the specific processes involved. Thus, interest is focused on that aspect of molecular genetics which may be abstractly formulated: Namely, DNA (deoxyribonucleic acid) transcription into m-RNA (messenger-ribonucleic acid) and m-RNA translation into protein.

The approach of this work is algebraic in nature. Briefly, DNA, RNA and protein molecules are represented as vectors in separate finite-dimensional vector spaces. Transcription and translation may then be realized as linear operators on certain of the spaces. Such a formulation allows one to express the abstract qualities of molecular genetics in a precise mathematical language. The underlying motivation is to develop a formalism which will facilitate a search for any inherent symmetry principles which operate at the level of very complex biological interactions. Such symmetry principles, if any exist, could be of importance in (i), reformulating (and, of course, re-assessing) existing theories mathematically; and (ii), guiding

future experimental work by positing questions which arise as natural extensions of a mathematical structure. The analogy to the rôle of symmetry in theoretical physics is obvious and intentional.

Two distinct vector space formulations will be presented, each differing from the other in field structure. The use of a continuous field, specifically the real field, allows one to develop a space which admits a geometric interpretation of the macromolecular vectors. However, this space is inadequate to describe the linear arrangement of information units (codons or amino acids) in the molecule. To overcome this difficulty, a space over a finite field is created, but in this second formulation the simple geometric interpretation is lost. The relative merits of these two separate representations of molecular genetics will be discussed.

For the convenience of the reader, we begin by giving a brief list of basic definitions of the necessary mathematics.

B. MATHEMATICAL FOUNDATIONS

(i) SETS

Underlying all of our investigations will be the concept of a set.

Definition:

A set is a collection of distinct elements.

The fundamental property of a set is inclusion; that is, whether or not a given element is a member of a given set. Let A be a set and x an element which may or may not be contained in A. Notationally, we have $x \in A$ (read "x is contained in A") in the first case and $x \notin A$ (read "x is not contained in A") in the second. If we wish to denote the elements of a set explicitly, then we write them contained in curly braces ({}) to indicate set-theoretic inclusion.

We denote a (proper or improper) subset B of the set A by $B \subset A$ (read "B is contained in A") or $A \supset B$ (read "A contains B"). This is to be interpreted in the following manner:

$B \subset A$ if and only if $x \in B \Longrightarrow$ (read "implies that") $x \in A$, for all $x \in B$.

If $B \subset A$ and $B \supset A$, then $B = A$; that is, the sets B and A are identical.

For convenience, we postulate the existence of a set which contains no elements, the empty or null set, denoted $\emptyset$. With the existence of this set, we may proceed to develop a notational calculus for sets.

If two sets A and B have no elements in common, then they are said to be disjoint, in symbols $A \circ B$. This is succintly emphasized in terms of the intersection, a binary operation on sets to be defined below.

Let A and B be two (not necessarily) disjoint sets. The union of A and B is the set $A \dot{+} B$, such that if $x \in A$ and/or $x \in B$, then $x \in A \dot{+} B$. When A is disjoint from B, we write the union as $A + B$.

The intersection of A and B is the set AB, such that if $x \in A$ and $x \in B$, then $x \in AB$. In case $A \circ B$, then $AB = \emptyset$.

The (proper) difference of two sets is defined only when $B \subset A$. In this case, the difference of A and B is the set $A - B$, such that if $x \in A - B$, then $x \in A$ but $x \notin B$. The difference is often termed the relative complement of B in A.

Countable (finite or infinite) generalizations of the above operations are obvious and will not be discussed.

An abstract set is totally determined by its cardinality. For a finite set (a set with a finite number of elements), the cardinality is simply the number of elements in the set. Such a cardinal number is termed a finite cardinal number. The existence of infinite sets (sets with an infinite number of elements), however, leads to the concept of transfinite cardinal numbers. We will introduce these only by example and refer the

interested reader to standard works.[2]

Consider the set of natural numbers $\mathcal{N} = \{1,2,3,\ldots\}$. This is the prototype countable infinite set and its cardinality is the first transfinite cardinal number, a. The only other infinite set with which we shall be concerned is the uncountable infinite set, having the transfinite cardinal number c (continuum). The set of real numbers is a representation of this abstract set.

We may define the sum of cardinal numbers as the cardinal number of a union of sets. The product of cardinal numbers is defined in terms of a Cartesian product of sets as follows. Let M and N be sets with cardinal numbers m and n, respectively. Then, M x N denotes the Cartesian product set which consists of all ordered 2-tuples of the elements of M and N; one member of the 2-tuple comes from M and one from N. The cardinality of M x N is $m \cdot n$. For example, let $M = \{a,b\}$, $N = \{c,d\}$, then

$$M \times N = \{(a,c), (a,d), (b,c), (b,d)\} \equiv P$$

and the cardinality of P is $2 \cdot 2 = 4$. The countable extension is obvious and will not be formally presented.

(ii) MAPPINGS

A mapping is a rule which assigns to each element (pre-image) of its domain A a distinct element (image) of its range B, in symbols $f:A \rightarrow B$.

If every image has only one pre-image, then f is said to be one-to-one or injective. If every element of B has at least one pre-image, then f is said to be onto or surjective. A mapping which is both one-to-one and onto is a bijective mapping, or more familiarly, a one-to-one correspondence.

(iii) GROUPS

Definition:

A Group is a set G and a binary combination rule (group product) which associates to every ordered pair (a,b) of elements of G an element ab of G in such a way that the following axioms are satisfied.

GA1. For all $a,b,c \in G$, $a(bc) = (ab)c$.

GA2. There exists $e \in G$ such that $ea = ae = a$ for all $a \in G$.

GA3. For every $a \in G$, there exists $a^{-1} \in G$ such that $aa^{-1} = a^{-1}a = e$.

GA1 ensures that the formation of the group product (group multiplication) is associative. GA2 postulates the existence of an identity element which is readily seen to be unique. GA3 postulates the existence of an inverse for every element of G, and these inverses are also readily seen to be unique.

In general, group multiplication is not commutative. In the event that it is, the group is said to be abelian. For an abelian group, the combination rule is usually denoted as + and the identity as 0. For non-abelian groups, we will use $\cdot$ (normally suppressed) to denote group multiplication and 1 to symbolize the identity element.

Some authors denote the group as the pair (G,f), where f is the group product $f: G \times G \to G$. This notation has the advantage of allowing one to symbolize groups of the same elements having different combination rules. We will refrain from employing this notation, however.

The groups with which we shall be concerned in this work are the additive group of real numbers, the multiplicative group of real numbers, the additive group of integers modulo n and the multiplicative group of integers modulo p, where p is prime. We shall assume that the reader is familiar with the first two groups and, consequently, we discuss only the last two in detail.

Additive group of integers modulo n:

We define congruence of two integers modulo the natural number n by $a = b + kn$, where k is an integer. This is shortened simply to $a = b \bmod n$. The equivalence class (or congruence class) of a modulo n is given by

$$[a]_n = \{x \in Z \mid x = a \bmod n\} \qquad \ldots.1$$

where Z is the set of integers. Simply put, $[a]_n$ is the set which contains all of the integers which are congruent to a modulo n.

It is easy to see that every $a \in Z$ is congruent modulo n to one of the numbers 0, 1, 2, ..., n-1. Now, consider the set

$$Z_n \equiv \{[0]_n, [1]_n, \ldots, [n-1]_n\} \qquad \ldots.2$$

under addition modulo n, Z_n becomes an additive abelian group of order n. The sum on Z_n is defined by

$$[a]_n + [b]_n = [a + b]_n \qquad \ldots.3$$

The identity element is $[0]_n$ and the inverse of an element $[a]_n$ is defined by

$$-[a_n] = [-a]_n = [n-a]_n \qquad \ldots.4$$

Multiplicative group of integers modulo p:

We may define multiplication on Z_p by

$$[a]_p[b]_p = [ab]_p \qquad \ldots.5$$

Hence, $[1]_p$ may obviously serve as the multiplicative identity. In addition, since p is prime,[3] every element has an inverse, excluding $[0]_p$. Thus the set

$$Z'_p \equiv \{[1]_p, [2]_p, \ldots, [p-1]_p\}$$

forms a group under multiplication modulo p. In addition, this group may be shown to be cyclic.

(iv) FIELDS:

Definition:

A field is a set $\mathcal{F}$ which satisifies the following axioms.

FA1. $\mathcal{F}$ is an additive abelian group with the identity denoted 0.

FA2. $\mathcal{F}^* \equiv \mathcal{F} - \{0\}$ is a multiplicative abelian group with the identity denoted 1.

FA3. Multiplication is distributive over addition; that is, for every $a,b,c \in \mathcal{F}$,

$$a(b+c) = ab+ac \text{ and } (b+c)a = ba+ca$$

We note that $0 \cdot a = a \cdot 0 = 0$ for all $a \in \mathcal{F}$.

It is easy to show that Z_p, where p is prime, forms a field. Since the groups involved are finite, this field is finite.

(v) VECTOR SPACES:

Definition:

A vector space over the field $\mathcal{F}$ is an additive abelian group V for which there is defined a binary rule, termed scalar multiplication, such that for every $c \in \mathcal{F}$ (a scalar) and $\underset{\sim}{\alpha} \in V$ (a vector) there exists the product $c\underset{\sim}{\alpha} \in V$, satisfying the following axioms.

VSA1. $c(d\underset{\sim}{\alpha}) = (cd)\underset{\sim}{\alpha}$ for every $c,d \in \mathcal{F}$, and $\underset{\sim}{\alpha} \in V$.

VSA2. $(c+d)\underset{\sim}{\alpha} = c\underset{\sim}{\alpha} + d\underset{\sim}{\alpha}$ for every $c,d \in \mathcal{F}$, and $\underset{\sim}{\alpha} \in V$.

VSA3. $c(\underset{\sim}{\alpha} + \underset{\sim}{\beta}) = c\underset{\sim}{\alpha} + c\underset{\sim}{\beta}$ for every $c \in \mathcal{F}$, and $\underset{\sim}{\alpha}, \underset{\sim}{\beta} \in V$.

VSA4. $1\underset{\sim}{\alpha} = \underset{\sim}{\alpha}$ for every $\underset{\sim}{\alpha} \in V$.

Definition:

A finite set of elements of V, $\{\underset{\sim}{\alpha}_1, \underset{\sim}{\alpha}_2, \ldots, \underset{\sim}{\alpha}_n\}$ is <u>linearly dependent</u> over $\mathcal{F}$ if there exist scalars $c_1, c_2, \ldots, c_n \in \mathcal{F}$ <u>not all zero</u> such that

$$c_1\underset{\sim}{\alpha}_1 + c_2\underset{\sim}{\alpha}_2 + \ldots + c_n\underset{\sim}{\alpha}_n = \underset{\sim}{0}$$

If the only relation which exists is the trivial one (that is, $c_i = 0$, $i = 1,2,\ldots,n$) then the set of vectors $\{\underset{\sim}{\alpha}_1, \underset{\sim}{\alpha}_2, \ldots \underset{\sim}{\alpha}_n\}$ is termed linearly independent over $\mathcal{F}$.

Definition:

Let V be a vector space over the field $\mathcal{F}$. $S \subset V$ is a spanning set for V if for every $\underset{\sim}{\alpha} \in V$, $\underset{\sim}{\alpha}$ may be written as a linear combination $\sum_i c_i \underset{\sim}{\sigma}_i$, where $c_i \in \mathcal{F}$ and $\underset{\sim}{\sigma}_i \in S$. If S is finite, then V is a finite dimensional vector space.

Definition:

Let V be a vector space. $B \subset V$ is a basis for V if B is a minimal spanning set for V.

We state without proof the following three propositions.

1. A basis for a vector space is a linearly independent set.

2. Let B be a basis for V over $\mathcal{F}$. Then every $\underset{\sim}{\alpha} \in V$ may be expressed uniquely as a linear combination of elements of B with coefficients in $\mathcal{F}$.

3. All bases for a finite-dimensional vector space have the same cardinality. Further, the cardinality of a basis for a finite-dimensional vector space is equal to the dimension of the space.

(vi) INNER-PRODUCT SPACES[4]:

Definition:

An inner-product is a scalar-valued function defined on a vector space V over a field $\mathcal{F}$, such that the following axioms are satisfied.

IPA1. $(\underset{\sim}{\alpha}, \underset{\sim}{\beta}) = (\underset{\sim}{\beta}, \underset{\sim}{\alpha})$ for every $\underset{\sim}{\alpha}, \underset{\sim}{\beta} \in V$

IPA2. $(a\underset{\sim}{\alpha} + b\underset{\sim}{\beta}, \underset{\sim}{\gamma}) = a(\underset{\sim}{\alpha}, \underset{\sim}{\gamma}) + b(\underset{\sim}{\beta}, \underset{\sim}{\gamma})$ for every $\underset{\sim}{\alpha}$, $\underset{\sim}{\beta}$, $\underset{\sim}{\gamma} \in V$ and $a, b \in \mathcal{F}$.

IPA3. $(\underset{\sim}{\alpha}, \underset{\sim}{\alpha}) \geq 0$ for all $\underset{\sim}{\alpha} \in V$; $(\underset{\sim}{\alpha}, \underset{\sim}{\alpha}) = 0$ if and only if $\underset{\sim}{\alpha} = \underset{\sim}{0}$. (positive-definiteness).

Definition:

An inner-product space is a vector space with an inner-product defined on the space.

C. THE GENETIC CODE

The genetic code may be considered to be a language based on the set of four elements $\{U,A,C,G\} \equiv \mathcal{B}$. These elements (U,A,C,G) represent the purine (A,G) and pyrimidine (U,C) nucleic acid bases which determine the functionality of a ribonucleic acid message. The linear sequence of these bases in a given messenger RNA template determines the linear sequence of amino acids in a nascent protein molecule. Each triplet (codon) of the base elements codes the introduction of a specific amino acid into a growing protein, a process which involves recognition of the anticodon sequence on a transfer RNA (t-RNA) molecule, the amino acid carrier. The codon-anticodon association occurs within a ribosome, one of the functions of which is to set the appropriate phase of translation (code interpretation). The reader is referred to Hayes[5] and Davidson[6] for a detailed description of the function of the genetic code in protein synthesis.

The full code is the set consisting of all possible ordered 3-tuples of the set $\mathcal{B}$. Thus, there are $4^3 = 64$ codons and this set will be denoted $\mathcal{C}$. The third set to be considered consists of the twenty amino acids and the operator TC (the terminator codon, which interrupts the process of protein synthesis). We will label this set $\mathcal{A}$. Hence, symbolically, we may denote the process of code interpretation by the mapping

$$f:\mathcal{C} \rightarrow \mathcal{A} \qquad \ldots.6$$

This mapping has been fully determined[6] by chemical and/or genetic methods and is presented in Table 1. A brief inspection of Table 1 characterizes

Table 1

The Genetic Code[1]

UUU Phe	UAU Tyr	UCU, UCA, UCC, UCG Ser	UGU Cys
UUA Leu	UAA TC		UGA TC
UUC Phe	UAC Tyr		UGC Cys
UUG Leu	UAG TC		UGG Trp
AUU, AUA, AUC Ile	AAU Asn	ACU, ACA, ACC, ACG Thr	AGU Ser
	AAA Lys		AGA Arg
	AAC Asn		AGC Ser
AUG Met	AAG Lys		AGG Arg
CUU, CUA, CUC, CUG Leu	CAU His	CCU, CCA, CCC, CCG Pro	CGU, CGA, CGC, CGG Arg
	CAA Gln		
	CAC His		
	CAG Gln		
GUU, GUA, GUC, GUG Val	GAU Asp	GCU, GCA, GCC, GCG Ala	GGU, GGA, GGC, GGG Gly
	GAA Glu		
	GAC Asp		
	GAG Glu		

[1] The amino acid (or terminator codon) to which each codon corresponds is written to the right of the codon. Standard abbreviations for the amino acids are used (see Table 2).

f as mapping $\mathfrak{C}$ onto $\mathfrak{A}$. Since the cardinality of $\mathfrak{C}(64)$ is greater than the cardinality of $\mathfrak{A}(21)$, the surjective nature of this mapping defines the redundancy of the gentic code. The number of elements of $\mathfrak{C}$ which map onto each element of $\mathfrak{A}$ under the function f is listed in Table 2. The combinational nature of this redundancy has been investigated group-theoretically by Findley and McGlynn.[7]

The linear sequence of codons in an m-RNA molecule is determined by the template DNA molecule. DNA differs from RNA in being composed of the nucleic acid bases $\{T,A,C,G\} \equiv \mathfrak{B}'$, where U has been replaced by T (thymine) in DNA. Additionally, DNA is a double-stranded moiety, whereas RNA is usually single-stranded. We will express the relation between $\mathfrak{B}$ and $\mathfrak{B}'$ as the one-to-one correspondence

$$h:\mathfrak{B}' \rightarrow \mathfrak{B} \qquad \ldots.7$$

where

$$h(T) = U;\ h(A) = A;\ h(C) = C;\ h(G) = G \qquad \ldots.8$$

and the inverse mapping is also defined.

Mathematically, we may express the gentic code as the Cartesian product

$$\mathfrak{B} \times \mathfrak{B} \times \mathfrak{B} = \mathfrak{C} \qquad \ldots.9$$

Hence, at the DNA level, the code becomes

$$h^{-1}(\mathfrak{C}) = \mathfrak{C}' \equiv \mathfrak{B}' \times \mathfrak{B}' \times \mathfrak{B}' \qquad \ldots.10$$

In DNA transcription only one strand of the double-stranded molecule is utilized as the template in synthesizing a specific m-RNA molecule. A further constraint is that m-RNA synthesis can proceed only from the 3′ terminus to the 5′ terminus of the DNA template. The polarity designations 5′, 3′ of a DNA template derive from the substituent positions on the deoxyribose unit of the DNA polymer. The 5′ position refers to the hydroxy

Table 2

Redundancy of the Genetic Code

Elements of $\mathcal{A}$	Order of Redundancy
Ser (Serine)	6
Arg (Arginine)	6
Leu (Leucine)	6
Ala (Alanine)	4
Val (Valine)	4
Pro (Proline)	4
Gly (Glycine)	4
Thr (Threonine)	4
Ile (Isoleucine)	3
TC (Terminator Codon)	3
Phe (Phenylalanine)	2
Tyr (Tyrosine)	2
Cys (Cysteine)	2
His (Histidine)	2
Gln (Glutamine)	2
Lys (Lysine)	2
Glu (Glutamic Acid)	2
Asp (Aspartic Acid)	2
Asn (Asparagine)	2
Trp (Tryptophan)	1
Met (Methionine)	1

substituted carbon external to the deoxyribose ring, while the 3′ position refers to the hydroxy substituted carbon internal to the ring.

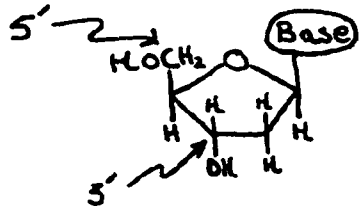

Adjacent deoxyribose units in the single-stranded DNA molecule are bonded together via a phosphodiester linkage, with the binding occurring at the 5′ position on one unit and at the 3′ position on the other.

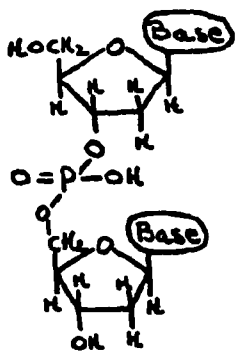

If we now consider the entire single-stranded DNA molecule, one end of the molecule terminates in a deoxyribose unit which is bonded to the rest of the molecule at the 3′ position, while the other end terminates in a unit bonded to the rest of the molecule at the 5′ position. These are termed the 5′ and 3′ ends of the molecule, respectively. In the double stranded DNA molecule, however, association occurs such that one strand has the opposite polarity of the other if we view the molecule in one direction, left-to-right say, along the chain. The importance of distinguishing the different polarities is simply that m-RNA synthesis occurs only in the 3′ → 5′ direction <u>along</u> a single strand of DNA.

Unlike transcription, translation (protein synthesis) proceeds in the 5′ → 3′ direction <u>along</u> the template m-RNA molecule. Care must be taken

when relating a given codon message back to the template DNA from which it arose. Consider a single-stranded DNA template. When m-RNA is made from this template the RNA molecule grows in the $5' \rightarrow 3'$ direction, since synthesis proceeds in the $3' \rightarrow 5'$ direction along the DNA template. However, the m-RNA codon message is read in the $5' \rightarrow 3'$ direction and, thus, the controlling DNA codon message must be interpreted in the $3' \rightarrow 5'$ direction.

D. FORMULATION OF MOLECULAR GENETICS AS AN n-DIMENSIONAL VECTOR SPACE

(i) R-FIELD:

Consider the 64-dimensional vector space over the field of real numbers R. We may choose the set $\mathcal{E}'$ as a basis for this space. In this case the space will be termed D_1. Let an inner-product be defined on D_1. Since $\mathcal{E}'$ is a linearly independent set, we may choose it to be orthogonal. Further, let the elements of $\mathcal{E}'$ be normalized. Thus,

$$(\underset{\sim}{\alpha}_i, \underset{\sim}{\alpha}_j) = \delta_{ij} \qquad \ldots.11$$

where $\underset{\sim}{\alpha}_i$, $\underset{\sim}{\alpha}_j \in \mathcal{E}'$, δ_{ij} is the Kronecker delta, and $\{i,j = 1,2,3, \ldots, 64\}$.

Since $\mathcal{E}'$ spans D_1, we have for every $\underset{\sim}{c} \in D_1$

$$\sum_{i=1}^{64} c_i \underset{\sim}{\alpha}_i = \underset{\sim}{c} \qquad \ldots.12$$

where $c_1, c_2, \ldots, c_{64} \in R$ are unique. Using (11), we may write

$$(\underset{\sim}{c}, \underset{\sim}{d}) = \sum_{i=1}^{64} c_i d_i \qquad \ldots.13$$

In view of (13), the 64-tuple $(c_1, c_2, \ldots, c_{64})$ may be considered to be a row vector $\langle c|$ while the 64-tuple $(d_1, d_2, \ldots, d_{64})$ is a column vector $|d\rangle$. $\langle c|$ and $|d\rangle$ are representations of $\underset{\sim}{c}$ and $\underset{\sim}{d}$ respectively.

The Euclidean norm is defined on D_1; that is

$$||\underset{\sim}{c}|| = (\underset{\sim}{c}, \underset{\sim}{c})^{\frac{1}{2}} \qquad \ldots.14$$

Hence, we have a geometrical interpretation of D_1, where the angle θ between two vectors $\underset{\sim}{c}$ and $\underset{\sim}{d}$ is given by

$$\theta = \cos^{-1}\left[\frac{(\underset{\sim}{c},\underset{\sim}{d})^{\frac{1}{2}}}{||\underset{\sim}{c}||\cdot||\underset{\sim}{d}||}\right] \qquad \ldots.15$$

Finally, we define the projection operator

$$P_i\underset{\sim}{c} = (\underset{\sim}{\alpha}_i, \underset{\sim}{c})\,\underset{\sim}{\alpha}_i = c_i\underset{\sim}{\alpha}_i \qquad \ldots.16$$

D_1 may be interpreted as a space of DNA vectors. Each vector having positive integral coefficients represents a single strand of a given DNA molecule. We shall return to the representation of the double-stranded moiety below.

The positive integral coefficients c_i represent the number of occurrences of a given DNA codon $\underset{\sim}{\alpha}_i$ in a single-stranded DNA. Mathematically, c_i is the projection of the vector along the $\underset{\sim}{\alpha}_i$ axis in 64-space. Hence we may write the total number of codons in a single-stranded DNA as

$$\sum_{i=1}^{64} (\underset{\sim}{\alpha}_i, P_i\underset{\sim}{c}) = \sum_{i=1}^{64} c_i = n \qquad \ldots.17$$

where $\underset{\sim}{c}$ is the vector representation of the molecule.

By convention, we let the space D_1 be composed of vectors which represent single-stranded DNA molecules having $3' \rightarrow 5'$ polarity. We define the associated space D_1^* as a space of vectors which represent single-stranded DNA molecules having $5' \rightarrow 3'$ polarity. It is obvious, of course, that $D_1 = D_1^*$. In fact, D_1^* serves merely to remind us that opposite strands of a total DNA molecule have opposite polarity with respect to one another. In D_1 the codons are read from the 5′ to the 3′ end of the single-stranded molecule in forming the basis set. Thus, if $\underset{\sim}{\alpha}_i$ = TAG, then $\underset{\sim}{\alpha}_i^*$ = GAT. We may view the transition from D_1 to D_1^* as the one-to-one correspondence

$$k: D_1 \rightarrow D_1^* \qquad \ldots.18$$

which simply reverses the polarity of the codon basis vectors.

Now, consider the base-antibase mapping, g, which is a one-to-one correspondence defined by

$$\begin{aligned} g(T) &= A \qquad g(C) = G \\ g(A) &= T \qquad g(G) = C \end{aligned} \qquad \ldots.19$$

Let $\underset{\sim}{c} \epsilon D_1$. We will denote the operation of g on $\underset{\sim}{c}$ as $g(\underset{\sim}{c}) = \bar{\underset{\sim}{c}}$. Thus, if $\underset{\sim}{\alpha}_i$ = TAC, then $\bar{\underset{\sim}{\alpha}}_i$ = ATG.

With the mappings k and g in mind, we proceed to define the representation of a double-stranded DNA. Let $\underset{\sim}{c} \epsilon D_1$ represent the $3' \rightarrow 5'$ strand of a given DNA molecule. Let $\underset{\sim}{d}^* \epsilon D_1^*$ represent the $5' \rightarrow 3'$ strand of the same molecule. It follows that $\underset{\sim}{c}$ and $\underset{\sim}{d}^*$ are related to the same double-stranded DNA if and only if $\underset{\sim}{c} = \bar{\underset{\sim}{d}}^*$. Thus, the total DNA is represented by the pair

$$[\underset{\sim}{c}, \underset{\sim}{d}^*] \qquad \ldots.20$$

where $\underset{\sim}{c} = \bar{\underset{\sim}{d}}^*$ (equivalently, of course, we may write $\bar{\underset{\sim}{c}} = \underset{\sim}{d}^*$).

More than one DNA molecule will be represented by the same vector pair. In fact, a given vector pair represents N distinct DNA molecules, where N is given by

$$N = \frac{n!}{c_1! c_2! \ldots c_{64}!} \qquad \ldots.21$$

where n is defined in (17), the c_i are defined in (12) and both n and the c_i are positive integral. However, for a given DNA molecule, only one vector pair is defined.

The particular form of (21) results from the manner in which information is encoded in a DNA molecule. This vector formalism adequately describes the number of codons of a given type which occurs in the molecule, but the

order of occurrence is disregarded. Thus, a DNA vector pair contains less information than the DNA molecule from which it is formed. This information may be recaptured only by a radical restructing of the field (vide infra).

The vector space D_1 contains vectors which do not represent physically-realizable DNA molecules; that is, those vectors with coefficients which are not positive integral. These vectors permit the continuous deformation of one physically-realizable DNA vector into another. Such a process may be interpreted as evolution, and an evolution operator $\mathcal{E}$ may be constructed. Geometrically, this operator simply acts to either rotate a vector in 64-space or change its length or both. That is, the evolution operator is a familiar linear transformation on the DNA vectors. Since evolution is a time-based phenomenon, however, $\mathcal{E}$ must be time-dependent. Thus, evolution may be viewed as a time varying linear operator $\mathcal{E}(t)$ on D_1. It should be noted, however, that the physical interpretation constrains $\mathcal{E}(t)$ to select physically-realizable DNA vectors. We shall not pursue this development further in the present work.

If the non-physical DNA vectors are excluded from D_1, then D_1 is no longer a vector space. Hence, these physically-unrealizable vectors are essential to the formalism. A space which contains only physically-realizable vectors can be constructed, but it requires a restructuring of the field (vide infra).

Transcription:

We next wish to develop a mapping from the set of DNA vector pairs into the space of RNA vectors. This, of course, is the process of transcription.

We postulate the existence of a transcription operator $\mathcal{T}$ which operates on a DNA vector pair to produce an RNA vector. This RNA vector represents, biologically, the transcription product of the $3' \rightarrow 5'$ DNA vector. Let the DNA vector pair $[\underset{\sim}{c}, \underset{\sim}{d}']$ be given. Then,

$$\mathcal{T}[\underset{\sim}{c},\underset{\sim}{d}^*] = h(\underset{\sim}{d}^*) = \underset{\sim}{r} \qquad \ldots.22$$

where h is defined in (7); and where $\underset{\sim}{r} \epsilon R_1$, the RNA vector space. The basis for R_1 is the orthonormal set $\mathcal{C}$. Note that in (22), $\underset{\sim}{r}$ is defined so as to have $5' \rightarrow 3'$ polarity.

The $5' \rightarrow 3'$ vector is transcribed by the operator $\mathcal{T}^*$.

$$\mathcal{T}^*[\underset{\sim}{c},\underset{\sim}{d}^*] = h(k(\underset{\sim}{c})) = \underset{\sim}{r}' \qquad \ldots.23$$

where k is defined in (18); and where $r' \epsilon R_1$. Again, note that $\underset{\sim}{r}'$ is defined so as to have $5' \rightarrow 3'$ polarity (this is a direct result of the fact that k acts to reverse the polarity of $\underset{\sim}{c}$).

Thus, $\mathcal{T}$ transcribes the $3' \rightarrow 5'$ vector, while $\mathcal{T}^*$ transcribes the $5' \rightarrow 3'$ vector.

Considered in its totality, the vector space R_1 may be defined as being isomorphic to D_1. Then, the one-to-one and onto mapping from D_1 to R_1 is

$$h: D_1 \rightarrow R_1 \qquad \ldots.24$$

Hence, R_1 is structurally identical to D_1, and its properties need not be investigated. The definition of the operators $\mathcal{T}$ and $\mathcal{T}^*$, however, allows us to focus attention directly on a fixed DNA vector pair and its transcription into the correct biologically related RNA vectors. It is for this reason that $\mathcal{T}$ and $\mathcal{T}^*$ were constructed.

As was the case for D_1, R_1 also contains vectors which are not physically realizable. In order to remain consistent, we will define the domain of $\mathcal{T}$ and $\mathcal{T}^*$ to be all DNA vector pairs, whether or not they are physically realizable. In addition, the number of RNA molecules corresponding to a given R_1 vector is equal to N, where N is defined analogously to (21). As for D_1, only one R_1 vector corresponds to a given RNA molecule.

Translation:

Translation of an m-RNA results in the formation of a protein molecule. The rule which assigns a particular amino acid to a given m-RNA codon is, of course, that defined by the mapping $f: \mathcal{C} \to \mathcal{A}$. Protein synthesis is initiated at the AUG codon[8] on an m-RNA molecule and proceeds in the $5' \to 3'$ direction along the template until one of the terminator codons is reached.

Consider the set of vectors $S_1 \subset R_1$ which represent all RNA molecules having an AUG codon at the $5'$ terminus and one of the terminator codons at the $3'$ terminus but containing no other terminator codons. Translation maps S_1 into P_1, the space of protein vectors. P_1 is a 20-dimensional vector space over the field R. We take as an (orthonormal) basis for P_1 the set $\mathcal{A}' \equiv \mathcal{A} - \{TC\}$. The translation operator is simply the mapping f defined in (6). Thus, given a $\underset{\sim}{\sigma} \in S_1$,

$$f(\underset{\sim}{\sigma}) = \underset{\sim}{\rho} \qquad \ldots.25$$

where $\underset{\sim}{\rho} \in P_1$.

We define P_1 to be an inner-product space, hence the analogs of (12), (13), (14), (15) and (16) in P_1 space are valid. This allows the length of a protein vector and the angle between two protein vectors to be determined. Since there is a relative abundance of protein sequences available in the literature, one immediate application of this formalism consists of the investigation of the norm and the angle relationships between protein vectors whose representative proteins are physically related. Such an investigation may lead to generalizations concerning structure/function/evolution relationships between proteins.

The combinational formula which enumerates the number of protein molecules related to a fixed vector in S_1 is more complicated than those given previously. This results from the constraint placed on the vectors of S_1 and the surjective nature of the mapping f. This will not be investigated in this work. However, the number N' of protein molecules related to a fixed vector of P_1 is given by

$$N' = \frac{n'!}{p_1!p_2! \cdots p_{20}!} \qquad \ldots.26$$

where n' is the total number of amino acids occuring in the protein molecule, and the p_i are the expansion coefficients of the protein vector. For the sake of completeness, we note that only one protein vector corresponds to a given protein molecule.

(ii) FINITE FIELD:

A DNA molecule contains information concerning the order in which the bases (and, ultimately, the m-RNA codons) are arranged linearly along the molecule. This information was not fully incorporated in the previous discussion, but it may be completely retained in the vector space structure through the use of a finite field. The field of interest is Z_5.

$$Z_5 \equiv \{[0]_5, [1]_5, [2]_5, [3]_5, [4]_5\} \qquad \ldots.27$$

We make the order-isomorphism

$$\{[0]_5, [1]_5, [2]_5, [3]_5, [4]_5\} \leftrightarrow \{0,T,A,C,G\} \qquad \ldots.28$$

Thus the field consists of the set $\mathcal{B}' + \{0\} \equiv \mathcal{H}'$, where 0 is an abstract element which serves as the additive identity. Since in any order-isomorphism we must have $[0]_5 \leftrightarrow 0$, then there are 24 (not necessarily distinct) order-isomorphisms of the form (28).

Let the set $\{\underset{\sim}{a}_1, \underset{\sim}{a}_2, \ldots, \underset{\sim}{a}_n\}$ be a finite set of cardinality n which is linearly independent over $\mathcal{H}'$. Let D_2 be an n-dimensional vector space over the field $\mathcal{H}'$ for which $\{\underset{\sim}{a}_1, \underset{\sim}{a}_2, \ldots, \underset{\sim}{a}_n\}$ is a basis. Thus, every $c \in D_2$ may be expressed as

$$c = \alpha_1\underset{\sim}{a}_1 + \alpha_2\underset{\sim}{a}_2 + \ldots + \alpha_{n-1}\underset{\sim}{a}_{n-1} + \alpha_n\underset{\sim}{a}_n \qquad \ldots.29$$

D_2 has the following physical interpretation. Every $\underset{\sim}{c}\epsilon D_2$ represents a physically-realizable, single-stranded DNA molecule which, by convention, we shall take to have $3' \rightarrow 5'$ polarity. The basis vectors simply serve as a place-keeping device, while the linear arrangement of DNA bases along the molecule becomes the ordered set of expansion coefficients of the vector.

We define the associated space D_2^* as the vector space representing single-stranded DNA molecules having $5' \rightarrow 3'$ polarity. Thus, we may represent a double-stranded DNA molecule as the vector pair

$$[\underset{\sim}{c}, \underset{\sim}{d}^*] \qquad \ldots.30$$

where $\underset{\sim}{c}\epsilon D_2$, $\underset{\sim}{d}^*\epsilon D_2^*$; and where $\underset{\sim}{c} = \underset{\sim}{\bar{d}}^*$. As before, the vector $\underset{\sim}{\bar{d}}^*$ is defined by $g(\underset{\sim}{d}^*) = \underset{\sim}{\bar{d}}^*$ where g is given in (19).

In analogy to (18), let k be the one-to-one correspondence which reverses vector polarity. For example, let $\underset{\sim}{c}\epsilon D_2$ be given as in (29). Then,

$$k(\underset{\sim}{c}) = \underset{\sim}{c}^* \qquad \ldots.31$$

where

$$\underset{\sim}{c}^* = \alpha_n \underset{\sim}{a}_1 + \alpha_{n-1} \underset{\sim}{a}_2 + \ldots + \alpha_2 \underset{\sim}{a}_{n-1} + \alpha_1 \underset{\sim}{a}_n \qquad \ldots.32$$

Obviously, $k(D_2) = D_2^*$

D_2 is isomorphic to R_2, the vector space representing RNA molecules. This is a field isomorphism given by

$$h:\mathcal{K}' \rightarrow \mathcal{K} \qquad \ldots.33$$

where $\mathcal{K} \equiv \{O,U,A,C,G\}$; and where the one-to-one correspondence h is defined in (7). Implicitly of course, we have the order-isomorphism

$$\{[0]_5, [1]_5, [2]_5, [3]_5, [4]_5\} \leftrightarrow \{O,U,A,C,G\} \qquad \ldots.34$$

Transcription:

The definitions of the transcription operators $\mathcal{T}$ and $\mathcal{T}^*$ are the same as those given in (22) and (23), respectively. Thus, we have

$$\mathcal{T}[\underset{\sim}{c},\underset{\sim}{d}^*] = h(\underset{\sim}{d}^*) = \underset{\sim}{r} \epsilon R_2 \qquad \ldots.35$$

and

$$\mathcal{T}^*[\underset{\sim}{c},\underset{\sim}{d}^*] = h(k(\underset{\sim}{c})) = \underset{\sim}{r}' \epsilon R_2 \qquad \ldots.36$$

where both $\underset{\sim}{r}$ and $\underset{\sim}{r}'$ have $5' \rightarrow 3'$ polarity; and where $\underset{\sim}{r}$ represents the transcription product of the $3' \rightarrow 5'$ vector, while $\underset{\sim}{r}'$ represents the transcription of the $5' \rightarrow 3'$ vector.

Translation:

Since the protein field would have to contain the set $\mathcal{A}$ - {TC}, it is not possible to form a field set of prime cardinality. Hence, a field is not defined, and a protein vector space with a structure similar to D_2 and R_2 cannot be constructed. However, the vectors of R_2 may be treated as RNA molecules and used to form S_1. The formalism of the last section is then applicable.

E. DISCUSSION

(i) COMPARISON OF THE TWO FORMALISMS:

For the purposes of this discussion, the system of vector spaces that was developed over the real field will be denoted VSI, while that developed over Z_5 will be termed VSII.

In both VSI and VSII DNA and RNA molecules are treated as vectors in finite-dimensional spaces. Double-stranded DNA molecules are treated as vector pairs. Transcription is formulated as a linear operator mapping DNA space into RNA space. In VSI a protein space is defined and protein synthesis

is treated as a mapping from a subset of RNA space to protein space. An analogous treatment of protein synthesis in VSII is not possible.

There exist vectors in VSI which do not represent physically-realizable molecules. This reflects the fact that VSI is more rich mathematically than the biological system demands. The physically-realizable vectors form a countable subset of the space, and the physically-unrealizable vectors permit continuous deformations of one physically-realizable vector into another. All vectors in VSII, however, represent actual molecules and, in this sense, VSII is a more economical representation of the system.

In VSI there is a combinational ambiguity in proceeding <u>from</u> a vector <u>to</u> a molecule: That is, more than one molecule corresponds to the same vector. This is a result of the loss of information that occurs when a unique vector is formed from a given molecule. The order of the arrangement of the codons in the molecule is not retained in the vector representation. This difficulty is removed in the VSII formulation.

A geometric interpretation of VSII does not exist for an arbitrarity-dimensioned space. This arises because a positive-definite scalar product for an arbitrarily-dimensioned space cannot be defined. This may be seen easily for any space whose dimension is a 5 (or a multiple of 5) --- simply form the norm of the vector

$$\underset{\sim}{v} = [1]_5\underset{\sim}{a}_1 + [1]_5\underset{\sim}{a}_2 + [1]_5\underset{\sim}{a}_3 + [1]_5\underset{\sim}{a}_4 + [1]_5\underset{\sim}{a}_5$$

This difficulty does not occur for VSI, and in fact, the existence of a geometrical interpretation leads to an immediate application of the formalism to existing experimental data (<u>vide infra</u>).

It appears that neither VSI nor VSII is ideal for the algebraic formulation of molecular genetics. Together, however, they achieve an

adequate description of the informational nature of the fundamental processes.

(ii) POSSIBLE APPLICATIONS:

The use of the geometrical interpretation of VSI to analyze protein sequence data has already been mentioned. An example of a specific type of investigation is the following.

There exist enzymatic reaction sequences of the form

$$A \xrightarrow{E_1} B \xrightarrow{E_2} C \xrightarrow{E_3} D$$

where E_1, E_2 and E_3 are enzyme catalysts of the reaction sequence; where A is a substrate; D is a product; and B and C act as both substrates and products. Since E_1, E_2 and E_3 are proteins (or, at least, are composed mainly of protein), a defined relationship between the three protein vectors $\underset{\sim}{E_1}$, $\underset{\sim}{E_2}$ and $\underset{\sim}{E_3}$ exists: Namely, the norms of all three vectors and the angle between any pair of vectors. In this fashion one may ascertain whether the angle between $\underset{\sim}{E_1}$ and $\underset{\sim}{E_2}$ is related in a simple fashion to the angle between $\underset{\sim}{E_2}$ and $\underset{\sim}{E_3}$ when a set of such sequence reactions from different species is considered; or whether $\underset{\sim}{E_1}$, $\underset{\sim}{E_2}$ and $\underset{\sim}{E_3}$ all lie in the same plane; or whether some simple relationship exists with respect to the norms of the three vectors. The list could go on almost indefinitely. More importantly, the questions may be composed in a precise and unambiguous manner so that correlation of large amounts of data becomes easily feasible.

Construction of evolutionary trees by a species comparison of the sequences of proteins having similar functions has been attempted in the past using metric space theory.[9] The thrust of this type of analysis has been to define a mathematically correct metric with which to gauge the distance, evolutionarily, between protein sequences. One basic type of metric which has been used is the Hamming metric[10] which, for this particular problem, simply counts the number of amino acid replacements that are necessary

to convert one protein sequence into another. More elaborate metrics may be defined to account for the redundancy in the genetic code in relating a protein sequence back to a DNA sequence. A similar analysis may be made using the formalism of VSI, but since the space involved is more rich mathematically than a metric space, more subtle questions may be posed. In fact, D_1, R_1 and P_1 become metric spaces if the metric is defined as $||\underset{\sim}{a}-\underset{\sim}{b}||$. More importantly, however, the application of this metric defines D_1, R_1 and P_1 as finite-dimensional Hilbert spaces. An investigation of the relationships between the elements of these spaces should prove fruitful. VSII may also be treated as a metric space, and one example of a correct metric in this space is, in fact, the Hamming metric.

Perhaps the most promising aspect of the agebraic structures developed i. this work is the ability to define evolution at a <u>dynamical</u> level rather than simply at a comparative level. The metric space formulations are restricted to investigating evolution by a comparison of specific protein sequences at a fixed point in evolutionary time. It may be possible, however, to use results obtained in this manner to construct a physically meaningful time-dependent linear operator that acts to select certain vectors in D_1. Certainly, the mathematics necessary for such an investigation is available.

F. REFERENCES

1. See, for example, "Elements of Abstract Algebra", Allan Clark, Wadsworth Publishing Co., Belmont, Calif. (1971).

2. See, for example, "Set Theory", Felix Hausdorff, 2nd Ed., Chelsea Publishing Co., New York (1962); "Theory of Sets", E. Kamke, Dover Publications, New York (1950).

3. There exist multiplicative groups modulo n, where n is not prime, if the equivalence classes which form the group elements are relatively prime to n. See Ref. 1, p. 23. These groups are not discussed, since they cannot be used to form a finite field.

4. Since we shall not deal with complex spaces, Hermitian symmetry for the scalar product is not invoked.

5. "The Genetics of Bacteria and Their Viruses", William Hayes, 2nd Ed., Halsted Press, New York (1968); Chap. 14 and references therein.

6. "The Biochemistry of Nucleic Acids", J. N. Davidson, 7th Ed., Academic Press, New York (1972).

7. G. L. Findley and S. P. McGlynn, "A Group-Theoretic Analysis of the Genetic Code", J. Chem. Phys., submitted for publication.

8. The codon GUG may sometimes act as the protein synthesis initiator (see Ref. (6) p. 363). This may be taken into account by a slight modification of S_1. However, at this time, the additional complexity does not seem to be warranted.

9. William A. Beyer, Myron L. Stein, Temple F. Smith and Stanislaw M. Ulam, Math. Biosciences, 19, 9 (1974). References to older works, in which the "metrics" used were axiomatically incorrect, are given in this paper.

10. R. W. Hamming, Bell System Technical J., 26, 147 (1950).

VIII. THE ORBITAL APPROXIMATION

VIII. THE ORBITAL APPROXIMATION

(See item 160)

The only item of Section II.A concerned with this topic is 160.

This work is concerned with the orderly extraction from theory of the following concepts:

---The concept of orbital interactions: This concept is heavily used but is rarely, if ever, discussed in terms of a meaningful MO approach.

---The various orbital types are labelled, in self-evident terminology: core, valence, Rydberg, continuum. The interrelations of these types of orbitals are rarely specified and the manner of their evolution from the same energy operator is not delineated.

Our aim is to relate orbital properties to state properties in a way which is at once useful and meaningful. In this connection, we pay considerable attention to the following topics:

---Koopmans' theorem: We focus interest not on the energy equivalence part of this approximation (i.e., $I(n) \simeq -\varepsilon_{nn}$) but rather on its importance as a selection rule.

---The Rydberg Equation: We show that the use of improved virtual orbitals (IVO's) leads to a Koopmans' theorem for Rydberg transitions and, thence, deduce a closed-form solution which yields the Rydberg equation and expressions for the quantum defect.

---A modified Koopmans' theorem for core orbitals has been deduced and applied. It has been shown that it leads directly to the point-charge model, and yields the standard empirical expressions for ESCA chemical shifts.

---The secular determinant $|F - ES|$ has been constructed in a formal way

for a molecule AB constituted of two bits A and B. The interaction of various blocks from this determinant (to the exclusion of other blocks which are presumed to be non-interacting) is shown to lead to such concepts as conjugation, hyperconjugation, through-bond interaction, through-space interaction, bond-bond interaction (i.e., LCBO), etc. As a result, the approximations inherent in such concepts become physically very clear. ---Continuation of the process specified above, but with explicit input of virtual orbitals, leads to concepts of polarization, locally-excited states, charge-transfer states, excimer states, the LCRO model, etc.

In sum, we speak to the problem of "How to avoid reducing chemistry to numerics while still benefitting from theory". We believe that we have done so in a way which retains rigor and makes the hierarchy of approximations self-evident.